ELUCIDATION OF THE PHYSIOLOGICAL, REGULATORY, AND SYMBIOTIC IMPACTS OF METHIONINE METABOLISM IN *XENORHABDUS* BACTERIA

A Dissertation Presented for the

Doctor of Philosophy

Degree

The University of Tennessee, Knoxville

Cameron Moore

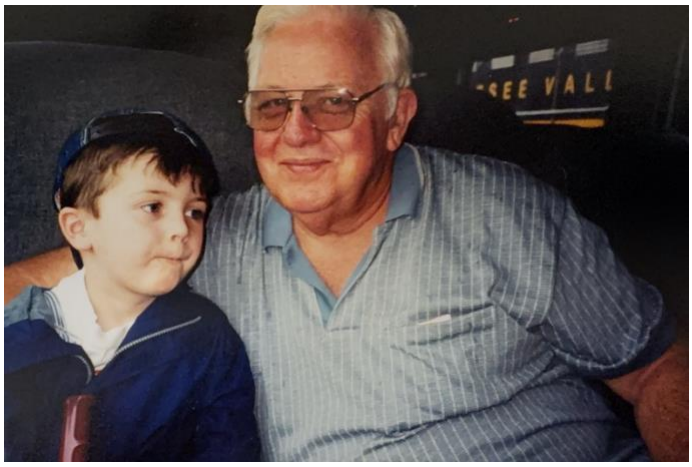
August 2026

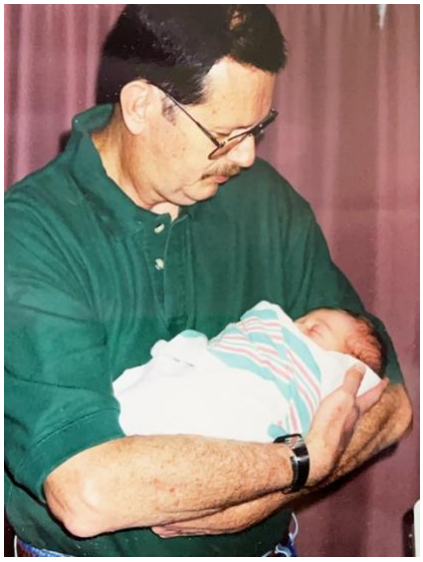
Copyright © 2026 by Cameron Moore

All rights reserved.

DEDICATION

In loving memory of Big Papaw and Little Papaw.





ACKNOWLEDGEMENTS

I want to first thank Dr. Heidi Goodrich-Blair for allowing me to join her research team and for providing kind and thoughtful mentorship during our time together. I also want to extend my gratitude to Dr. Elizabeth 'Liz' Fozo, Dr. Gladys Alexandre, and Dr. Erik Zinser, for their willingness to serve on my dissertation committee and their collective efforts to help me "see the forest through the trees." I want to thank my former committee member Dr. Jeremiah Johnson for his prior contributions to my research project while serving on my committee. I also want to thank other faculty who did not serve on my committee but provided helpful insights to my research throughout my tenure in the Microbiology Department including Dr. Jennifer Heppert, Dr. Todd Reynolds, Dr. Lindsay Burcham, Dr. Alison Buchan, and Dr. Andrew Monteith.

The Goodrich-Blair lab has become one of my strongest support systems and it is here I have met incredible, selfless individuals who have dedicated their time to train me in the ways of microbiology, nematology, and entomology. I attribute all of my laboratory skill to the amazing training I received from Sarah Kauffman, Dr. Jennifer Heppert, and Dr. Alex Grossman. I am forever grateful for their mentorship and, most importantly, their friendship. I have also had the privilege of forming meaningful friendships with current and former lab mates: Dr. Erin Mans, Dr. Nick Mucci, Emmanuel Allwell, Jahirul Rafi, Dr. Ryan Awori, Dr. Paula Rozo-Lopez, Dr. Jayashree Ramakrishnan, Tyler Myers, Matthew Traywick, Grace Pullen, Omar Alani, and Nick Pawlowski. Each aforementioned individual has enriched my life, and I am grateful to have journeyed in the laboratory alongside you all.

Outside of the Goodrich-Blair Lab, I am also the unofficial member of the Reynolds Lab as it was here, I met some of the best scientific “sisters” a guy could ask for. Mikayla Mangrum, Ainsley King, and Kaley Taylor have been my dearest confidants in graduate school and have supported me through my myriad ups and downs. Thank you all for being there when I needed you most. I also want to thank the friends across the Microbiology department who have helped make graduate school an absolute delight: Dr. Alex Truchon, Dr. Jill Walton, Dr. Jéssica Mendonça, Abbey Behler, and Emily Landolt, and Dr. Selene Shore. Each friend has offered new perspectives on my view of the world and science, while also bringing levity to my life when I desperately needed it.

My family is a constant source of love in my life and distract me from my research as often as they can. My mother, Sherri Fowler, and stepfather, Jeffery Fowler have been my fiercest supporters and have always pushed me to be the best that I can be. They sacrificed their time, their money, and possibly their sanity in order to help me get to this point, but I know they would do it all again if I asked them to. My father, Bradley Moore, and my stepmother, Angie Moore, always find new ways to make me laugh and while they are probably disappointed, I did not earn my degree in cryptozoology, I am grateful for their support, nonetheless. To the rest of my family, if y’all ever actually read this, I’m sorry I didn’t mention you individually; however, I love you and am grateful to have you in my life. My partner, Eric Coleman, and my very own “Smokey-dog”, Beau, have been necessary and blessed additions to my family. Together, they made graduate school seem possible and gave me a reason to keep going. I am grateful to Eric for believing in me at every stage of the graduate school process, for driving me to the laboratory at 3-o-clock in

the morning, and for loving me no matter what. I love you dearly and cannot wait for what the next stage of our life together.

I want to use the last section of my acknowledgements to thank my amazing grandfathers: Kenneth (Little Papaw) Moore and Herman (Big Papaw) Long. Words cannot express how much I loved these two men and words also cannot express how devastated I am that they are not here to see me complete my Ph.D. Both men played a critical role in making me the person I am today and are the kind of grandfathers any kid would dream of. I know that you both were extremely proud of me, and I only hope that I continue to make you proud.

ABSTRACT

All animal life, in some form, interacts with bacteria. These associations are highly contextual and can change depending on host or microbial nutrient status. Amino acids are important nutritional cues that influence various animal-microbe symbioses by modulating dynamics of microbial physiology within animal hosts. Symbiotic *Xenorhabdus* bacteria are established models for symbiosis, but very little is known regarding their general physiology *in vitro* or *in vivo*. Chapter 1 of this dissertation reviews what is presently known about *Xenorhabdus* physiology and compares what is known to other symbiotic bacteria. In Chapter 2, I interrogate the growth dynamics of *Xenorhabdus* bacteria in chemically, defined media and identify the aspartate-derived amino acids as growth-modulatory nutrients among certain species. Chapter 3 investigates how methionine metabolism in *X. bovienii* impacts colonization and fecundity of its nematode host *Steinernema feltiae*. Chapter 4 explores how Lrp-dependent phenotypic variation in *X. nematophila* changes during *in vitro* and *in vivo* growth conditions. In Chapter 5, we address the novel questions generated by this work and propose studies that can fill these knowledge gaps and enhance our understanding of *Xenorhabdus* physiology during symbiotic interactions.

TABLE OF CONTENTS

CHAPTER 1: INTRODUCTION 1

REFERENCES 16

CHAPTER 2: *XENORHABDUS* BACTERIA HAVE VARIABLE LAG TIMES IN AMINO ACID-DEFICIENT GROWTH CONDITIONS THAT ARE LINKED TO METABOLIC DEMAND FOR METHIONINE 29

ABSTRACT 30

INTRODUCTION 31

MATERIALS AND METHODS 36

RESULTS 42

DISCUSSION 67

REFERENCES 75

APPENDIX 89

CHAPTER 3: SYMBIONT METHIONINE BIOSYNTHESIS POSITIVELY INFLUENCES MUTUALISTIC ASSOCIATIONS WITH *S. FELTIAE* NEMATODES BY OPTIMIZING INTESTINAL COLONIZATION AND SUPPORTING FECUNDITY. 97

ABSTRACT 98

INTRODUCTION 99

MATERIALS AND METHODS 103

RESULTS 112

DISCUSSION 130

REFERENCES 135

CHAPTER 4: FIXED LRP EXPRESSION IN XENORHABDUS NEMATOPHILA IS DETRIMENTAL FOR SURVIVAL IN NUTRIENT-LIMITED NICHES..... 144

ABSTRACT..... 145

INTRODUCTION 147

MATERIALS AND METHODS..... 150

RESULTS 155

DISCUSSION..... 177

REFERENCES 186

CHAPTER 5: CONCLUSIONS AND FUTURE DIRECTIONS 195

INTRODUCTION 196

QUESTION 1: 197

QUESTION 2: 200

QUESTION 3: 205

CONCLUDING STATEMENT 208

REFERENCES 210

VITA..... 215

LIST OF TABLES

Table 2.1: Bacterial strains utilized in this study. 38

Table 3.1: Bacterial Strains and Plasmids 105

Table 3.2: Primers used in this study 108

Table 3.3*:* Proportions of wild-type and *ΔmetE X. bovienii*-Sf-FL strain on LA at 0 and 10 d post inoculation. 116

Table 3.4: Met auxotrophy confers a competitive disadvantage to *X. bovienii*-Sf-FL during *S. feltiae*-FL nematode colonization. 125

Table 4.1: Bacterial Strains and Growth Conditions 152

Table 4.2: The *X. nematophila* high-*lrp* P_{fliC}-*gfp* positive isolate maintains high P_{fliC}-*gfp* expression homogenously during growth in LB broth at the colony-level. 163

Table 4.3: List of metabolism-associated genes (locus tags and annotations) that are differentially expressed in the *X. nematophila lrp-2::kan* mutant. 174

LIST OF FIGURES

Figure 2.1: The aspartate-derived amino acids (ADAA; Asp, Met, Thr, and Lys) improve growth of *X. nematophila* in defined media. 45

Figure 2.2: Reconstruction of the predicted ADAA superpathway in *X. nematophila* reveals genomic distinctions from the characterized pathway in *E. coli* MG1655. . 48

Figure 2.3: Assessment of varying carbon and nitrogen sources on *X. nematophila* lag phase 52

Figure 2.4: The lag time of *X. nematophila* in GMM is primarily responsive to methionine. 55

Figure 2.5: A prolonged lag in GMM is not conserved among *Xenorhabdus* species. 59

Figure 2.6: Most Xenorhabdus exhibit Met-responsive lag times in GMM. 60

Figure 2.7: Comparative genomic analyses reveal genomic diversity in ADAA-related genes among *Xenorhabdus* bacteria. 66

Figure 2.8: *X. nematophila* growth in GMM is not due to eventual accumulation of a minority population adapted to growth in this condition. 89

Figure 2.9: The lag time of X. nematophila in GMM is primarily responsive to methionine. 90

Figure 2.10: *X. nematophila* lag in GMM is minimally influenced by intraspecific variation. 91

Figure 2.11: Phylogenetic tree of tested *Xenorhabdus* species (and other selected Enterobacterales). 92

Figure 2.12: Phylogenetic tree of MetB, MetC, MetY, MtcC, and MtcC-like proteins encoded in the genomes of *Xenorhabdus* species (and other selected *Enterobacterales*)..... 93

Figure 2.13: Genomic neighborhood of *Xenorhabdus* mtcC locus. Predicted ORFs with lines through them indicate if the sequence is not contiguous..... 94

Figure 2.14: Inoculum density but not growth phase alters *X. nematophila* lag phase length..... 95

Figure 2.15: Correlation between PixA Met richness and *Xenorhabdus* lag length..... 96

Figure 3.1: Deletion of the *X. bovienii*-Sf-FL *metE* gene does not alter wild-type growth and survival characteristics on Met-replete media..... 115

Figure 3.2: Fewer mature, *S. feltiae*-FL IJs emerge from lipid agar plates and are colonized by fewer bacterial cells when reared on methionine auxotrophic *X. bovienii*-Sf-FL..... 118

Figure 3.3: Complementation with the *metE* ortholog of *X. nematophila* fully and partially restores *S. feltiae*-FL IJ emergence and *X. bovienii*-Sf-FL colonization, respectively. 119

Figure 3.4: Increased levels of exogenous Met restores the emergence defect but not attenuated colonization of *ΔmetE*-reared *S. feltiae*-FL IJs..... 121

Figure 3.5: Average emergence of *S. feltiae*-FL IJs reared on mixed culture populations (green) phenocopies IJ emergence from a *ΔmetE* monoculture (pink) instead of wild type (blue). 122

Figure 3.6: A) *S. feltiae* nematodes exhibit decreased reproduction when reared on a *ΔmetE* (pink) *X. bovienii* symbiont than when reared on wild type (blue) or *ΔmetE attTn7::metE*$_{Xn}$ (purple) symbionts after 6 d. 127

Figure 3.7: Bacterial burden of unaged (A) and aged (B) *S. feltiae* IJs prior to natural infection assays when reared on wild type (blue), *ΔmetE* (pink), and *ΔmetE attTn7::metE*$_{Xn}$ (purple) strains. 128

Figure 3.8: Unaged (A and C) and Aged (B and D) *S. feltiae* IJs reared on a *ΔmetE* mutant (pink) exhibited similar virulence and emergence phenotypes to IJs reared on wild-type (blue) and *ΔmetE attTn7::metE*$_{Xn}$ (purple) strains when infecting *G. mellonella.* 129

Figure 4.1: Constitutive *lrp* expression is detrimental for *X. nematophila* persistence within *S. carpocapsae* IJs. 158

Figure 4.2: Spot dilution assay of *X. nematophila* wild-type, *lrp-2::kan*, low-*lrp*, and high-*lrp* strains on LB when revived from glycerol stocks stored at -80℃ for 7 d. 160

Figure 4.3: Fixed high-*lrp* expressing *X. nematophila* cells (blue) grow poorly in amino acid limiting growth conditions compared to wild-type (purple), *lrp-2::kan* (red), and fixed low-*lrp* (pink) strains. 165

Figure 4.4: The length of lag phase (A, D, G, J, M, P), growth rate (B, E, H, K, N, Q), and maximum OD_{600} (C, F, I, L, O, R) determined from the growth curves in Figure 4.3. 166

Figure 4.5: The presence of *lrp* influences gene expression of 25% of genes encoded in the *X. nematophila* genome when grown to stationary phase in a complex, rich medium. 170

Figure 4.6: *X. nematophila* Lrp negatively regulates carbon and amino acid metabolism during early stationary phase growth in LB. 173

Figure 4.7: The majority of predicted essential genes negatively regulated by Lrp in *X. nematophila* are associated with protein synthesis and metabolism. 176

Figure 4.8: Variation in Lrp-dependent P_{fliC}-*gfp* in *X. nematophila* colonies grown in minimal medium supplemented with casamino acids (solid lines, right y-axis) correlates with bacterial growth yield in minimal medium supplemented with glucose (dashed lines, left). 184

Figure 5.1: Emergence behavior of *Steinernema* nematodes when reared on wild-type and *metE*-deficient *Xenorhbadus* symbionts. 204

CHAPTER 1: INTRODUCTION

Authors: Cameron Moore and Heidi Goodrich-Blair

Bacteria are metabolically diverse and versatile organisms whose evolutionary success stems from niche-specific metabolic adaptation.

Bacteria occupy almost every explored Earth ecosystem [1, 2]. This evolutionary success can be attributed, in part, to their metabolic diversity and versatility which allows them to leverage a multitude of chemical and physical resources to derive energy and then proliferate [3-5]. Metabolic versatility among bacteria can vary considerably. In the laboratory, the chemoheterotroph *Escherichia coli* utilizes 74 distinct carbon sources to support growth in culture, while *Rhodopseudmonas palustris* can apply chemoheterotrophic, chemoautotrophic, photoheterotrophic, and photoautotrophic metabolic strategies in a condition-dependent manner [6, 7]. In natural contexts, bacteria generally take on specialized metabolic roles where they consume a few select nutrients to support growth and proliferation [8]. This suggests that evolutionary forces act upon bacterial species and drive metabolic specialization, thus allowing them to dominate within their respective niches. In order to determine the fitness benefits of metabolic versatility and specialization in natural contexts, it is imperative to identify the impact individual nutrients have on a bacterium's ability to proliferate and to determine the environmental contexts for which these nutrients represent a critical resource.

The availability of exogenous nutrients is one of the primary determinants of bacterial growth [9]. Nutrient availability can be highly variable within and across environmental contexts. Within soil ecosystems, nitrogen and phosphorous abundances are growth-limiting for bacteria in a soil-type dependent manner; however, carbon appears to be a common limiting nutrient in spite of the soil type [10]. In both marine and freshwater

ecosystems, phosphorous availability limits bacterial growth while carbon and nitrogen abundances vary in their impact [11]. Furthermore nutrient availability in either soil or aquatic ecosystems is not steady-state and fluctuates depending on geography, climate, and biodiversity [12, 13]. Bacteria are adept at persisting in the face of such variability and are thought to spend the majority of their lifespan transitioning between states of feast and famine [14]. In such dynamic natural environments, bacteria have evolved myriad strategies by which they can meet their metabolic demands in the presence or absence of nutrients.

At the cellular-level, nutrient-responsive motility, high-affinity nutrient import systems, and deployment of extracellular degradative enzymes aid bacteria in their efforts to forage for nutrients, while endogenous catabolic and biosynthetic processes allow bacteria to leverage their acquired resources [15-19]. To not expend excess energy in conditions where these mechanisms may be superfluous and costly, bacteria tightly coordinate these processes using regulatory hierarchies to control gene expression (e.g, transcription, post-transcription, translation, and post-translation) [20, 21]. In contexts where bacteria have access to multiple nutritional resources, these regulatory systems are also essential for governing priority uptake and degradation of these nutrients. For example, *E. coli* prioritizes the consumption of preferred carbon sources (e.g, glucose) over unideal ones (e.g, lactose) via differential regulation of gene targets by the Crp transcription factor in a process termed carbon catabolite repression (CCR) [19, 22]. Similar carbon prioritization hierarchies have been described in other related gammaproteobacteria (e.g, *Salmonella, Klebsiella,* and *Vibrio*), as well as in distantly related bacteria such as *Bacillus*

[19, 23-26]. Alternative prioritization has been observed in other gammaproteobacteria such as *Pseudomonas* and *Acinetobacter* species in which organic acids, such as citrate, malate, and succinate are utilized as their primary source of carbon over glucose [27]. These examples highlight a critical facet of microbial biology: related bacterial species do not share related diets. Logically, microorganisms evolving from the same lineage in the same environment may ultimately become competitors of one another for nutritional resources [28]. Diverse gammaproteobacteria occupy terrestrial, aquatic, plant, and animal niches yet they evolved from a common ancestor [29]. Therefore, it is advantageous for organisms of shared ancestry to evolve distinct feast and foraging behaviors rather than competing with their "kin" for a few, limited resources [30]. They must continue to evolve adaptations that permit them to better forage for shared resources or exploit underutilized ones. In both contexts, a bounty of mechanisms have been described, and they highlight an on-going arms race for bioavailable nutrients among bacteria.

Bacteria employ cooperative and competitive metabolic strategies when interacting with other living organisms.

Bacteria also compete for resources with other life forms, and this competition has led to the evolution of inter-organismal antagonistic or cooperative metabolic strategies [31, 32]. As antagonists, bacteria can employ two strategies, exploitation or inhibition competition [31]. Exploitative competition is generally characterized by rapid and efficient bacterial growth that limits the growth of competing organisms by depleting essential nutrients. The secretion and uptake of siderophores – high affinity, iron-chelating compounds – represents a classical mechanism of exploitation competition as the

siderophore-lacking competitor is unable to proliferate to the same level as the siderophore competent competitor and is ultimately outcompeted [33]. Inhibitory competition generally is characterized by the production of harmful compounds that damage (or kill) other living organisms. As an example, bacteriocins – protein-based antimicrobials that are synthesized via ribosomal activity – mediate competition between closely related bacteria and allow competitive dominance of the producer by killing off the competition [34, 35].

In a cooperative context, bacteria form partnerships with other life forms where nutritional or defensive support is exchanged, engendering a reciprocal fitness benefit. For example, the soil bacterium *Delftia* sp. DT-2 lacks the ability to utilize glucose as a carbon source but can grow in conditions where pyruvic acid is available. *Bacillus* sp. BP-3, which utilizes glucose, secretes sufficient levels of pyruvic acid under glucose-rich environmental conditions to allow growth of *Delftia* sp. DT-2 [36]. In turn, *Delftia* sp. DT-2 produces a toxin that inhibits the growth of competing soil bacteria, but not *Bacillus* sp. BP-3, promoting survival of both bacterial partners [36]. Metabolic cooperation between bacteria has been observed in a variety of ecosystems and is effective at conferring a strong competitive advantage for participating bacterial species [37, 38].

Competitive and cooperative metabolic schemes are employed in interkingdom interactions between bacteria and eukaryotes as well. Indeed, eukaryotic hosts, such as plants and animals, are nutrient-replete reservoirs and predictably experience fluctuations in nutrient availability [39, 40]. However the majority of these nutrients are made inaccessible by physical barriers (e.g, cell membranes), eukaryote immunity, and competition with other host-associated microorganisms [5, 26, 39]. Despite these barriers,

many bacteria readily occupy eukaryotic ecosystems persistently forming symbioses, that allow them to acquire preferred or essential dietary components. Much like in microbe-microbe competition, symbioses between bacteria and other organisms can vary in their effect on their eukaryotic partner's fitness, ranging from antagonistic to beneficial [5, 26, 41]. Symbiotic associations have been best studied in the context of bacterial pathogens particularly those that harm animals, including humans; however, there is a growing body of knowledge regarding bacteria that associate with other forms of eukaryotic life. For the purposes of this chapter, I will hereafter focus on symbiotic associations between animals and bacteria.

Bacteria lose and acquire metabolic traits that improve their ability to interact with eukaryotic hosts

The basis of many, but not all, animal-bacterium symbioses are metabolic in nature with the participating bacteria utilizing host-derived nutrients to support their metabolic activity and proliferation. The evolution of these relationships is often accompanied by the acquisition and loss of metabolic traits in response to selective pressure from symbiotic partners or the shared environment. Although genes associated with bacterial metabolism rarely engender the initiation of a symbiosis, they can be adaptive allowing symbiotic bacteria to thrive in their host ecosystem [42, 43]. In the next section, I will explore specific examples of how aspects of gene gain and gene loss associated with metabolic processes have enhanced symbiotic associations between bacteria and their animal hosts.

The acquisition of novel metabolic traits usually via horizontal gene transfer has led to bacterial adaptation during associations with animals. In its evolutionary history,

Salmonella enterica serovar Typhimurium acquired two distinct pathogenicity islands that allowed it to invade and survive within the mammalian intestine in both extracellular and intracellular contexts [44]. These islands encode virulence factors (e.g, Type 3 secretion systems) as well as metabolic genes. Pathogenicity Island-2 includes genes that encode enzymes for tetrathionate respiration – a host-derived metabolite that increases in abundance as a result of *Salmonella* infection [45] - indicating that Pathogenicity Island-2 enhances *S. enterica* growth and survival during infection by permitting utilization of an abundant host-specific resource [46]. Similar themes have been observed in mutualistic symbioses. For example, spirochete bacteria that occupy the hindgut of specific termite species like *Nasutitermes takasagoensis* have acquired, via horizontal gene transfer, the capacity to degrade the lignocellulose derivative hemicellulose [47]. This trait is adaptive for the termite host and its hindgut symbionts as it permits access to an otherwise recalcitrant nutrient source [47]. The acquisition of genes that confer novel metabolic traits can impart strong fitness benefits to both pathogens and symbionts of animals and represents key evolutionary milestones in the bacterium's co-adaptation to its host.

The loss of metabolism-associated genes can also be imperative for the evolutionary success of symbiotic bacteria [48, 49]. The intracellular bacterium *Buchnera aphidicola* has undergone significant gene loss as the result of its obligate, mutualistic association with the Hemipteran insect *Acyrthosiphon pisum.* Metabolic redundancy between the host and bacterium is thought to have selected for the loss of many metabolic genes within the bacteria, including those involved in vitamin and amino acid biosynthesis [50, 51]. While this is commonly seen as a fitness trade-off given that *Buchnera* is unable

to grow and live independently of its host, such gene loss also has been shown to contribute to the reorganization of metabolic flux in the symbiont which promotes production of essential metabolic products like amino acids required by the aphid host for survival [52]. This phenomenon is not restricted to just *Buchnera* and *A. pisum*, as the formation of obligate, mutualistic symbioses independently occurred at least 16 times across the insect clade [42]. The formation of these mutualisms is correlated with a shift among insect hosts from a more generalized diet (e.g, herbivory) to a specialized one (e.g, plant phloem sap) [42]. Similar themes were observed in a "synthetic" animal-bacterium symbiosis where a non-cognate symbiont, *E. coli*, was experimentally evolved to mutualistically associate with the stinkbug *Plautia stali* – a Hemipteran insect that naturally forms an obligate, mutualistic symbiosis with gut-associated *Pantoea* bacteria [53]. The ancestral *E. coli* strain, which shares common ancestry with *Pantoea*, could minimally colonize insect host tissue and support host development at low levels, in the absence of *Pantoea* [53]. After several generations of development with the colonizing *E. coli*, some *P. stali* lines exhibited improved fitness. The *E. coli* strains derived from these insects had acquired mutations disrupting CCR regulation genes like *cyaA* and *crp* that regulate carbon source utilization [53]. Although mutation of these genes reduced the fitness of *E. coli in vitro,* they improved the host symbiotic outcome. It was speculated that activation of CCR in *E. coli* during colonization may have come at a metabolic cost for the *P. stali*; therefore, this suggested that host-association selected against the symbiont's CCR [53]. However, the native symbiont of *P. stali*, *Pantoea*, was predicted to encode functional CCR genes, signifying that in this organism an alternative regulatory hierarchy may be employed.

These data intimate that mutualistic animal-bacterium symbioses require metabolic adaptation by bacterial symbionts. However, gene loss is not exclusive to beneficial bacterial symbionts as many pathogens have also lost metabolic genes as the result of host association. Dependencies on animal hosts for essential growth factors, like amino acids and vitamins, has been documented in both obligate, intracellular pathogens (e.g, *Chlamydia trachomatis* and *Rickettsia prowazekii*) and free-living pathogens (e.g, *Pseudomonas aeruginosa* and *Yersinia pestis*) [54-57]. Furthermore the loss of metabolism genes in the context of pathogenesis can be adaptive. For example, enteroinvasive *E. coli* and *Shigella* species have lost the *cadA* locus, encoding a lysine decarboxylase enzyme, that is encoded by closely related, non-pathogenic *E. coli* [58]. Induction of *cadA* engenders resistance of non-pathogenic *E.* coli to weak organic acids during carbohydrate fermentation, a trait that is speculated to be advantageous in the mammalian intestine [59]. However, a by-product of the enzyme's activity, cadaverine, reduces effectiveness of *S. flexneri* enterotoxins during host infection, indicating that *cadA* loss can enhance enterotoxin-mediated virulence, a fitness benefit that may counterbalance the predicted increase in acid sensitivity [58]. Taken together, these examples demonstrate that symbiotic associations with animals select against bacterial metabolic traits, but that the impact on the animal host or the symbiont depends on the context.

Given that bacterial metabolic adaptation is seemingly universal in the context of antagonism and mutualism, then it could be inferred that these symbiotic designations are fixed. However, bountiful examples exist of commensal or beneficial bacteria becoming antagonistic to their host. For example, the abundant human gut commensal *Bacterioides*

fragilis degrades unusable plant-derived polysaccharides into short chain fatty acids the host's intestinal cells can use for their own metabolic processes [60]. However, *B. fragilis* also causes infections that manifest in a variety of forms including abscesses or colorectal cancer [60]. Even in "model" mutualisms like the *Buchnera* and *A. pisum* symbiosis, there is natural variation in *Buchnera* levels among aphids that leads to physiological adaptations in the host. Aphids that bear higher *Buchnera* titers must supply more metabolites to their symbiont at the expense of their fitness [61]. While this is not inherently an antagonistic interaction, these findings indicate that even essential mutualisms do not always evenly distribute the metabolic burden. From these observations an important question is revealed: *How does nutrient limitation within animal hosts influence the diet and growth behavior of host-associated bacteria?* In this dissertation, I utilize the symbiosis between *Xenorhabdus* bacteria and their *Steinernema* nematode hosts to address this question and describe my rationale for this model system below.

Xenorhabdus bacteria as models for metabolic adaptation in the context of symbiosis

Xenorhabdus bacteria are obligately host-associated bacteria that form mutualistic symbioses with nematodes of the *Steinernema* clade and antagonistic associations with insects [62]. These associations require *Xenorhabdus* to reversibly transition between mutualistic and pathogenic states. *Xenorhabdus* physiology has evolved in response to the alternating selective pressures of their two invertebrate hosts over evolutionary time. Arguably, the strongest host-associated selective pressures are imparted by the *Steinernema* host as their associations with *Xenorhabdus* symbionts are highly specific with only certain *Xenorhabdus* species colonizing certain nematode hosts [63, 64]. In well-

studied *Steinernema-Xenorhabdus* pairs, 1-2 bacterial cells initially colonize the anterior intestine of developing infective juvenile (IJ) nematodes – the only free-living, migratory stage of the *Steinernema* lifecycle – but can proliferate within a specialized tissue called the receptacle to reach up to 100-200 cfu [65, 66]. Although colonization of the receptacle by *Xenorhabdus* does reduce the longevity of mature *Steinernema* IJs, these organisms can survive for extended periods of time in their soil environment [67-69]. IJ nematodes are considered nutrient-limited as they are non-feeding, with a collapsed intestine and with their natural openings occluded by a protective, chitinous double cuticle [70-72]. During this stage *Xenorhabdus* must metabolically cooperate with their host as depletion of essential nutrients would be lethal for both organisms. Although *Xenorhabdus* can persist within IJs long-term, their population size decreases over time suggesting that one or more nutrients becomes growth limiting as the association progresses [71]. It is unknown if such metabolic cooperativity between *Steinernema* and *Xenorhabdus* is bi-directional (e.g, direct cross-feeding) or uni-directional (e.g, nematodes supply nutrients to the bacteria or vice versa); however, it is essential for both organisms to persist in order to effectively parasitize an insect host [68, 69]. When a naïve insect host is identified, *Steinernema* IJs will invade the insect and deposit the *Xenorhabdus* symbiont into the insect hemolymph where the bacteria will proliferate and kill the insect using an arsenal of virulence factors, this stage is referred to as early infection [73-75]. This stage of infection represents where *Xenorhabdus* likely uses competitive metabolic strategies to overcome its insect host, while also impeding the invasion of the insect by other *Xenorhabdus-Steinernema* pairs. Indeed, *Xenorhabdus* utilize exploitative and inhibitory strategies during early-stage infection to

ensure competitive dominance over other entomopathogenic bacteria [35, 76]. In the middle stage of infection, *Xenorhabdus* continue to proliferate by secreting degradative enzymes that breakdown the insect cadaver [18, 73, 77, 78]. In turn, the bacterivorous *Steinernema* host feeds on its *Xenorhabdus* symbiont during this stage to support growth, development, and reproductive processes [79]. At this stage, *Xenorhabdus* likely transitions to a state of metabolic cooperativity where it inadvertently supplies nutrients to its nematode host. During this same stage, the insect's microbiome constituents and soil-derived saprophytes will also begin to invade and/or proliferate in the insect cadaver [80, 81]. *Xenorhabdus* continues to utilize competitive strategies, including secondary metabolite production, to maintain competitive dominance within the environment [80, 81]. During the final stage of infection, changes in the insect cadaver environment, mediated by alterations in nutrient availability and/or nematode and bacterial population size, trigger the development of IJ nematodes who, along with their colonized *Xenorhabdus*, return to the soil in search of a viable host [82, 83]. This brief review of the *Xenorhabdus* life cycle demonstrates that these bacteria are effective models for investigating bacterial adaption to host-derived nutrients as they must transition between two distinct host environments (nematodes and insects) and experience dynamic nutritional changes in both environments resulting in proliferative and persistent states. Our understanding of *Xenorhabdus* adaptation to host conditions is limited by a dearth of information regarding the primary metabolism of *Xenorhabdus* bacteria. Despite this field-wide oversight, observations from a variety of studies suggest that aspects of primary metabolism, particularly pathways associated with carbohydrate and/or amino acid

degradation and synthesis, play an integral role in both antagonistic and mutualistic host associations [71, 72, 82, 86, 87]. Furthermore, the ability of *Xenorhabdus* to transition between both host environments is possibly linked to the recognition and response to metabolic cues. In *X. nematophila* activity of the Leucine-responsive regulatory protein (Lrp) is required for both mutualistic and antagonistic host associations [75, 88-92]. While the nutritional cues that alter *X. nematophila* Lrp-dependent gene expression are unknown, work in other bacteria suggest that the presence of specific amino acids and carbohydrates can alter Lrp activity, directly or indirectly [93, 94]. In this dissertation, I address current knowledge gaps regarding our understanding of *Xenorhabdus* physiology and examined how these findings integrate into the symbiotic lifestyle of these bacteria.

In **Chapter 2**, I utilize chemically defined media to identify nutrients that significantly impact the growth dynamics of *X. nematophila in vitro.* Under amino acid-limiting growth conditions, I observed that *X. nematophila* undergoes a prolonged lag phase that can be significantly reduced in the presence of the aspartate-derived amino acids (ADAA), namely L-methionine (Met). Although a prolonged lag time is not shared among all *Xenorhabdus* species, I demonstrate that a Met-dependent shortening of lag is conserved among the majority of tested species. Comparative genomics of the tested *Xenorhabdus* bacteria revealed that clade-wide variation in lag time in amino-acid limiting growth conditions is associated with the presence of predicted accessory Met metabolism genes and a Met-rich inclusion protein. Taken together, these data suggest that differential demand for the ADAA *in vitro* is likely driven by efficacy in methionine biosynthesis/acquisition.

In **Chapter 3,** I interrogate the role of Met biosynthesis in mediating the mutualistic interactions of *X. bovienii*-Sf-FL and its nematode host *S. feltiae*-FL. I discover that disruption of Met biosynthesis in *X. bovienii* significantly reduces the reproduction of *S. feltiae* nematodes, as fewer IJ stage worms develop and emerge during *in vitro* experiments. Both genetic and chemical complementation rescue this reproduction phenotype suggesting that *Steinernema* fitness depends both on its symbiont's ability to produce and/or acquire exogenous Met. Furthermore, Met biosynthesis is required for optimal outgrowth of *X. bovienii* within the receptacle of *S. feltiae* IJs. Despite the impacts of symbiont Met metabolism on colonization and fecundity, *S. feltiae* IJs-reared on a Met-deficient symbiont were able to infect, kill, and reproduce within *Galleria mellonella* larvae. However, aged *S. feltiae* IJs colonized by a Met-deficient symbiont exhibited significantly reduced reproduction *in vivo* compared to unaged IJs. Together, these data suggest that *X. bovienii* Met proficiency is essential for mutualistic associations with *S. feltiae*-FL nematodes.

In **Chapter 4,** I investigate how metabolic demands in *X. nematophila* are impacted *in vitro* and *in vivo* by Lrp-dependent phenotypic variation. During colonization and persistence within *S. carpocapsae* IJs, the proportion of *X. nematophila* cells expressing high levels of *lrp* decrease over time. When grown in amino acid deficient media, *X. nematophila* cells with fixed high-*lrp* expression are unable to grow over a 168-h growth curve, while fixed low and *lrp* deficient cells can grow but are distinct from wild-type growth. Supplementation of Met supports the growth of fixed high-*lrp X. nematophila* strain suggesting a high physiological demand for this amino acid *in vitro*. Transcriptomic

analyses expand our present understanding of the Lrp regulon in *X. nematophila* as we find that Lrp negatively regulates a plethora of essential genes involved in carbon metabolism, amino acid metabolism, and cellular replication. Together, our data suggest that variability in *X. nematophila* Lrp levels is required for optimal metabolic adaptation and that selection against homogenously high *lrp* expression *in vivo* may be driven by nutrient limitation in regard to amino acids.

REFERENCES

1. Horner-Devine, M.C., K.M. Carney, and B.J. Bohannan, *An ecological perspective on bacterial biodiversity.* Proc Biol Sci, 2004. **271**(1535): p. 113-22.
2. Cockell, C.S., *Are microorganisms everywhere they can be?* Environmental Microbiology, 2021. **23**(11): p. 6355-6363.
3. Douglas, A.E., *The microbial exometabolome: ecological resource and architect of microbial communities.* Philosophical Transactions of the Royal Society B: Biological Sciences, 2020. **375**(1798).
4. Lucius, S. and M. Hagemann, *The primary carbon metabolism in cyanobacteria and its regulation.* Frontiers in Plant Science, 2024. **Volume 15 - 2024**.
5. Bhagwat, A., et al., *Bacterial metabolism in the host and its association with virulence.* Virulence, 2025. **16**(1): p. 2459336.
6. Tong, M., et al., *Gene Dispensability in Escherichia coli Grown in Thirty Different Carbon Environments.* mBio, 2020. **11**(5).
7. Brown, B., M. Wilkins, and R. Saha, *Rhodopseudomonas palustris: A biotechnology chassis.* Biotechnology Advances, 2022. **60**: p. 108001.
8. Johnson, D.R., et al., *Metabolic specialization and the assembly of microbial communities.* Isme j, 2012. **6**(11): p. 1985-91.
9. Monod, J., *THE GROWTH OF BACTERIAL CULTURES.* Annual Review of Microbiology, 1949. **3**(Volume 3, 1949): p. 371-394.
10. Aldén, L., F. Demoling, and E. Bååth, *Rapid method of determining factors limiting bacterial growth in soil.* Appl Environ Microbiol, 2001. **67**(4): p. 1830-8.

11. Elser, J.J., L.B. Stabler, and R.P. Hassett, *Nutrient limitation of bacterial growth and rates of bacterivory in lakes and oceans: a comparative study.* Aquatic Microbial Ecology, 1995. **09**: p. 105-110.

12. Chao, C.-F., et al., *Heavy rainfall shifts microbial control from nutrient–temperature to precipitation dependence in subtropical coastal waters.* Estuarine, Coastal and Shelf Science, 2026. **334**: p. 109811.

13. Shipley, J.R., et al., *Consumer biodiversity increases organic nutrient availability across aquatic and terrestrial ecosystems.* Science, 2024. **386**(6719): p. 335-340.

14. Finkel, S.E., *Long-term survival during stationary phase: evolution and the GASP phenotype.* Nature Reviews Microbiology, 2006. **4**(2): p. 113-120.

15. Raina, J.-B., et al., *The role of microbial motility and chemotaxis in symbiosis.* Nature Reviews Microbiology, 2019. **17**(5): p. 284-294.

16. Davies, J.S., et al., *Selective Nutrient Transport in Bacteria: Multicomponent Transporter Systems Reign Supreme.* Frontiers in Molecular Biosciences, 2021. **Volume 8 - 2021**.

17. Kamalanathan, M., et al., *Exoenzymes as a Signature of Microbial Response to Marine Environmental Conditions.* mSystems, 2020. **5**(2).

18. Park, D. and S. Forst, *Co-regulation of motility, exoenzyme and antibiotic production by the EnvZ-OmpR-FlhDC-FliA pathway in Xenorhabdus nematophila.* Mol Microbiol, 2006. **61**(6): p. 1397-412.

19. Buffing, M.F., et al., *Capacity for instantaneous catabolism of preferred and non-preferred carbon sources in Escherichia coli and Bacillus subtilis.* Scientific Reports, 2018. **8**(1): p. 11760.

20. Kroner, G.M., M.B. Wolfe, and L. Freddolino, *Escherichia coli Lrp Regulates One-Third of the Genome via Direct, Cooperative, and Indirect Routes.* J Bacteriol, 2019. **201**(3).

21. Fic, E., et al., *cAMP Receptor Protein from Escherichia coli as a Model of Signal Transduction in Proteins – A Review.* Journal of Molecular Microbiology and Biotechnology, 2008. **17**(1): p. 1-11.

22. Görke, B. and J. Stülke, *Carbon catabolite repression in bacteria: many ways to make the most out of nutrients.* Nature Reviews Microbiology, 2008. **6**(8): p. 613-624.

23. Fisher, S.H., *Regulation of nitrogen metabolism in Bacillus subtilis: vive la différence!* Molecular Microbiology, 1999. **32**(2): p. 223-232.

24. Green, V.E., et al., *The molecular mechanism for carbon catabolite repression of the chitin response in Vibrio cholerae.* PLoS Genet, 2023. **19**(5): p. e1010767.

25. Lin, C.T., et al., *Role of the cAMP-dependent carbon catabolite repression in capsular polysaccharide biosynthesis in Klebsiella pneumoniae.* PLoS One, 2013. **8**(2): p. e54430.

26. Pokorzynski, N.D. and E.A. Groisman, *How Bacterial Pathogens Coordinate Appetite with Virulence.* Microbiology and Molecular Biology Reviews, 2023. **87**(3): p. e00198-22.

27. Park, H., et al., *Pseudomonad reverse carbon catabolite repression, interspecies metabolite exchange, and consortial division of labor.* Cellular and Molecular Life Sciences, 2020. **77**(3): p. 395-413.

28. Pekkonen, M., T. Ketola, and J.T. Laakso, *Resource Availability and Competition Shape the Evolution of Survival and Growth Ability in a Bacterial Community.* PLOS ONE, 2013. **8**(9): p. e76471.

29. Williams, K.P., et al., *Phylogeny of gammaproteobacteria.* J Bacteriol, 2010. **192**(9): p. 2305-14.

30. Blount, Z.D., C.Z. Borland, and R.E. Lenski, *Historical contingency and the evolution of a key innovation in an experimental population of Escherichia coli.* Proceedings of the National Academy of Sciences, 2008. **105**(23): p. 7899-7906.

31. Hibbing, M.E., et al., *Bacterial competition: surviving and thriving in the microbial jungle.* Nat Rev Microbiol, 2010. **8**(1): p. 15-25.

32. Ayres, J.S., *Cooperative Microbial Tolerance Behaviors in Host-Microbiota Mutualism.* Cell, 2016. **165**(6): p. 1323-1331.

33. Leventhal, G.E., M. Ackermann, and K.T. Schiessl, *Why microbes secrete molecules to modify their environment: the case of iron-chelating siderophores.* J R Soc Interface, 2019. **16**(150): p. 20180674.

34. Suleman, M., et al., *Pyocins and Beyond: Exploring the World of Bacteriocins in Pseudomonas aeruginosa.* Probiotics Antimicrob Proteins, 2025. **17**(1): p. 240-252.

35. Kauffman, S.J., et al., *Genomic Diversification and Tailocin-Mediated Competition in Animal-Associated Xenorhabdus Bacteria.* ISME Communications, 2026.

36. Ge, Z.B., et al., *Two-tiered mutualism improves survival and competitiveness of cross-feeding soil bacteria.* Isme j, 2023. **17**(11): p. 2090-2102.

37. Bechtold, E.K., et al., *Metabolic interactions underpinning high methane fluxes across terrestrial freshwater wetlands.* Nature Communications, 2025. **16**(1): p. 944.

38. Consuegra, J., et al., *Metabolic Cooperation among Commensal Bacteria Supports Drosophila Juvenile Growth under Nutritional Stress.* iScience, 2020. **23**(6): p. 101232.

39. Rohmer, L., D. Hocquet, and S.I. Miller, *Are pathogenic bacteria just looking for food? Metabolism and microbial pathogenesis.* Trends Microbiol, 2011. **19**(7): p. 341-8.

40. Sharp, C. and K.R. Foster, *Host control and the evolution of cooperation in host microbiomes.* Nature Communications, 2022. **13**(1): p. 3567.

41. Douglas, A.E., *Symbiosis as a general principle in eukaryotic evolution.* Cold Spring Harb Perspect Biol, 2014. **6**(2).

42. Cornwallis, C.K., et al., *Symbioses shape feeding niches and diversification across insects.* Nat Ecol Evol, 2023. **7**(7): p. 1022-1044.

43. Passalacqua, K.D., M.-E. Charbonneau, and M.X.D. O'Riordan, *Bacterial Metabolism Shapes the Host-Pathogen Interface.* Microbiology spectrum, 2016. **4**(3): p. 10.1128/microbiolspec.VMBF-0027-2015.

44. Bustamante, V.H., et al., *HilD-mediated transcriptional cross-talk between SPI-1 and SPI-2.* Proceedings of the National Academy of Sciences, 2008. **105**(38): p. 14591-14596.

45. Hensel, M., et al., *The genetic basis of tetrathionate respiration in Salmonella typhimurium.* Mol Microbiol, 1999. **32**(2): p. 275-87.

46. Winter, S.E., et al., *Gut inflammation provides a respiratory electron acceptor for Salmonella.* Nature, 2010. **467**(7314): p. 426-9.

47. Tokuda, G., et al., *Fiber-associated spirochetes are major agents of hemicellulose degradation in the hindgut of wood-feeding higher termites.* Proc Natl Acad Sci U S A, 2018. **115**(51): p. E11996-e12004.

48. Murray, G.G.R., et al., *Genome Reduction Is Associated with Bacterial Pathogenicity across Different Scales of Temporal and Ecological Divergence.* Mol Biol Evol, 2021. **38**(4): p. 1570-1579.

49. McCutcheon, J.P. and N.A. Moran, *Extreme genome reduction in symbiotic bacteria.* Nature Reviews Microbiology, 2012. **10**(1): p. 13-26.

50. Feng, H., et al., *Trading amino acids at the aphid–Buchnera symbiotic interface.* Proceedings of the National Academy of Sciences, 2019. **116**(32): p. 16003-16011.

51. Chong, R.A., H. Park, and N.A. Moran, *Genome Evolution of the Obligate Endosymbiont Buchnera aphidicola.* Molecular Biology and Evolution, 2019. **36**(7): p. 1481-1489.

52. Blow, F., et al., *Impact of Facultative Bacteria on the Metabolic Function of an Obligate Insect-Bacterial Symbiosis.* mBio, 2020. **11**(4).

53. Koga, R., et al., *Single mutation makes Escherichia coli an insect mutualist.* Nat Microbiol, 2022. **7**(8): p. 1141-1150.

54. McClarty, G., H.D. Caldwell, and D.E. Nelson, *Chlamydial interferon gamma immune evasion influences infection tropism.* Current Opinion in Microbiology, 2007. **10**(1): p. 47-51.

55. Driscoll, T.P., et al., *Wholly Rickettsia! Reconstructed Metabolic Profile of the Quintessential Bacterial Parasite of Eukaryotic Cells.* mBio, 2017. **8**(5).

56. Barth, A.L. and T.L. Pitt, *Auxotrophic variants of Pseudomonas aeruginosa are selected from prototrophic wild-type strains in respiratory infections in patients with cystic fibrosis.* J Clin Microbiol, 1995. **33**(1): p. 37-40.

57. Seif, Y., et al., *Metabolic and genetic basis for auxotrophies in Gram-negative species.* Proc Natl Acad Sci U S A, 2020. **117**(11): p. 6264-6273.

58. Maurelli, A.T., et al., *"Black holes" and bacterial pathogenicity: a large genomic deletion that enhances the virulence of Shigella spp. and enteroinvasive Escherichia coli.* Proc Natl Acad Sci U S A, 1998. **95**(7): p. 3943-8.

59. Moreau, P.L., *The lysine decarboxylase CadA protects Escherichia coli starved of phosphate against fermentation acids.* J Bacteriol, 2007. **189**(6): p. 2249-61.

60. Patrick, S., *A tale of two habitats: Bacteroides fragilis, a lethal pathogen and resident in the human gastrointestinal microbiome.* Microbiology (Reading), 2022. **168**(4).

61. Smith, T.E. and N.A. Moran, *Coordination of host and symbiont gene expression reveals a metabolic tug-of-war between aphids and Buchnera.* Proc Natl Acad Sci U S A, 2020. **117**(4): p. 2113-2121.

62. Goodrich-Blair, H. and D.J. Clarke, *Mutualism and pathogenesis in Xenorhabdus and Photorhabdus: two roads to the same destination.* Molecular Microbiology, 2007. **64**(2): p. 260-268.

63. Cowles, C.E. and H. Goodrich-Blair, *The Xenorhabdus nematophila nilABC genes confer the ability of Xenorhabdus spp. to colonize Steinernema carpocapsae nematodes.* J Bacteriol, 2008. **190**(12): p. 4121-8.

64. McMullen, J.G., 2nd, et al., *Fitness costs of symbiont switching using entomopathogenic nematodes as a model.* BMC Evol Biol, 2017. **17**(1): p. 100.

65. Martens, E.C., K. Heungens, and H. Goodrich-Blair, *Early colonization events in the mutualistic association between Steinernema carpocapsae nematodes and Xenorhabdus nematophila bacteria.* J Bacteriol, 2003. **185**(10): p. 3147-54.

66. Stilwell, M.D., et al., *Studying the Symbiotic Bacterium Xenorhabdus nematophila in Individual, Living Steinernema carpocapsae Nematodes Using Microfluidic Systems.* mSphere, 2018. **3**(1).

67. Grewal, P.S., *Anhydrobiotic potential and long-term storage of entomopathogenic nematodes (Rhabditida: Steinernematidae).* International Journal for Parasitology, 2000. **30**(9): p. 995-1000.

68. Mitani, D.K., H.K. Kaya, and H. Goodrich-Blair, *Comparative study of the entomopathogenic nematode, Steinernema carpocapsae, reared on mutant and wild-type Xenorhabdus nematophila.* Biological Control, 2004. **29**(3): p. 382-391.

69. Emelianoff, V., et al., *Effect of bacterial symbionts Xenorhabdus on mortality of infective juveniles of two Steinernema species.* Parasitology Research, 2007. **100**(3): p. 657-659.

70. Snyder, H., et al., *New insights into the colonization and release processes of Xenorhabdus nematophila and the morphology and ultrastructure of the bacterial receptacle of its nematode host, Steinernema carpocapsae.* Appl Environ Microbiol, 2007. **73**(16): p. 5338-46.

71. Flores-Lara, Y., et al., *Influence of nematode age and culture conditions on morphological and physiological parameters in the bacterial vesicle of Steinernema carpocapsae (Nematoda: Steinernematidae).* J Invertebr Pathol, 2007. **95**(2): p. 110-8.

72. Martens, E.C., F.M. Russell, and H. Goodrich-Blair, *Analysis of Xenorhabdus nematophila metabolic mutants yields insight into stages of Steinernema carpocapsae nematode intestinal colonization.* Mol Microbiol, 2005. **58**(1): p. 28-45.

73. Cowles, K.N. and H. Goodrich-Blair, *Expression and activity of a Xenorhabdus nematophila haemolysin required for full virulence towards Manduca sexta insects.* Cell Microbiol, 2005. **7**(2): p. 209-19.

74. Sicard, M., et al., *Stages of infection during the tripartite interaction between Xenorhabdus nematophila, its nematode vector, and insect hosts.* Appl Environ Microbiol, 2004. **70**(11): p. 6473-80.

75. Casanova-Torres, A.M., et al., *The Global Transcription Factor Lrp Is both Essential for and Inhibitory to Xenorhabdus nematophila Insecticidal Activity.* Appl Environ Microbiol, 2017. **83**(12).

76. Bashey, F., H. Hawlena, and C.M. Lively, *Alternative paths to success in a parasite community: within-host competition can favor higher virulence or direct interference.* Evolution, 2013. **67**(3): p. 900-7.

77. Richards Gregory, R. and H. Goodrich-Blair, *Examination of Xenorhabdus nematophila Lipases in Pathogenic and Mutualistic Host Interactions Reveals a Role for xlpA in Nematode Progeny Production.* Applied and Environmental Microbiology, 2010. **76**(1): p. 221-229.

78. Jubelin, G., et al., *Studies of the dynamic expression of the Xenorhabdus FliAZ regulon reveal atypical iron-dependent regulation of the flagellin and haemolysin genes during insect infection.* Environ Microbiol, 2011. **13**(5): p. 1271-84.

79. Mucci, N.C., et al., *Chemical ecology of an apex predator life cycle.* bioRxiv, 2021: p. 2021.02.13.430781.

80. Singh, S., et al., *Role of secondary metabolites in establishment of the mutualistic partnership between Xenorhabdus nematophila and the entomopathogenic nematode Steinernema carpocapsae.* Appl Environ Microbiol, 2015. **81**(2): p. 754-64.

81. Engel, Y., et al., *The Global Regulators Lrp, LeuO, and HexA Control Secondary Metabolism in Entomopathogenic Bacteria.* Front Microbiol, 2017. **8**: p. 209.

82. Mucci, N.C., et al., *Apex Predator Nematodes and Meso-Predator Bacteria Consume Their Basal Insect Prey through Discrete Stages of Chemical Transformations.* mSystems, 2022. **7**(3): p. e0031222.

83. San-Blas, E., S.R. Gowen, and B. Pembroke, *Steinernemafeltiae: Ammonia triggers the emergence of their infective juveniles.* Experimental Parasitology, 2008. **119**(1): p. 180-185.

84. Neubacher, N., et al., *Symbiosis, virulence and natural-product biosynthesis in entomopathogenic bacteria are regulated by a small RNA.* Nat Microbiol, 2020. **5**(12): p. 1481-1489.

85. Lam, Y.C., et al., *The Xenorhabdus nematophila LrhA transcriptional regulator modulates production of γ-keto-N-acyl amides with inhibitory activity against mutualistic host nematode egg hatching.* Appl Environ Microbiol, 2024. **90**(7): p. e0052824.

86. Richards, G.R., et al., *Isolation and characterization of Xenorhabdus nematophila transposon insertion mutants defective in lipase activity against Tween.* J Bacteriol, 2009. **191**(16): p. 5325-31.

87. Holdbrook, R., et al., *Nutribloods: Novel synthetic lepidopteran haemolymphs for understanding insect–microbe nutritional interactions in vitro.* Physiological Entomology, 2025. **50**(3): p. 264-276.

88. Cao, M. and H. Goodrich-Blair, *Xenorhabdus nematophila bacteria shift from mutualistic to virulent Lrp-dependent phenotypes within the receptacles of Steinernema carpocapsae insect-infective stage nematodes.* Environ Microbiol, 2020. **22**(12): p. 5433-5449.

89. Heungens, K., C.E. Cowles, and H. Goodrich-Blair, *Identification of Xenorhabdus nematophila genes required for mutualistic colonization of Steinernema carpocapsae nematodes.* Mol Microbiol, 2002. **45**(5): p. 1337-53.

90. Cao, M., et al., *High Levels of the Xenorhabdus nematophila Transcription Factor Lrp Promote Mutualism with the Steinernema carpocapsae Nematode Host.* Appl Environ Microbiol, 2017. **83**(12).

91. Hussa, E.A., A.M. Casanova-Torres, and H. Goodrich-Blair, *The Global Transcription Factor Lrp Controls Virulence Modulation in Xenorhabdus nematophila.* J Bacteriol, 2015. **197**(18): p. 3015-25.

92. Cowles, K.N., et al., *The global regulator Lrp contributes to mutualism, pathogenesis and phenotypic variation in the bacterium Xenorhabdus nematophila.* Cell Microbiol, 2007. **9**(5): p. 1311-23.

93. Hart, B.R. and R.M. Blumenthal, *Unexpected coregulator range for the global regulator Lrp of Escherichia coli and Proteus mirabilis.* J Bacteriol, 2011. **193**(5): p. 1054-64.

94. Chen, C.F., et al., *Metabolic regulation of lrp gene expression in Escherichia coli K-12.* Microbiology (Reading), 1997. **143 (Pt 6)**: p. 2079-2084.

CHAPTER 2: *XENORHABDUS* BACTERIA HAVE VARIABLE LAG TIMES IN AMINO ACID-DEFICIENT GROWTH CONDITIONS THAT ARE LINKED TO METABOLIC DEMAND FOR METHIONINE

Authors: Cameron Moore and Heidi Goodrich-Blair

Author Contributions

I developed the methodology and performed all experimental and computational analyses presented in this chapter, except for the generation of synteny maps and the coding required to generate the whole genome *Xenorhabdus* phylogeny. I also contributed to project conceptualization, statistical analysis, and writing the manuscript.

Heidi Goodrich-Blair secured funding and contributed to project conceptualization, manuscript editing and writing, and generated the synteny maps presented in this chapter.

Alex Truchon, who is credited in the acknowledgements section, contributed to the coding required to generate the whole genome *Xenorhabdus* phylogeny.

ABSTRACT

Lag phase is the time required for microorganisms to recognize and respond to nutritional shifts in their environment and initiate cell proliferation. *Xenorhabdus* bacteria experience major shifts in nutrients during their entomopathogenic lifecycle where they transition between *Steinernema* nematode and insect host niches. We investigated how *Xenorhabdus* respond to nutrient shifts by assaying the growth of these bacteria when transitioning from nutrient rich into nutrient-limiting growth conditions. We determine that *Xenorhabdus* exhibit variable lag phase lengths (e.g. long, intermediate, or short) when transitioned into amino-acid-deficient media that are responsive to the addition of the aspartate-derived amino acids (Asp, Lys, Met, Thr), namely Met. These data suggest that metabolic demand for Met governs the length of time *Xenorhabdus* spend in lag phase when grown in amino acid limiting growth conditions. While there was not an apparent association between these lag length phenotypes and the bacterial phylogeny, comparative genomic analyses revealed predictors of prolonged or shortened lag among *Xenorhabdus* species. Our data suggest that this physiology may be due to niche-specific adaption, and we hypothesize that this is linked to the specific interactions among *Xenorhabdus* and their *Steinernema* hosts.

INTRODUCTION

Bacteria experience dynamic fluctuations in nutrient availability in their natural environments and must optimize their physiology to assimilate available exogenous resources and resume exponential growth in a transient phase of population growth denoted as lag phase (1, 2). The length of lag phase can be influenced by a multitude of factors (e.g. bacterial population history, population size, temperature, pH, and environmental insults) but adaptation to accessible nutrients represents the most fundamental determinant of a bacterium's lag time (1). Many types of nutritional shifts have been described in *E.* coli and have variable influences on lag time. Classically, *E. coli* experiences a diauxic shift, often denoted as a growth lag, when cultivated in the presence of two or more carbon sources where the duration of the diauxie reflects the time required for the cells to acclimate to a less preferred carbon source (3). Experimental studies investigating *E. coli* transitions between carbon sources have revealed that lag phase can be subdivided into two phases: 1) bacterial cells grow in biomass and upregulate genes involved in the catabolism of the available carbon source and 2) bacterial cells begin proliferating and upregulate genes involved in cell growth, biosynthetic metabolism, and division (2). Lag time can also depend on the type of carbon-to-carbon transition faced by a bacterium. For example, the aforementioned studies focused on transitions between glycolytic, PTS (phosphotransferase) regulated carbon sources. Although the initial steps of these carbon source's catabolism varies, metabolic flux will ultimately move through glycolysis. Contrastingly, shifts from glycolytic to a gluconeogenic carbon source (e.g. glucose to acetate), requires a complete reversal in metabolic flux that temporarily diminishes

metabolite pools in early glycolysis creating a metabolic bottleneck that impedes growth initiation until the stoichiometric ratios of the carbon metabolism are restored (4). Depletion of these early glycolytic metabolite pools during this carbon-to-carbon shift also impedes the rate of translation as many of these metabolic intermediates serve as precursors to other essential growth factors like nucleic and amino acids; therefore, supplementation of these molecules can alleviate this bottleneck and reduce the lag time of *E. coli* (4). Indeed, carbon-to-carbon shifts do not solely represent the changes bacteria experience as much broader feast to famine shifts can occur where the abundance of exogenous growth factors can impact bacterial adaptation time. For example, in conditions where amino acids are replete, the majority of the *E. coli* cell protein content is associated with protein synthesis (5). When cells are introduced into amino acid deficient conditions, the abundances of protein synthesis machinery diminishes as the proportion of amino acid biosynthetic enzymes increases sequentially based on the metabolic demands of the cells and thus elongates the time required to initiate exponential growth (5). The extent of bacterial lag can be elongated by the presence of external growth factors such as the nucleobase adenine which inhibits nucleotide biosynthetic processes and causes a stall in bacterial growth until the metabolic block can be overcome (6). The impact of nutritional shifts on bacterial lag phase and the mechanisms underlying these shifts have been well-studied in a limited array of bacteria namely bacterial models used in systems biology and/or human-relevant pathogens (1-4, 7-9). To this end, we lack a broader understanding of how bacteria overcome nutritional shifts the physiological relevance of these adaptation in their ecological context.

Most, if not all, bacteria are thought to persist in natural environments in a stationary phase-like state where they are subject to famine conditions as well as exogenous stressors (10). When nutrient conditions become amenable for bacteria to proliferate again, the length of a bacterium's lag phase can be adaptive in situations where unique biotic and abiotic pressures may enhance or impede growth resumption (1). For example, invasive serotypes of the human pathogen *Streptococcus pneumoniae* experience a prolonged lag phase in nutrient-rich media relative to nasopharynx-colonizing serotypes as they produce larger quantities of extracellular capsule, a trait that is advantageous for evading human host immunity but necessitates a reduction in proliferation (11, 12). Likewise, the lag time of the marine, bacterium *Phaeobacter inhibens* is reduced via the assimilation of methylated compounds produced by its algal partner *Emiliana huxleyi* which can allow this organism to exploit an ecologically abundant nutrient source and potentially outcompete other marine microorganisms (13). Supported by these aforementioned examples, a bacterium's optimal lag time is context dependent and alterations in lag duration is associated with the amount of predictability or stochasticity a bacterium faces in its natural environment (3). Augmentation of a bacterium's lag time is also subject to physiological trade-offs where the energetic investment of a faster lag leads to less efficacious growth, while slower adaptation reduces energetic costs and promotes robust growth (3). Given that nutrient abundance can fluctuate predictably or stochastically, we can infer that bacterial lag times have evolved in response to these pressures in order to optimize fitness in particular niche(s).

Bacteria of the clade *Xenorhabdus* present a unique opportunity by which to study bacterial adaption to fluctuations in environmental nutrients as they are transmitted between two nutritionally distinct animal host environments: entomopathogenic *Steinernema* nematodes and insects (14, 15). The *Xenorhabdus*-*Steinernema* association is mutualistic, and these organisms have evolved species or strain-level partnerships that are co-adapting and co-evolving (16, 17). *Xenorhabdus* colonize the anterior intestinal region of *Steinernema* nematodes across multiple life stages and are eventually vectored by infective juvenile (IJ) stage nematodes to naive insect hosts (17-19). The IJ stage is considered nutrient-limiting as acquisition of exogenous nutrients is impaired by the formation of a protective double cuticle that occludes the organism's natural openings (20). Given this limitation, both the *Steinernema* IJ and its *Xenorhabdus* symbiont must rely on endogenous nutrient reserves in order to persist together in the soil. During this stage, the bacteria are restricted to a specialized tissue of their nematode host called the receptacle and here *Xenorhabdus* can proliferate and persist for extended periods of time (18). For example, *X. nematophila* can grow at a rate of 0.085 hr^{-1} within the IJ receptacle and can reach levels around 500 bacterial cells per *S. carpocapsae* nematode (21). In order to achieve these levels *in vivo*, *X. nematophila* must synthesize essential growth factors such as amino acids **(**Thr, Met, Leu, Trp, Tyr, and Phe**) ,** vitamins (pyroxidine, p-aminobenzoic acid), and nucleobases (thymine and uracil) (22-24). *Xenorhabdus* are essential cargo for their nematode host as they are robust insect pathogens and within the insect host niche they additionally serve as the primary food source of their *Steinernema* host (25-27). During early infection, *Xenorhabdus* are released into the blood cavity of their insect host

and proliferate on nutrients derived from the insect hemolymph, growing at a rate of 0.41 hr^{-1} (20, 28, 29). Recent work has identified that optimal population growth in synthetic hemolymph is largely associated with utilization of carbohydrates and free amino acids (29). After killing their insect host, *Xenorhabdus* employ an arsenal of degradative enzymes to liberate bioavailable nutrients from the insect tissue (27, 30-33). This ultimately leads to stage-specific nutritional shifts where metabolites involved in central carbon, amino acid, and nucleotide metabolism fluctuate from infection initiation to IJ development and emergence (25). Taken together, it is likely that the ability of *Xenorhabdus* bacteria to adapt and grow within insect or nematode host niches is dependent upon the unique nutrient composition of each host environment.

In this report, we investigated how *Xenorhabdus* adapt to nutrient limitation and initially hypothesized that one or more of the aforementioned nutrient groups (e.g, carbohydrates, amino acids, nucleobases, and vitamins) significantly altered the growth dynamics of these bacteria. Growth assays in chemically defined media revealed that the absence of aspartate-derived amino acids (ADAA, Asp, Lys, Thr, and Met) prolonged the lag time of *X. nematophila* when grown in amino acid deficient growth conditions. While a few *Xenorhabdus* species exhibited similar physiology to *X. nematophila*, we observed variable lag times across the clade when grown under similar conditions. Of the ADAA, Met had the most significant reductive impact on the lag time of the majority of *Xenorhabdus* bacteria including *X. nematophila.* This suggested that *Xenorhabdus* species experience differential metabolic demand for Met that contributes to their variable lag lengths in amino acid limited growth conditions. Using phylogenetics and comparative

genomics, we determine that the prolonged lag phenotype seen in some *Xenorhabdus* is not likely associated with the evolutionary emergence of *Xenorhabdus* bacteria and may instead be driven by niche-specific adaptation to one or more of their host conditions.

MATERIALS AND METHODS

Bacteria and Growth Conditions

The bacteria utilized in this study are shown in **Table 1.** All *Xenorhabdus* were grown at 30˚C. For *Xenorhabdus* growth, Luria-Bertani (LB) medium was supplemented with 0.1% sodium pyruvate (agar plates) or kept in the dark (liquid) to protect cells from reactive oxygen species generated by exposure to natural light (80). Bacteria were revived from frozen stocks by inoculation and overnight growth on LB agar plates, that were then used as the source for inoculation into LB liquid medium for overnight growth with aeration (56 rpm; New Brunswick Scientific). All defined media used in this study were described previously (81). Briefly, both the rich, defined medium (RDM) and minimal media (MM) were buffered with 3-(N-morpholino)- propanesulfonic acid (40 mM, MOPS, MP Biomedicals), contained glucose as a primary source of carbon (11 mM, Fisher Scientific), and had ammonium sulfate as the primary source of nitrogen (9.5 mM, Fischer Scientific), unless stated otherwise. The final concentrations of all medium components and nutritional supplements are provided in **JBac_DefinedMediumComponents_6_23_26.xlsx.** The amino acids aspartate (Thermo Fisher), lysine (Thermo Fisher), and threonine (Thermo Fisher) were added to media as supplements at a final concentration of 0.4 mM each and methionine (Sigma Aldrich) was

added at a final concentration of 0.2 mM. All defined media were sterilized using a 0.22 μm pore filter (Avantor).

Growth Curve Assays

The OD_{600} of overnight LB cultures was measured on a Genesys 50 spectrophotometer (Thermo Fisher). Cultures were then normalized to an OD_{600} of 1.0, washed three times with 1X PBS, and diluted to an OD_{600} of 0.01 into sterile media, unless stated otherwise. For 96-well plate assays, cells were grown with double orbital shaking (282 cycles per min) in a total volume of 250 μL of media in a Synergy H1 plate reader (Agilent). The plate reader was programmed to measure OD_{600} every 0.25 h. For growth in 17x100 mm, disposable culture tubes (hereafter, test tubes), 5 mL of cultures were grown in a cell rotator (New Brunswick Scientific) at 56 rpm. For cultures in baffled, Erlenmeyer flasks, 50 mL of culture were grown in a chest incubator (New Brunswick Scientific) at 200 rpm. All growth data were blanked using OD_{600} readings measured from a sterile media control. If negative values were calculated after blanking the OD_{600} readings, during data analysis, the lowest negative number in the dataset was identified, and an additional 0.0001 was added to the absolute value of the lowest number. The combined total (e.g, absolute value + 0.0001) was added to all the data points in the dataset so that they could be plotted logarithmically. To assess viable cell counts during growth, samples (2.5 μL, 200 μL, and 2 mL from 96-well, test tube, and flask cultures, respectively) were taken from cultures every 12 h, serial diluted in 1X PBS and plated on LB agar for colony counts.

Table 2.1: Bacterial strains utilized in this study.

Bacterial Genotype	HGB Stock	Cognate Nematode Host
X. nematophila ATCC19061	HGB800	*S. carpocapsae*
X. nematophila ATCC19061	HGB007	*S. carpocapsae*
X. nematophila ATCC19061 2˚ Form	HGB1061	*S. carpocapsae*
X. nematophila ATCC19061 2˚ Form	HGB1056	*S. carpocapsae*
X. nematophila AN6/1	HGB081	*S. carpocapsae*
X. nematophila F1	HGB1849	*S. carpocapsae*
X. nematophila Websteri	HGB1419	*S. websteri*
X. nematophila Anatoliense	HGB1418	*S. anatoliense*
X. bovienii-Sf-FL	HGB1699	*S. feltiae* - FL
X. bovienii-Sa-IN-78	HGB1738	*S. affine* – IN - 78
X. cabanillasii	HGB2490	*S. riobrave*
X. innexi	HGB1681	*S. scapterisci*
X. szentirmaii	HGB0836	*S. rarum*
X. miraniensis	HGB2240	Unknown
X. beddingii ATCC 49542	HGB084	*S. longicaudum*
X. poinarii ATCC 49121	HGB086	*S. glaseri* and *S. cubanum*
X. doucetiae	HGB1413	*S. diaprepesi*
X. griffiniae	HGB2511	*S. hermaphroditum*
X. ehlersii	HGB834	*S. longicaudum*
X. thuongxuanensis	HGB2382	*S. sangi*
P. laumondii TT01	HGB801	*H. bacteriophora*
P. mirabilis	HGB0994	n/a
E. coli MG1655	HGB1006	n/a

Growth Dynamics Determinations and Statistical Analyses

To determine the lag time and average growth rate for each generated curve, we utilized the following equation to calculate the rate of growth (μ, hr^{-1}) between consecutive times points: $\mu = \ln (OD_2/OD_1)/T_2-T_1)$ (82)**.** This calculation was done for all consecutive pairs of data points from the initiation to the termination of each growth curve. The end of lag phase was considered the time for which this calculated growth rate was greater than 0 for three timepoints in a row after inoculation indicating the initiation of exponential growth phase. The end of exponential growth phase was determined when the growth rate was consistently less than or equal to 0 for three consecutive timepoints. The average exponential growth rate was taken for all data points between the termination of lag phase and the initiation of stationary phase. Maximum OD_{600} was determined using the 'maximum function' in Microsoft Excel for each growth curve. Growth curves were plotted and analyzed statistically (Student's t-tests and One-Way ANOVA) in GraphPad Prism version 10.6.1.

Assessing for the growth of a mutant sub-population for shortened lag

To determine if a mutant sub-population of *X. nematophila* was responsible for the shortened lag phase phenotype rather than the whole population, cells were allowed to reach stationary phase and then re-inoculated in the same media to determine if lag time was altered. Wild-type *X. nematophila* was grown in 5 mL LB cultures in biological triplicate to create inoculum cultures. Upon reaching stationary phase, cells were washed and diluted into LB, MM + Glucose (GMM), or GMM + Aspartate, Threonine, Lysine, and Methionine (GMM+ADAA). The remaining inoculum was stored at -80˚C. The LB,

GMM, and GMM+ADAA sub-cultures were grown to stationary phase ($OD_{600} \geq 0.9$, 12 – 144 h depending on the media condition) before harvesting and storage at -80˚C, hereafter referred to as passaged. To determine if a sub-population had grown resulting in a shortened lag time, inoculum and passaged cells were revived, prepared, and grown in the tested media for 168 h in a 96-well plate. The lag time of each biological replicate under each growth condition was determined as described above and the change in lag time (Δlag) was calculated by subtracting the lag time of the passaged cells from the lag time of the inoculum cells. A $\Delta\text{lag} \leq 0$ was interpreted to mean that a shortened lag phenotype had not arisen from a mutant sub-population, while a $\Delta\text{lag} > 0$ indicated the passaged cells displayed shortened lag relative to the original wild-type inoculum. A shorter lag time for the passaged cells relative to inoculum cells was interpreted as support for the idea that passaged cells were merely a mutant sub-population that were adapted for growth in that medium. The experiment was repeated three times, and the average change in lag for each biological replicate, in each growth condition, was calculated.

Comparative Genomics

Forward BLASTp (83) queries and Reciprocal Best Hits (RBH) analyses were conducted in MicroScope MaGe (84) and Galaxy v.0.1.5 (85), respectively. For the forward analyses, amino acid query sequences were aligned against the tested *Xenorhabdus* genomes. Putative orthologs were selected based on sequence identity (≥ 40%) and query length (≥ 50%). RBH analysis was used to confirm orthology. Protein sequence orthology was confirmed via RBH analysis using the same sequence parameters mentioned above.

The data summarizing the results of these searches are presented in **JBac_SupplementalSequenceAlignmentData_ForwardAndRBH_6_23_26.xlsx.**

Phylogenetic Tree Generation

Phylogenetic analyses were performed as described previously to determine the relatedness of *Xenorhabdus, Photorhabdus, Proteus,* and *Escherichia* species (16, 51). The genomes were compared using MicroScope MaGe Gene Phyloprofile to identify conserved, non-paralogous gene homologs (984 homolog sets in total) (84). Homolog sets were individually aligned using MAFFT v7.490 (86, 87), concatenated using Sequence Matrix v1.8 (88) and trimmed nucleotide gaps using TrimAL v1.3 (89). To construct a phylogeny of Met-metabolism associated protein orthologs, the protein sequences of *Xenorhabdus* MetB, MetC, MetY, MtcC, and the MtcC-like orthologs were downloaded from MicroScope Mage and aligned in Geneious Prime v 2026.0.2 (https://www.geneious.com) using MUSCLE v5.1 (90). Phylogenetic tree construction was performed via IQ-Tree 2 v2.4.0 (91) using ultrafast bootstrap analysis (1000 replicates) (92). ModelFinder was used to determine that GTR+F+I+R6 was the appropriate substitution model for maximum likelihood analysis for the whole genome analysis and LG+R5 was the appropriate model for the maximum likelihood analysis of the protein orthologs (93). Results from both analyses were visualized and edited using Interactive Tree of Life v7.5 (94) and nodes with less than 80% bootstrap support were collapsed. The phylogenetic tree of the whole-genome analysis is shown in **Supplemental Figure 4**, while a cladogram of these data is presented in **Figure 5.** The phylogeny of the Met-metabolism protein orthologs is presented in **Supplemental Figure 5**.

RESULTS

Wild-type *X. nematophila* exhibits a prolonged lag phase in aspartate-derived amino acid deficient growth conditions.

We first sought to identify the effects of specific subsets of nutrients (e.g., glucose, amino acids, nucleobases, vitamins, and nicotinic acid) on the population-level growth dynamics of *X. nematophila* using formulations of rich-defined medium (RDM) where each of these nutrient groups were absent **(Figure 2.1A)**. Six biological replicates of *X. nematophila* were grown in each of these conditions at 30˚C for 24 h. After a 1.92 h (± 0.44) lag phase, *X. nematophila* grew at an average rate of 0.34 hr^{-1} (± 0.03) and reached a maximum OD_{600} of 0.61 (± 0.06) in the standard RDM (**JBac_SupplementalGrowthDynamics_6_23_26.xlsx**). Growth was observed in all nutrient-deficient conditions except for the amino acid deficient condition, which had a maximum OD_{600} of 0.02 and was significantly different from all the other tested conditions (± 0.002; $p < 0.0001$, One-Way ANOVA, Tukey's HSD). While significant alterations in *X. nematophila* growth dynamics were observed in the absence of the other nutrients relative to replete RDM conditions, the absence of the amino acids had the most profound effect on *X. nematophila* growth. This phenotype was unexpected given that *X. nematophila* still had access to sources of carbon, nitrogen, and sulfur in the RDM and is prototrophic for all twenty of the supplemented amino acids (**Figure 2.1CD,** 28, 34, 35).

To identify if specific amino acids could improve growth of *X. nematophila* in amino acid deficient RDM, we conducted amino acid auxanography (**Figure 2.1B**). Briefly, groups of amino acids were pooled together based on their shared metabolic

pathways (11 in total) and the majority of tested amino acids, excluding alanine, were represented twice across the pools (36). *X. nematophila* growth was assessed in each condition via maximum OD_{600} after a 24 h incubation at 30˚C and compared to an amino acid replete control (**Figure 2.1B**). In amino-acid-replete RDM, all eight biological replicates grew by 24 h, reaching an average maximum OD_{600} of 0.53 (± 0.04; **Figure 2.1B**). The maximum OD_{600} of *X. nematophila* in all auxanography pools after 24 h was significantly lower than in the amino acid replete condition ($p < 0.0001$, One-way ANOVA, Tukey's HSD). The aspartate-derived amino acids (ADAA; Asp, Thr, Lys, and Met) pool consistently supported modest growth of *X. nematophila* across the eight replicates, reaching a maximum OD_{600} of 0.19 (± 0.03; **Figure 2.1B**). *X. nematophila* growth in the ADAA supplemented condition was significantly higher than the other ten auxanography pools indicating that these four amino acids were sufficient to stimulate growth in RDM ($p < 0.0001$, One-way ANOVA, Tukey's HSD). In traditional auxanography, disruption of a single biosynthetic pathway generally results in bacterial growth in at least two auxanography pools. Growth was not observed in the additional pools containing Lys and Met, but growth among a few biological replicates was observed in three additional pools, including those that contained Asp and Thr (**Figure 2.11B**). Overall, the auxanography data clearly point to the ADAA as enhancing growth under amino acid deficient RDM conditions. Interpretation of the lack of reproducible observable growth in other conditions (e.g., pools containing Met and Cys) is prevented by two limitations of the assay: that some conditions may require more than 24 h (the endpoint of the assay) to yield observable growth and that the presence of an inhibitory amino acid in

some combinations could mask the positive impacts of other amino acids. For example, *E. coli* is sensitive to elevated exogenous and endogenous L-cysteine (Cys) as it can increase sensitivity to hydrogen peroxide and disrupt metabolic processes, like threonine biosynthesis (37, 38). If these phenomena are conserved in *X. nematophila* then supplementation of Cys with Met may impede our ability to assess the impact of Met on growth under amino acid limiting conditions. Furthermore, amino acid-deficient RDM still contains vitamins and nucleobases, which could have growth inhibitory impacts on *X. nematophila* (39, 40).

To address these limitations, we next assessed the impact of the ADAA on *X. nematophila* growth by monitoring both OD_{600} (**Figure 2.1C**) and colony forming units (CFU; **Figure 2.1D**) in glucose minimal medium (GMM; **Figure 2.1CD**) a condition which lacks the amino acids, vitamins, and nucleobases unlike the RDM. In GMM, *X. nematophila* population growth, as indicated by an increase in OD_{600} and CFU, began around 45-48 h post-inoculation and continued to increase until both experiments were terminated. By contrast, GMM supplemented with the ADAA or all twenty of the amino acids displayed significantly shorter lag time (14.5 ± 2.57 h, $p = 0.0001$, GMM+ADAA, 2.0 ± 1.73 h, $p < 0.0001$, GMM+AA) relative to no supplementation (One-way ANOVA, Tukey's HSD). This pattern held true regardless of the culture vessel (96-well, tube, or flask) or volume utilized to culture *X. nematophila* (**Figure 2.1D**).

We also investigated whether the eventual observed growth in GMM was the result of wild-type *X. nematophila* dividing after a long, population-wide lag, or due to the eventual rise of a minority mutant population of cells (**Figure 2.8)**. The former scenario is

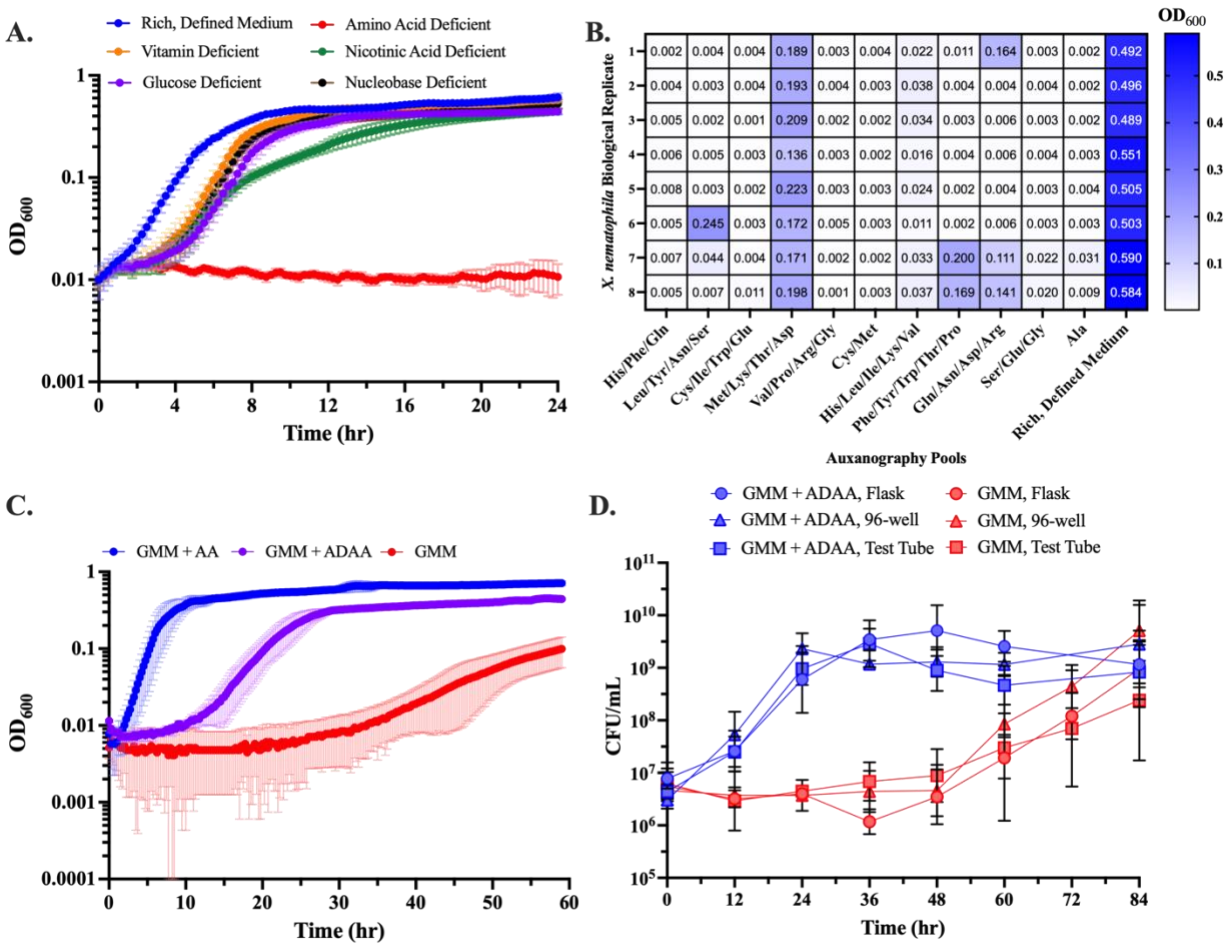


Figure 2.1: The aspartate-derived amino acids (ADAA; Asp, Met, Thr, and Lys) improve growth of *X. nematophila* in defined media.

A) Growth (OD_{600}) of *X. nematophila* in replete rich, defined medium (RDM) (blue line) or RDM lacking specific classes of nutrients (vitamins, orange; glucose, purple; amino acids, red; nicotinic acid, green; nucleobases, black). **B)** Maximum growth yield (OD_{600}) of *X. nematophila* after 24 h incubation in replete RDM (right column) or amino-acid-deficient RDM supplemented with auxanography pools comprising nutrients listed at the bottom of each column. **C)** Growth (OD_{600}) of *X. nematophila* in glucose minimal medium (GMM) with either the twenty, proteinaceous amino acids (AA) or with a pool of ADAA. **D)** Viable cell counts of *X. nematophila* in GMM with (blue) or without (red) the ADAA over an 84-h time course. The growth vessel type utilized is denoted based on shape: 96-well plate (triangle), test tube (square), and baffled flask (circle).

predicted to have relatively stable lag phase length for both naive and passaged cells, while the latter scenario is predicted to result in shorter lag phase length in cells that have been passaged. In all tested media passaged cells exhibited the same (GMM+ADAA and LB), or longer (GMM) lag phase as the initial inoculum suggesting that indeed wild-type *X. nematophila* cells are growing in GMM. Taken together, these growth assays demonstrate that wild-type *X. nematophila* can grow in the absence of the amino acids but exhibit a prolonged lag phase that is responsive to supplementation of the ADAA.

***X. nematophila* is predicted to synthesize the aspartate-derived amino acids similar to other *Enterobacterales*.**

We next considered the possibility that, despite being prototrophic for the ADAA, some aspect of the ADAA pathway in *X. nematophila* may be distinct from other well-characterized members of the *Enterobacterales* like *E. coli* MG1655. Using a forward and reciprocal BlastP approach, we searched the *X. nematophila* ATCC19061 genome for homologs of the functionally characterized *E. coli* MG1655 ADAA pathway protein sequences (**Figure 2.2**). The initial branch of the ADAA pathway converts oxaloacetate to aspartate, which is then used as a precursor for the synthesis of Lys, Thr, and Met. In *E. coli*, the early steps of the pathway (oxaloacetate to L-aspartate-semialdehyde) are catalyzed by the enzymes AspC, ThrA, MetL, LysC, and Asd (41-43) for which we found an ortholog for each enzyme in the *X. nematophila* genome. Similarly, the Lys and Thr branches both appear to be reciprocally conserved with respect to *E. coli* enzyme orthologs found in *X. nematophila*. This included the presence of ThrA and The shared sequence similarity between XNC1_1035 and *E. coli* MG1655 MetB suggested that this putative

enzyme may have function in some aspect of *X. nematophila* Met metabolism, though this warranted further interrogation. We also found that *X. nematophila* lacks an ortholog of *E. coli* MalY. Since MalY has functional redundancy to MetC (46) in *E. coli*, its absence is not predicted to impact Met prototrophy in *X. nematophila.* Other *E. coli* enzymes such as MetH and MmuM, that can also catalyze reactions in the final steps of Met biosynthesis (**Figure 2.2**, 44), were not identified. MetE, the cobalamin-independent methionine synthase, is sufficient to engender methionine prototrophy in *E. coli*, though it exhibits reduced enzymatic activity compared to the cobalamin-dependent MetH (47). Taken together with our growth data, we have strong evidence that the Lys, Thr, and Met biosynthesis pathways are likely functional in *X. nematophila*; however, the regulation or efficiency of these pathways in amino acid limiting growth conditions remain unclear.

Utilization of Asp as a nitrogen source, but not a carbon source, modestly impacts *X. nematophila* lag time in minimal medium.

Based on the *in vitro* growth data (**Figure 1)** and comparative genomic data (**Figure 2**), we considered that the prolonged lag phase of *X. nematophila* may be caused by insufficient flux through the ADAA pathway. An alternative explanation was that one or more of the ADAA may serve as a preferential source of carbon or nitrogen. To address these possibilities, we first monitored *X. nematophila* growth in minimal media supplemented with the individual ADAA or glucose as carbon sources. Note that the concentration of all tested carbon sources in the minimal medium were added at 11mM. Only Asp, but not Lys, Thr, or Met, was sufficient to support *X. nematophila* growth as a

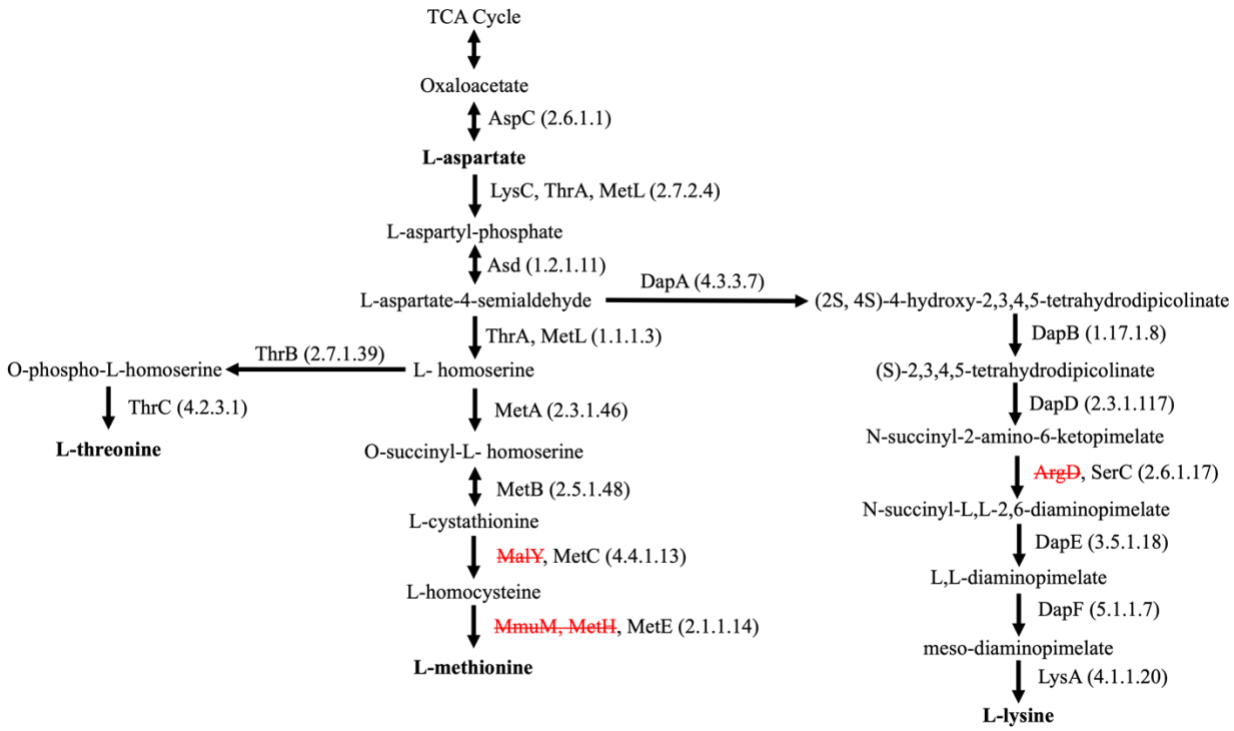


Figure 2.2: Reconstruction of the predicted ADAA superpathway in *X. nematophila* reveals genomic distinctions from the characterized pathway in *E. coli* MG1655.

Each amino acid produced in this pathway (Asp, Lys, Thr, and Met) is bolded. Orthologous proteins identified in genomes of *E. coli* MG1655 and *X. nematophila* ATCC19061 are listed in black to the right or above their respective reaction arrows. The E.C. numbers corresponding to each enzymatic reaction are written parenthetically next to the enzyme name. Enzymes found in *E. coli* MG1655 but not in *X. nematophila* are presented in red with a strikethrough line. AspC – aspartate aminotransferase, ThrA – fused aspartate kinase/homoserine dehydrogenase 1, MetL – fused aspartate kinase/homoserine dehydrogenase 2, LysC – aspartate kinase 3, Asd – aspartate-semialdehyde dehydrogenase, DapA – 4-hydroxy-tetrahydrodipicolinate synthase, DapB – 4-hydroxy-tetrahydrodipicolinate reductase, DapD – tetrahydrodipicolinate succinylase, ArgD – *N*-acetylornithine aminotransferase/ *N*-succinyldiaminopimelate aminotransferase, SerC – phosphoserine/phosphohydroxythreonine aminotransferase, DapE – succinyl-diaminopimelate desuccinylase, DapF – diaminopimelate epimerase, LysA – diaminopimelate decarboxylase, ThrB – homoserine kinase, ThrC – threonine synthase, MetA – homoserine *O*-succinyltransferase, MetB – *O*-succinylhomoserine(thiol)-lyase/ *O*-succinylhomoserine lyase, MalY – negative regulator of MalT activity/cystathionine β-lyase, MetC – cystathionine β-lyase/L-cysteine desulfhydrase/alanine racemase, MmuM – homocysteine *S*-methyltransferase, MetH – cobalamin-dependent methionine synthase, MetE – cobalamin-independent homocysteine transmethylase.

carbon source. Additionally, the length of *X. nematophila* lag phase when grown on Asp as a carbon source was comparable to that of GMM **(Figure 2.3A)**. We next assessed whether the dosage of carbon supplemented to the medium had a significant impact on *X. nematophila* lag, as increasing levels of glucose were previously shown to positively impact the growth rate and carrying capacity of *X. nematophila in vitro* ((48), **Figure 2.3B**). In the absence of a carbon source, no growth was observed; however, the presence of glucose gave rise to similar lag phase lengths, regardless of the tested concentration (ranging from 11-55 mM).

Finally, we tested if the effect of ADAA supplementation on *X. nematophila* lag varied depending on the carbon source provision in the medium. Here we tested carbon sources predicted to be taken up via phosphotransferase systems (PTS, e.g. glucose, mannose, *N*-acetyl-glucosamine, and trehalose) and non-PTS transported carbon sources (e.g. acetate, glycine, maltose, glycerol, and serine, **Figure 2.3C)**. In the absence of the ADAA, *X. nematophila* growth was observed for all predicted PTS carbon sources and some non-PTS sources (e.g., serine, glycerol, and maltose) over the 168-h experiment. In the absence of the ADAA, *X. nematophila* exhibited comparable lag times when grown on glucose, L-serine, mannose, trehalose, and *N*-acetyl-glucosamine as sole carbon sources. *X. nematophila* was able to exit lag phase and grow in minimal medium containing maltose as a carbon source (127.8 ± 2.7 h), however this took significantly longer than the aforementioned carbon sources ($p < 0.0001$, One-Way ANOVA, Tukey's HSD). No growth was observed within the 168-h experiment, when *X. nematophila* was provided acetate or glycine, suggesting that under these conditions, *X. nematophila* cannot use these

compounds as sole sources of carbon or require more time to adjust their physiology to grow on them. ADAA supplementation into the acetate, glycine, and no-carbon conditions, permitted *X. nematophila* growth. This supported our previous observation that Asp can be utilized as a sole source of carbon and suggests that it may be preferentially utilized over acetate and glycine. However, the results of these experiments suggest that *X. nematophila* lag phase does not vary considerably across the type of carbon source. Supplementation with the ADAA significantly reduced the lag time of *X. nematophila* in all tested minimal media regardless of the provisioned carbon source ($p<0.0001$, One-Way ANOVA, Tukey's HSD).

Given that *X. nematophila* lag times were not significantly altered by variation in the supplied carbon pool, we ruled out the possibility that utilization of the ADAA as carbon sources caused the reduction of *X. nematophila* lag in GMM. We next tested if one or more of the ADAA could serve as a sole nitrogen source in GMM. Note that to this point, ammonium sulfate has been provisioned in all defined media utilized as the primary source of inorganic nitrogen. The ADAA were individually supplemented into nitrogen-deficient GMM. Asp, but not Lys, Thr, or Met, served as nitrogen source for *X. nematophila* **(Figure 2.3D).** Furthermore, we noted that when Asp was supplied as a nitrogen source in GMM, the lag time was significantly shorter (16.8 ± 3.8h) than in GMM with ammonium sulfate (86 h ± 24.5 h, $p = 0.0001$, One-Way ANOVA, Tukey HSD). Given that the lag times were different from one another, we considered the possibility that utilization of Asp as a carbon source was responsible for the reduced lag time we observed previously in GMM. In previous experiments, Asp had been added at a much lower

concentration (0.4 mM) compared to in this experiment (9.4mM). To address this discrepancy, we assessed if a lower dosage of Asp could sufficiently reduce *X. nematophila* lag in GMM (**Figure 2.3E**). There was no concentration-dependent effect between *X. nematophila* lag with Asp or ammonium sulfate as the sole nitrogen source. Furthermore, supplementation of Asp did not recapitulate the ~16h lag observed in the previous experiment (**Figure 2.3D)** although it was still shorter relative to the condition containing ammonium sulfate. Taken together, these data indicate that utilization of Asp as a sole nitrogen source can modestly reduce lag, and that *X. nematophila* lag time in GMM (regardless of nitrogen source) can vary considerably across experiments. Finally, we assessed if the type of nitrogen source had an impact on *X. nematophila* lag in GMM (**Figure 2.3F**). Ammonium sulfate, serine, and glutamate, but not nitrate, urea, or arginine, could each serve as a sole nitrogen source allowing *X. nematophila* to exit lag phase without ADAA supplementation. Compared to the condition containing ammonium sulfate (86 ± 24.5 h), glutamate had a comparatively shorter lag time in GMM (48.2 ± 8.4 h, $p = 0.0001$, One-Way ANOVA, Tukey HSD) suggesting a possible role of this amino acid as a preferential nitrogen source for *X. nematophila*, similar to Asp. Supplementation with the ADAA significantly reduced the lag in GMM for all tested nitrogen sources except for glutamate ($p < 0.0001$, One-Way ANOVA, Tukey HSD). Overall, theses data suggested that *X. nematophila* lag phase duration is significantly shortened by ADAA supplementation but is likely only modestly influenced by the utilization of Asp as a sole nitrogen source.

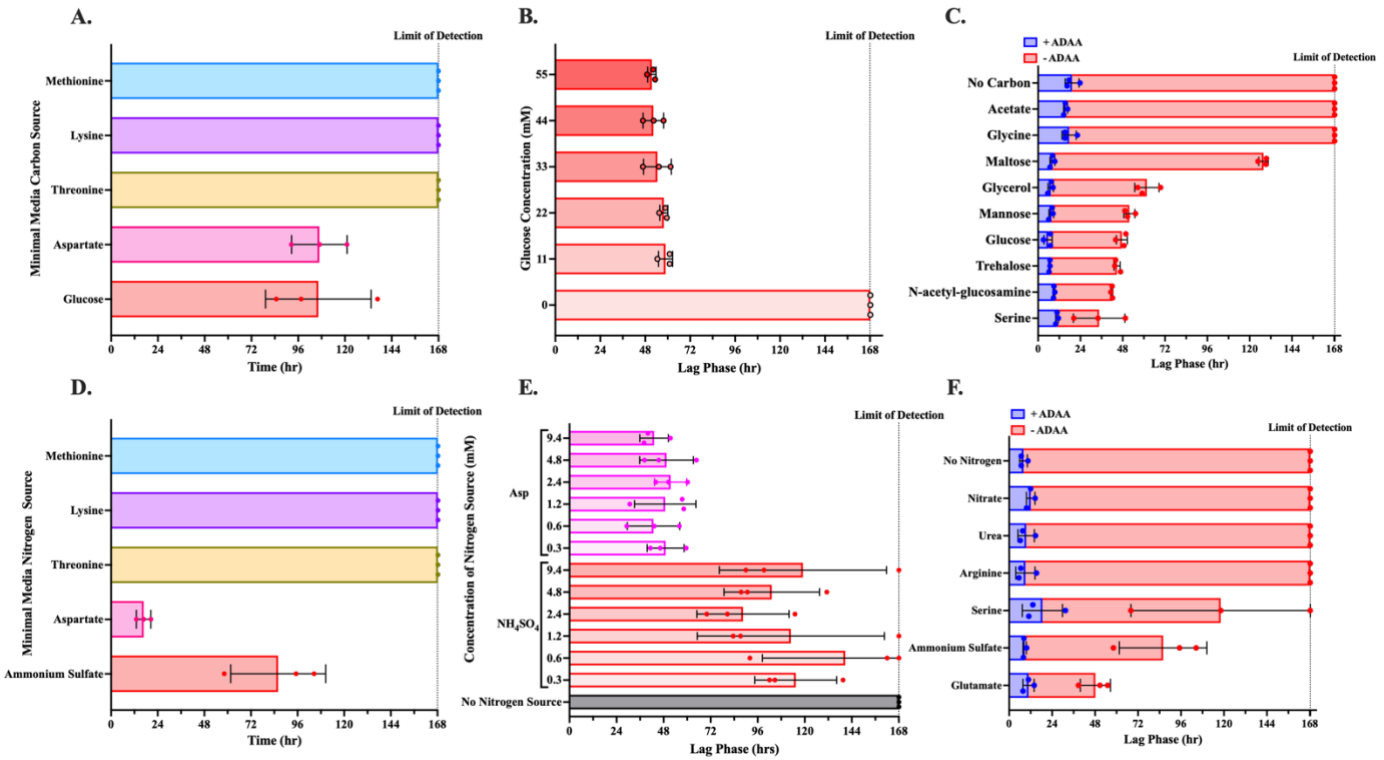


Figure 2.3: Assessment of varying carbon and nitrogen sources on *X. nematophila* lag phase

Lag time (h) of *X. nematophila* grown in various media conditions: **A)** minimal medium with the individual ADAA (Met, Lys, Thr, Asp) or Glucose provisioned as a sole source, **B)** GMM with varying concentrations of glucose, **C)** minimal medium with PTS (Mannose, Glucose, Trehalose, and N-acetyl-glucosamine) and non-PTS (Acetate, Glycine, Maltose, Glycerol, and Serine) carbon sources in the presence (blue boxes) or absence (red boxes) of the ADAA, **D)** GMM with individual ADAA provisioned as a sole source of nitrogen, **E)** GMM with varying concentrations of ammonium sulfate and aspartate as the sole nitrogen source, **F)** GMM supplemented with various nitrogen sources in the presence or absence of the ADAA. Error bars indicate ±1SD.

The prolonged lag phase of *X. nematophila* in GMM is methionine-responsive.

Given that Asp only modestly reduced *X. nematophila* lag when supplied as a nitrogen source, we predicted that one of the remaining ADAA (Lys, Thr, and Met) or a specific combination of these amino acids could shorten the length of lag in GMM. To investigate this possibility, we cultivated *X. nematophila* in GMM with 16 different combinations of Asp, Thr, Lys, and Met and then determined the impact of these combinations on the length of the lag (**Figure 2.4A and Figure 2.9**). The addition of Met alone significantly shortened the lag phase of *X. nematophila* (28.9 h ± 4.4 h) relative to unsupplemented GMM (57.1 h ± 7.6 h), while the individual additions of Asp, Thr, and Lys did not (**Figure 2.9)**. However, combinatorial addition of Asp, Thr, and Lys (33.5 ± 11.5 h) was sufficient to reduce the average lag time of *X. nematophila* in GMM similar to the lag observed with GMM + Met.

This suggests that alleviating metabolic flux through the Thr and Lys biosynthetic pathways and/or increasing flux through the Met biosynthetic pathway is sufficient to reduce the lag time of *X. nematophila* in GMM. Though not significantly different from GMM + Met, it is worth noting that conditions where methionine was supplemented with one or more of the other ADAA the average lag time could be shortened to as low as 13.3 h ± 2.4 h (GMM + ADAA). Altogether, these results suggest that *X. nematophila* exit from lag in GMM depends on metabolic flux through the methionine biosynthesis pathway and is therefore responsive to Met supplementation.

***Xenorhabdus* bacteria have variable and methionine-responsive lag phases when grown in glucose minimal medium.**

A prolonged, Met-responsive lag has not been reported previously for *X. nematophila* or any other *Xenorhabdus* bacteria. We considered the possibility that this physiology might be specific to the laboratory isolate we have been using throughout this study *X. nematophila* ATCC19061 – HGB800. To explore this, we examined the lag lengths of various *X. nematophila* isolates that were from derived from *S. carpocapsae* (e.g., ATCC19061-HGB800, AN6/1, ATCC19061-HGB007, and F1), *S. anatoliense,* and *S. websteri* nematodes (**Figure 2.10A).** We noted that all tested *X. nematophila* isolates exhibited a prolonged lag phases in GMM, ranging from 47.7 h (±4.5; Websteri) to >80h (AN6/1). The AN6/1 isolate did not grow in our initial experiment but did grow in a subsequent growth assay (**Figure 2.10C**). Regardless of lag phase duration in GMM alone, all tested *X. nematophila* isolates exhibited ADAA-responsive lag times when the ADAA were supplemented to GMM (**Supplemental Figure 2.10A**). *Xenorhabdus* bacteria, including *X. nematophila,* can spur "secondary form" variants that are phenotypically distinct (e.g., exoenzyme production, motility) from their "primary form" parental lineage (27, 49, 50). We tested if form variation had any impact on *X. nematophila* lag time in GMM and observed a meager reduction in the length of lag among secondary form variants compared to primary form variants (**Supplemental Figure 2.10B**); however the secondary form variants, like the primary form, exhibited an ADAA-responsive lag phase when grown in GMM. Overall, these data suggest that ADAA-dependent shortening of lag phase duration is a conserved trait among *X. nematophila* forms and isolates.

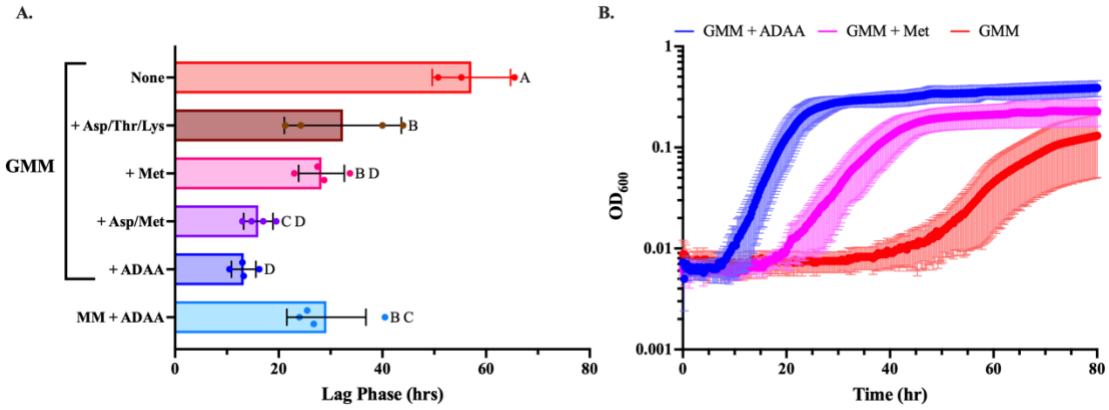


Figure 2.4: The lag time of *X. nematophila* in GMM is primarily responsive to methionine.

A) The average lag time of *X. nematophila* (3-4 biological replicates, ±1SD) in GMM alone (none) or supplemented (+) with different combinations of the ADAA. The data were analyzed via a One-way ANOVA and significance is shown using letter designations (A-D). **B)** Growth curves of *X. nematophila* (3-4 biological replicates, ±1SD) in GMM without (red) or with supplementation with the ADAA (blue) or Met alone (pink).

Given the conservation in lag length among *X. nematophila* isolates, we next tested if other *Xenorhabdus* species also exhibit a prolonged, Met-responsive lag phase in GMM (**Figure 2.5**). The *Xenorhabdus* species tested represent the breadth of the clade and were selected based on previous phylogenetic analyses conducted by our group (51). We also examined the growth behavior of closely related bacterial species, all members of the *Enterobacterales* (*E. coli* MG1655, *Proteus mirabilis,* and *P. laumondii* TT01) (15). Given that we previously showed experiment-to-experiment variation in the length of lag phase in *X. nematophila*, we assessed the lag time of 8-9 biological replicates of each selected species over the course of three independent experiments. To investigate if there were any correlations between the observed lag phenotypes and the evolutionary history of *Xenorhabdus*, we also generated a phylogeny of our tested bacterial species using whole-genome data analyzed via maximum likelihood methodologies as previously reported (51).

Interspecific diversity in the length of lag phase was observed across the *Xenorhabdus* clade when cultivated in GMM with lag times ranging from 6.8 h (± 1.7; *X. ehlersii*) to 107.6 h (± 21.58; *X. bovienii*-Sf-FL). *E. coli* MG1655 (4.3h ± 0.4) and *P. mirabilis* (7.4h ± 0.6), the most distantly related species to *Xenorhabdus,* exhibited shorter lag times in GMM (e.g. <24 h) and were not statistically significant from one another. Likewise, six *Xenorhabdus* species (*X. cabanillasii, X. miraniensis, X. beddingii, X. doucetiae, X. ehlersii,* and *X. thuongxuanensis*) exhibited comparably short lag times in GMM ranging from 6.8 h-18.6 h. Hereafter we will refer to these *Xenorhabdus* species as 'short lag' *Xenorhabdus*. Excluding *X. cabanillasii*, all of these *Xenorhabdus* are found within a sub-clade apical to the phylogeny. In addition to *X. nematophila*, three

Xenorhabdus species (*X. bovienii*, *X. innexi*, and *X. szentirmaii*), exhibited prolonged lag phases in GMM. The longest of these lag times was observed in *X. bovienii*-Sf-FL as reported above, one of two isolates tested, which was significantly longer than all other lag phases measured ($p<0.0001$, One-Way ANOVA, Tukey's HSD). While not isolated to a single clade like the 'short lag' *Xenorhabdus*, it was worth noting that the majority of these species diverged earlier in the phylogeny. Going forward, we will refer to this group as the 'long lag' *Xenorhabdus*. The remaining outgroup, *P. laumondii* TTO1, exhibited a significantly longer lag time (42.7 h ± 15.32, $p \leq 0.0002$, One-Way ANOVA, Tukey's HSD) in GMM compared to *E. coli* and *P. mirabilis,* but it was also significantly shorter than certain 'long lag' *Xenorhabdus* species, including *X. bovienii* ($p \leq 0.0001$, One-Way ANOVA, Tukey's HSD). Like *Xenorhabdus*, but unlike *E. coli* and *P. mirabilis, Photorhabdus* species, including *P. laumondii,* form a mutualistic relationship with insect-parasitic nematodes, suggesting that the physiology associated with a prolonged lag phase in GMM may be associated with the nematode-symbiont lifestyle. *X. poinarii* (42.4 ± 9.6 h) and *X. griffiniae* (30.44 ± 1.5 h) exhibited lag times similar to that of *P. luminescens*; however, they could not be easily grouped with either the 'short' or 'long' lag *Xenorhabdus* based on statistical significance. In congruence with their intermediary phenotype, we classified them as 'intermediate lag' *Xenorhabdus*. Taken together, our data suggest that the physiology associated with a prolonged lag phase in GMM is not associated with the emergence of the *Xenorhabdus* lineage, but rather may be associated with niche-specific adaptation to their nematode or insect host conditions.

We next examined if the lag times of the tested *Xenorhabdus* species are responsive to the addition of the ADAA and/or Met (**Figure 2.6)**. As before, we also tested the outgroup species for a point of comparison. The average lag times of *E. coli* and *X. thuongxuanensis* in GMM were unresponsive to supplementation with either Met or the ADAA. Given that these organisms were observed to have 'short' lag times in GMM, these data suggest that exit from lag for *E. coli* and *X. thuongxuanensis* is not limited by metabolic demand for these amino acids. Other 'short' lag *Xenorhabdus* (e.g., X. *ehlersii* and *X. cabanillasii*) also did not exhibit Met-responsive lag times in GMM but exhibited significantly shorter lag times in the presence of the ADAA ($p < 0.01$, One-way ANOVA, Tukey's HSD). This suggests that demand for Thr, Lys, and/or Asp does limit exit from lag in these *Xenorhabdus* species. Seven *Xenorhabdus* species (*X. bovienii*, *X. innexi*, *X. szentirmaii*, *X. poinarii*, *X. miraniensis*, *X. beddingii,* and *X. nematophila*) as well as *P. laumondii*, exhibited Met-responsive lag times in GMM that were not significantly different from their lag times in GMM + ADAA. This suggests that demand for Met synthesis alone determines the length of these species' lag time. *X. griffiniae*, *X. doucetiae*, and the outgroup *P. mirabilis* also exhibited Met-responsive lag times in GMM, but the reduction of their lag was further enhanced by the presence of Thr, Lys, and/or Asp ($p < 0.05$, One-way ANOVA, Tukey's HSD). This suggests that metabolic demand for more than one ADAA drives the length of lag in these species. Given that both *P. mirabilis* and *P. laumondii* exhibited Met-responsive lag times in GMM in addition to the majority of the tested *Xenorhabdus* species, we speculate that this physiological trait may be associated

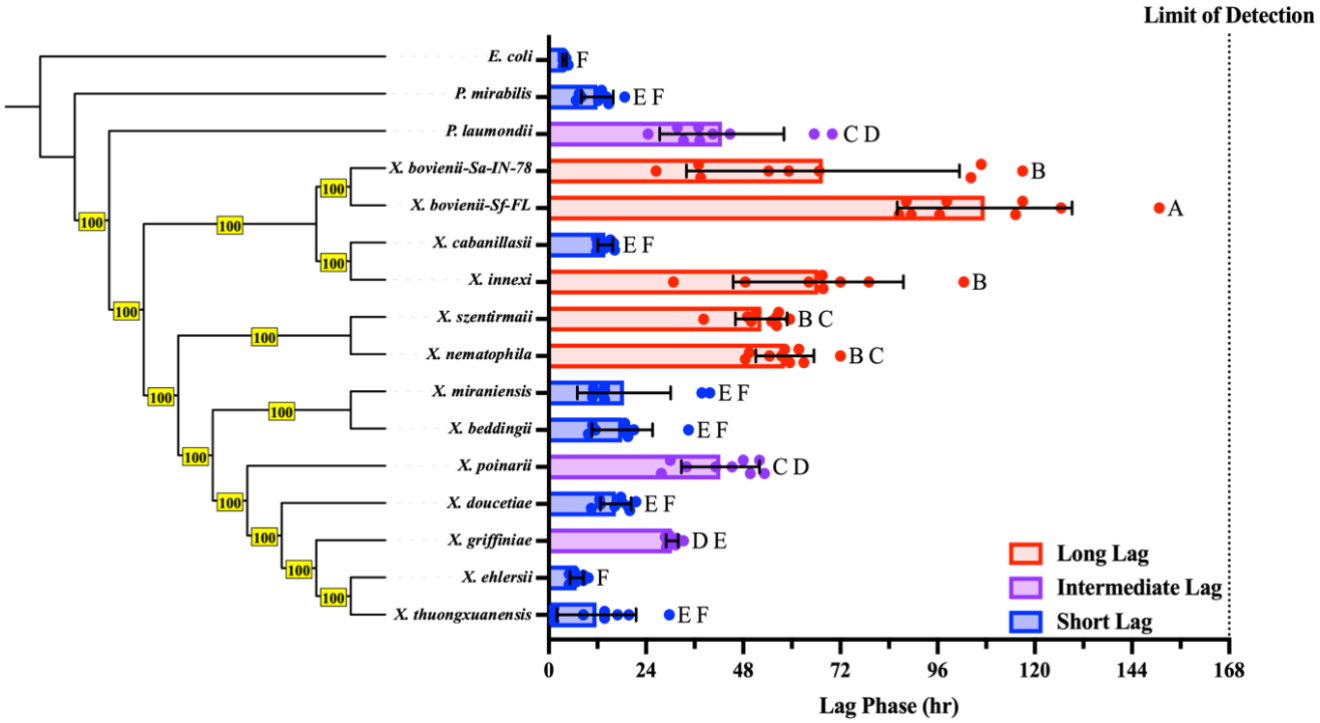


Figure 2.5: A prolonged lag in GMM is not conserved among *Xenorhabdus* species.

A) Cladogram of tested *Xenorhabdus* species (and other selected *Enterobacterales*). Numbers on the branches indicated bootstrap support values. Only bootstraps greater than 80% are shown. Dashed lines connect the bacterial species presented in panel B to their respective position on the cladogram. **(B)** Lag times of various *Xenorhabdus* species strains (and *Enterobacterales*) in GMM over a 168-h time course color coated by long (red), intermediate (purple), and short (blue) lag length. Data points shown represent biological replicates (8-9 total) and error bars indicate ±1SD. A One-Way ANOVA was used to test statistical differences among the lag times and letters (A-F) indicate statistical significance groupings.

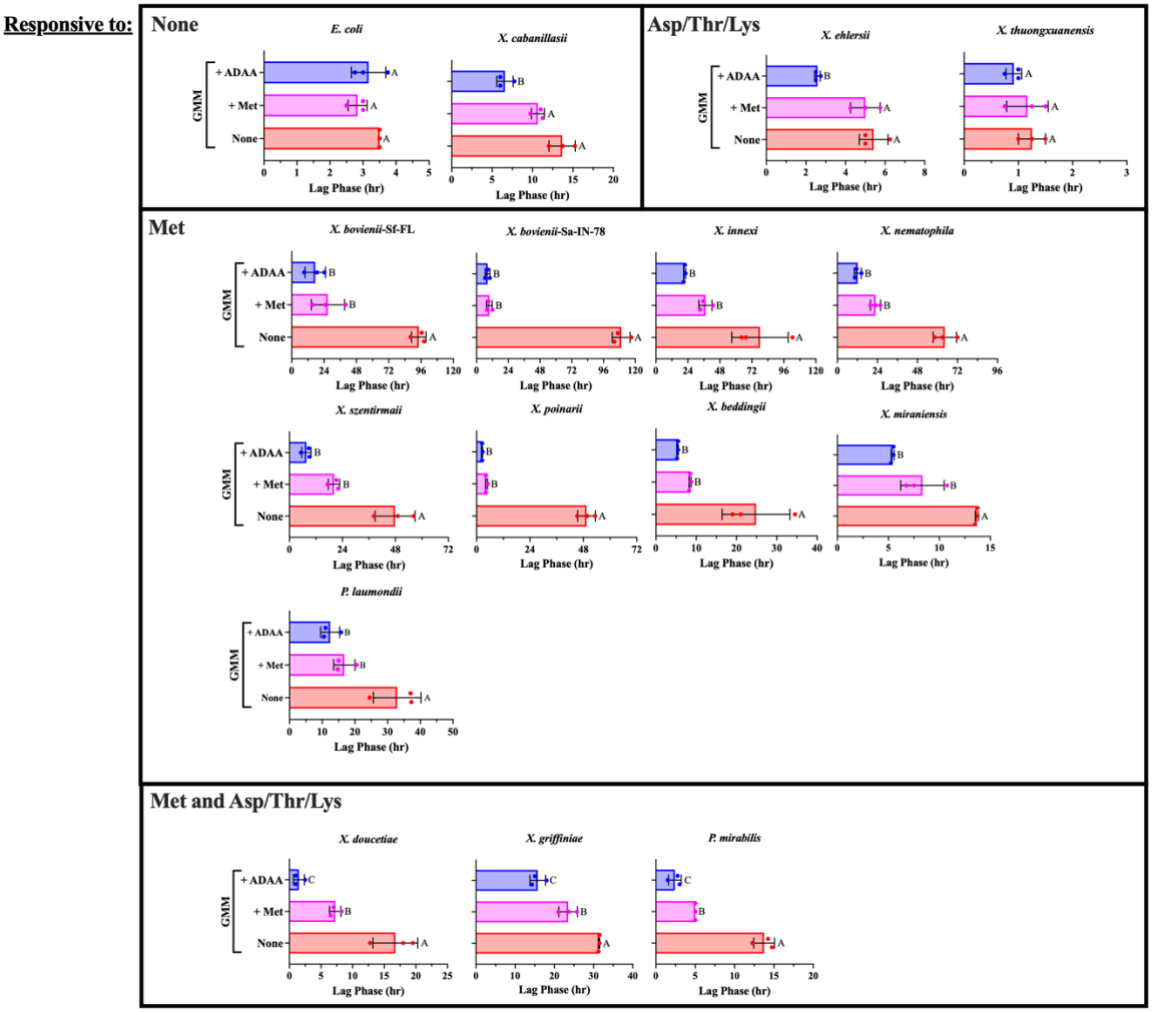


Figure 2.6: Most Xenorhabdus exhibit Met-responsive lag times in GMM.

Lag times of *Xenorhabdus* and outgroup species when grown in GMM with the ADAA (blue), Met alone (pink), or no supplementation (red) over the course of 168 h experiment. Graphs are organized into groups based on lag length responsiveness to the ADAA. The lag data presented here in GMM are also reported in Fig. 2.5. The x-axes of each graph are scaled according to improve data visualization. Data shown represent 2-3 biological replicates per bacterial species tested and error bars indicate ±1 SD.

with the evolution of organisms within the clade *Morganellaceae* which includes *Proteus, Photorhabdus,* and *Xenorhabdus* species.

Comparative genomic analyses reveal three methionine metabolism-associated loci that serve as possible lag length predictors.

The variations in *Xenorhabdus* lag length in GMM were striking and suggested to us that execution of Met biosynthesis among these bacteria was likely distinct between the short, intermediate, and long lag species. We sought to identify possible source of genomic variation among these closely-related *Xenorhabdus* species using the comparative genomics approach we described above. We first compared if all of *Xenorhabdus* bacteria contained genes predicted to function in ADAA biosynthesis as we observed for *X. nematophila*. We found that the early stages of the ADAA superpathway (oxaloacetate to L-aspartate semialdehyde) and the Thr pathway were conserved across all examined *Xenorhabdus* genomes (13 total). In contrast, we noted variation in the Lys pathway.

Orthologs of *E. coli* ArgD were only identified in seven of the tested genomes, including *X. nematophila*, *X. miraniensis*, *X. beddingii*, *X. doucetiae*, *X. griffiniae*, *X. ehlersii*, and *X. thuongxuanensis*. Of the genomes where ArgD was not identified (*X. bovienii, X. cabanillasii*, *X. innexi*, *X. szentirmaii,* and *X. poinarii*), only *X. cabanillasii* genome is considered complete making it difficult to conclude if *argD* is truly absent in the remaining species. Excluding *X. cabanillasii* (a 'short' lag and non-Met-responsive *Xenorhabdus*), these bacteria exhibit either 'long' or 'intermediate', Met-responsive lag times in GMM. In *E. coli* MG1655, ArgD is a bifunctional metabolic enzyme that contributes to both Lys and arginine biosynthesis; however, the absence of *argD* does not

result in auxotrophy for either amino acid as enzymes such as SerC and AstC serve functionally redundant roles (52). Taken together, these data support the prediction that the Lys pathway across the *Xenorhabdus* clade is likely functional even in the possible absence of ArgD in certain genomes.

E. coli MG1655 Met biosynthesis genes MetA, MetB, MetC, and MetE were identified in all thirteen tested genomes. During the query of MetB, we again noted that, in addition to MetB orthologs, each *Xenorhabdus* genome encoded at least one additional non-orthologous protein sequence. The majority of these proteins were annotated as *metC* but were not orthologous to *E. coli* MetC. We also identified that every tested *Xenorhabdus* genome encoded an ortholog to XNC1_1035 and that these sequences were identified in the initial query with the *E. coli* MetB amino acid sequence. Together these data suggested that each *Xenorhabdus* genome examined had one ortholog to *E. coli* MetB, MetC, and XNC1_1035 from *X. nematophila*. In addition to the XNC1_1035 orthologs identified in each tested genome, we noted five additional protein sequences that were non-orthologous to XNC1_1035 but shared sequence similarity. These five predicted proteins were annotated as *metC* and were encoded in the genomes of 'short' and 'intermediate' lag *Xenorhabdus* species: *X. poinarii*, *X. griffiniae*, *X. doucetiae* (though this protein was fragmented), *X. ehlersii,* and *X. thuongxuanensis*. Using the protein sequence from the genome of *X. griffiniae* (XGHIN1_v1_3989), we determined that these 5 proteins were orthologs of one another. Taken together, *Xenorhabdus* are predicted to encode orthologs for Met biosynthesis enzymes from *E. coli* MG1655 and also encode conserved

(XNC1_1035 orthologs) and non-conserved (XGHIN1_v1_3989 orthologs) proteins predicted to be involved in Met metabolism.

The presence of the Met-associated protein of unknown function in the tested *Xenorhabdus* genomes led us to investigate the potential for alternative pathways for Met metabolism among *Xenorhabdus.* We examined the selected genomes for the presence of homologs implicated in the Met direct sulfurylation pathway that occurs in *Pseudomonas* species and the Met reverse trans-sulfurylation pathway that occurs in *Klebsiella pneumoniae* (53-56). *Pseudomonas* can synthesize methionine by both the trans-sulfurylation (like in *E. coli* MG1655) or direct sulfurylation pathways (56). In the latter process, the *Pseudomonas* enzymes MetX and MetW convert L-homoserine into *O*-acetyl-homoserine rather than O-succinyl-homoserine (the product of MetA in *E. coli*), though this mechanism has been disputed (**Figure 2.7A**) (55, 57). Regardless, the activated homoserine molecule is then converted by the homocysteine synthase, MetY, into homocysteine using H_2S rather than Cys as the sulfur donor. All thirteen *Xenorhabdus* genomes tested encode one ortholog of *Pseudomonas aeruginosa* PAO1 MetY, but no orthologs of either MetX or MetW. These data suggest that *Xenorhabdus* bacteria are likely to utilize the canonical *E. coli* Met trans-sulfurylation pathway but not the alternative direct sulfurylation pathway.

In the reverse trans-sulfurylation pathway, exogenous and/or endogenous methionine is converted into *S*-adenosyl-methionine (AdoMet) via MetK and is eventually re-cycled via the AdoMet cycle into L-homocysteine. The proteins facilitating this process are conserved among *Xenorhabdus* (**Supplemental File 2**). L-homocysteine is then

converted by the cystathionine-β-synthase enzyme, MtcB, into L-allo-cystathionine. MtcC, a cystathionine-γ-lyase, then transforms L-allo-cystathionine into L-cysteine replenishing the cells endogenous sulfur levels (54). All *Xenorhabdus* species encode one ortholog to MtcC and MtcB (**Supplemental File 2**). We further noted that the MtcC orthologs were identical to the XNC1_1035 orthologs. Based on this, we hereafter refer to XNC1_1035 homologs as MtcC. The presence of both MtcB and MtcC in all tested genomes suggests that *Xenorhabdus* have the potential to execute reverse transulfurylation. The five XGHIN1_v1_3989 orthologs (hereafter called MtcC-like proteins) shared high sequence similarity with the MtcC amino acid sequence from *K. pneumoniae* but were not considered orthologs based on the RBH analysis. This was supported via phylogenetic analyses as the MtcC-like proteins grouped closest with the true MtcC orthologs rather than MetB, MetC, or MetY (**Figure 2.11**). To infer potential function of the MtcC-like proteins, we examined their genomic neighborhoods compared to those of the bona fide MtcC orthologs (**Figure 2.12 and Figure 7B**) The genomic neighborhoods of the *Xenorhabdus* MtcC orthologs were syntenic with one another and exhibited a similar genomic structure to that reported in *K. pneumoniae*, further supporting their putative role in reverse sulfurylation. The genomic loci of the MtcC-like proteins were not syntenic to those of the MtcC orthologs and shared limited synteny with each other. Across all 5 genomes that contained them, the MtcC-like genes were encoded proximally to an ortholog of the *yihN* gene of *E. coli* MG1655. This gene is predicted to encode a putative transport protein of unknown function whose expression is negatively influenced by the presence of exogenous cystine, the reduced form of cysteine (58). In *X. poinarii, X. doucetiae, X. thuongxuanensis,* and *X.*

ehlersii, an ortholog of the *E. coli dcyD* gene is also encoded downstream of the *yihN* ortholog. The protein product of this gene, if functional, would contribute to the degradation of D-cysteine into H_2S, ammonia, and pyruvate (59, 60). It is worth noting that orthologs of DcyD were not identified in other *Xenorhabdus* species. Taken together, these data suggest that the MtcC-like proteins may play an unknown role at the metabolic interface of Met and Cys metabolism. It is enticing to hypothesize that these MtcC-like proteins engage in the detoxification of inhibitory metabolites like L-cysteine. If so, the presence of these genes could help explain the 'short' and 'intermediate' lag phenotypes observed among some *Xenorhabdus*.

In addition to diversity in Met biosynthesis pathways, variable metabolic demand for Met, or variable pathways for Met recycling and acquisition could contribute to differences in lag phase phenotypes among *Xenorhabdus*. Met can be synthesized endogenously, taken up from the environment, or sourced from pre-existing proteins via degradation (44, 61). In *Xenorhabdus*, intracellular inclusion proteins, PixA and PixB, are hypothesized to act as reservoirs for amino acids during nutritional stress, particularly within infective juvenile nematodes (62-64). PixA is methionine rich as 8.1% of the PixA amino acid sequence is comprised of Met in *X. nematophila*, while most proteins are 2.9% Met on average (62, 65). We identified orthologs of PixA in each of the 'long' lag *Xenorhabdus* genomes (five total), as well as the genome of *X. doucetiae* ('short' lag; **Figure 7C**). Excluding PixA from *X. szentirmaii* (5.4% Met), all of the PixA orthologs had 8.1% or greater Met richness which exhibited a weak positive correlation with the lag

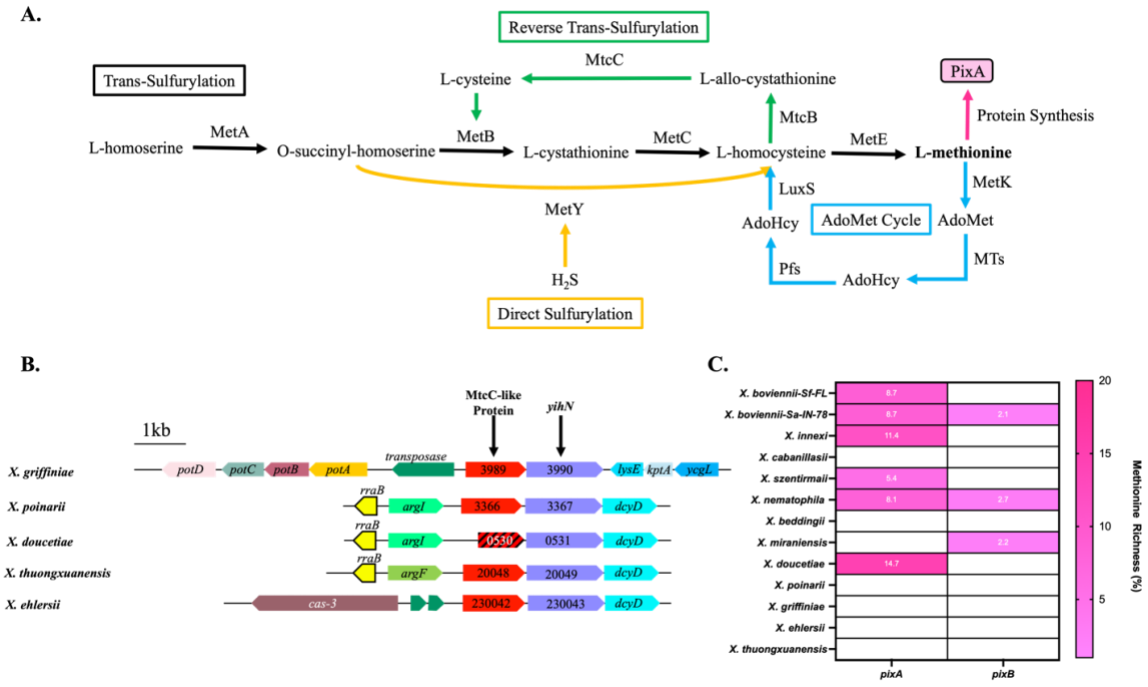


Figure 2.7: Comparative genomic analyses reveal genomic diversity in ADAA-related genes among *Xenorhabdus* bacteria.

A) The predicted Met biosynthesis pathway in *Xenorhabdus* bacteria. Black arrows denote the Met trans-sulfurylation pathway (as occurs in *E. coli*), orange denotes the direct sulfurylation pathway, and light blue denotes the AdoMet cycle. The Met-rich inclusion protein, PixA, is shown in the pink-shaded box. B) Aligned genomic neighborhoods of predicted MtcC-like proteins found in the 'short' lag, but not other examined *Xenorhabdus* species. C). Heat map of presence and methionine richness of *X. nematophila* PixA and PixB orthologs across the tested *Xenorhabdus* species. White boxes indicate the absence of orthologs, while pink boxes indicate presence. The intensity of pink color indicates the Met richness of the PixA or B orthologs (100% × (# of Met/# of total AA)).

time of *Xenorhabdus* bacteria (**Figure 2.15)**. These data suggest that there is a possible link between the presence of PixA and a prolonged lag in GMM.

DISCUSSION

Xenorhabdus bacteria exhibit variable lag phase lengths in conditions where amino acids are limiting. In RDM lacking the 20 common amino acids, where other sources of carbon and nitrogen are present, *X. nematophila* is unable to initiate growth in 24h. Furthermore, growth is observed in GMM after at least 48h of incubation. Based on our observations in GMM, we are confident that *X. nematophila* is likely to grow in amino acid deficient RDM, but likely requires additional time to initiate exponential growth. While later experiments revealed that Met could significantly reduce *X. nematophila* lag in GMM (>24h), this phenotype was only observed in the amino acid deficient RDM during our auxanographic analyses when it was supplemented with Lys, Thr, and Asp, but not when supplemented with Cys. Given that Cys has been previously described as an inhibitor of growth in other closely related bacterial species, like *E. coli*, it is possible that Cys exerts similar growth suppressive effects on *X. nematophila*, thereby masking the lag reducing effects of Met (37).

One notable discrepancy among our data is the occasional variability of *Xenorhabdus* lag times in GMM. For example, across six experiments evaluating the influences of carbon and nitrogen source on *X. nematophila* lag in minimal medium, we noted variation experiment to experiment. For example, in **Figure 2.3D** when Asp was supplemented as the sole nitrogen source, the lag of *X. nematophila* was 16.8h in length, but in **Figure 2.3E** under the same condition, the lag was 43.1h. Furthermore other

Xenorhabdus species, particularly *X. bovienii* – Sa – IN – 78 exhibited variable lag times in GMM across nine biological replicates in three independent experiments (**Figure 2.5**). Variable lag times have been reported and investigated previously in other bacteria. In one such study, *E. coli* exhibited variation at the single-cell level in regard to growth resumption, particularly when shifting from glucose as the sole carbon source to lactose (7). Using iterative rounds of carbon starvation and nutrient replenishment in the form of lactose, they isolated strains of *E. coli* that exhibited shorter and less variable lag times (7). Using evidence from mathematical modelling, they asserted that there are possible evolutionary trade-offs associated with evolving long or short lag times in response to changes in environmental nutrients (7). In this case, *E. coli* cells with shorter lag times ensure greater reproductive success in nutrient-replete conditions, while risking susceptibility to environmental stressors (7). Opposingly, *E. coli* with longer lag times, though considered less fit in nutrient-replete conditions, can persist longer in the face of environmental stress via tolerance by lag (7, 8). Variation in lag is apparent across the *Xenorhabdus* clade and suggests that distinct evolutionary pressures faced in their natural environments may select for or against long, variable lag times. Additionally, we noted that *X. nematophila* cultures inoculated at an initial optical density of 0.01, exhibited greater variation in lag than those inoculated at a density of 0.1, suggesting a population size-dependent effect on lag variation (**Supplemental Figure 2.14)**.

Of the ADAA, only Asp was demonstrated to serve as a source of carbon or nitrogen. When supplied as the sole form of nitrogen, Asp modestly reduced the lag of *X. nematophila* relative to cultures where ammonium sulfate was the sole nitrogen source,

regardless of the concentration. Utilization of Asp as a nitrogen source is mediated by AspA in which Asp is converted to fumarate and ammonia (66). Although ammonia is the preferred nitrogen source for *E. coli*, Asp exerts comparable effects on the organism's ability to grow *in vitro* (66, 67). Our data suggest that Asp may be a preferred nitrogen source for *X. nematophila* based on its ability to support earlier exit from lag in *vitro.* Given that *X. nematophila* grow in both insects and *Steinernema* IJs, two distinct, metabolically dynamic niches, it is possible that acquisition of ideal and non-ideal nitrogen sources may partially contribute to these *in vivo* observations. Nitrogen source utilization has not been studied in *Xenorhabdus* species *in vitro* or *in vivo*; however, Asp and ammonia have been shown to increase in abundance over the course of a *Xenorhabdus-Steinernema* insect infection, the latter of which is implicated in the emergence of infective juvenile nematodes (25, 68). It is also unknown what nitrogen sources *Xenorhabdus* utilizes within the receptacle of *Steinernema* IJs; however, some amino acids are accessible in this environment and could serve as sources of both nitrogen and carbon (23).

Strikingly, the type and amount of carbon source had little to no impact on the length of *X. nematophila* lag despite observations made in other closely related bacteria (2, 7). Initially, we considered that glucose may not be the ideal carbon source for *Xenorhabdus* species as they do not encode a homolog to the phosphotransferase system *ptsG,* which has been implicated in the uptake of glucose (69). The loss of this transporter in *E. coli* led to significant growth defects in GMM, despite having an additional PTS system capable of taking up glucose, *manXYZ* (70). *Xenorhabdus* species do encode homologs to the *manXYZ* PTS system, and its uptake of glucose has been shown previously

(69). Furthermore, the transcriptional and post-transcriptional regulators, SgrR and *sgrS*, which maintain metabolic homeostasis during phosphosugar stress by coordinating the repression of *ptsG* and *manXYZ* mRNAs, have not been identified in *Xenorhabdus* species, but have been identified in the closely related *Photorhabdus laumondii* TT01 (71). The regulation and execution of *Xenorhabdus* carbon metabolism has not been studied directly, but a plethora of studies have implicated sugar metabolism as a driver of *Xenorhabdus* fitness within its insect and nematode niches (29, 72-74).

Xenorhabdus exhibit both 'short', 'intermediate', and 'long' lag phases in GMM. The majority of them exhibit Met-responsive lag times in GMM, but the effect is most profound in the 'long' lag *Xenorhabdus*. The influence of Met on the length of a bacterium's lag phase has been investigated recently in the marine Roseobacter *P. inhibens,* which forms a symbiotic association the algae *Emiliana huxleyi* (13). Exit from lag for *P. inhibens* is associated with the uptake and assimilation of algal-derived methylated compounds that feed into the methionine cycle and stimulate production of the polyamine spermidine (13). In contrast to our study, however, Met supplementation extended the lag time of *P. inhibens,* a possible effect of negative feedback inhibition that reduced activity in the Met cycle (13, 44). In addition to their Met-responsive lag times, *Xenorhabdus* are not predicted to synthesize spermidine as they lack an ortholog to the enzyme SpeC; however, some species have been shown to encode and reduce expression of the spermidine transport protein *potD* over the course of IJ nematodes colonization (75). Overall, this suggests that the physiology described in *P. inhibens* is distinct from the

physiology we are observing in *Xenorhabdus* and that the Met-responsive lag times are not likely associated with elevated spermidine levels.

We revealed three possible explanations for the variable, Met-responsive lag times among *Xenorhabdus*. The first is that the loss of the ArgD enzyme among some 'long' and 'intermediate' lag *Xenorhabdus* altered metabolic flux in the Lys and Thr biosynthesis pathways reducing their efficacy. Our experiments support this hypothesis as supplementation of Met significantly improves the lag of 'long' and 'intermediate' *Xenorhabdus* bacteria *in vitro,* which could lead to elevated flux through both the Lys and Thr pathway. Furthermore, deletion of *argD* from *E. coli* is not growth inhibitory due to the redundant functions of SerC and AstC; however, the loss of *argD* does alter *E. coli* growth dynamics and was reported to cause a prolonged, variable lag time in GMM compared to the wild-type (52). We would predict in this condition that reducing cellular demand for Met, permits increased metabolic activity in the Thr and Lys pathways via inhibition of Met biosynthesis via MetA, MetL, and MetJ (76-78). Indeed, X. *bovienii* (Sf-FL and Sa-IN-78) and *X. innexi* exhibited 'long', variable lag times in GMM and are not predicted to encode an ArgD ortholog. However, one strong limitation of this approach is that the genomes of these three strains are not considered complete. Of the tested genomes, only the *X. nematophila*, *X. griffiniae*, and *X. cabanillasii* genomes are complete. Furthermore, *X. nematophila,* which is predicted to encode ArgD, also has a 'long' lag in GMM and considerable experiment-to-experiment variation. *X. cabanillasii*, a 'short' lag *Xenorhabdus* that groups phylogenetically with the 'long' lag *Xenorhabdus*, does not have an ArgD ortholog. Taken together, these data suggest that the absence of ArgD may be a

predictor of a longer lag time in *Xenorhabdus* but is not alone sufficient to explain the clade-wide variability.

The second explanation is that the presence of the MtcC-like proteins in some 'short' and 'intermediate' lag *Xenorhadus* may confer a unique metabolic trait that ameliorates the prolonged lag phenotypes observed in other *Xenorhabdus* species. The *mtcC* and *mtcB* genes in *K. pneumoniae* conferred the ability of this bacterium to use Met as a sole source of sulfur and was predicted to be adaptive in host conditions where inorganic sulfate or Cys was limiting (54). The minimal medium used in our study is not limiting for inorganic sulfate, and we do not predict that utilization of Met as a sulfur source is associated with the observed lag phenotype in *X. nematophila*. Furthermore, the high sequence similarity of the MtcC-like proteins to MetB and MtcC is not a sufficient predictor of protein function as enzymes that share similar sequences can be functionally distinct (79). Given that MtcC-like proteins are generally encoded alongside *dcyD* and *yihN*, genes associated with Cys metabolism, we hypothesize that this protein may function in the detoxification of metabolic intermediates produced from Met or Cys metabolism, although this requires further testing. Accumulation of metabolites involved in Met and Cys metabolism have been shown to negatively alter bacterial growth by impeding other metabolic pathways like branched chain amino acid biosynthesis (37, 38, 60). If a prolonged *Xenorhabdus* lag is associated with an accumulation of toxic metabolites, then a putative detoxification system would be advantageous. However, other 'short' lag *Xenorhabdus* like *X. cabanillasii, X. miraniensis*, and *X. beddingii* do not appear to encode MtcC-like proteins, suggesting an alternative mechanism responsible for the evolution of

'short' lag times among *Xenorhabdus*. Furthermore, *X. doucetiae*, although it encodes an MtcC-like protein, the ORF is fragmented, suggesting that either the protein is not functional or only a domain of the protein is functional. Altogether, as with ArgD, the presence of an MtcC-like protein ortholog is a predictor of short lag among *Xenorhabdus* species.

The final proposed explanation is that 'long' lag *Xenorhabdus* utilize an alternative Met acquisition mechanism to promote exit from lag phase in GMM via the degradation of intracellular inclusion proteins. The physiological role of PixA and PixB are elusive, but there is a strong correlation between the presence of PixA and the length of *Xenorhabdus* lag time in GMM. Only one 'short' lag *Xenorhabdus, X. doucetiae*, encodes for an ortholog of PixA; however, the initial predictor of its shorter lag phenotype (e.g. the presence of an MtcC-like protein) is flawed as the protein is likely fragmented as stated above. Furthermore, the PixA ortholog of *X. doucetiae* has the highest Met richness observed (14%). One hypothesis that has been proposed previously is that PixA and/or PixB serve as endogenous reservoirs for amino acids and are degraded during starvation to restore intracellular amino acid pools (62, 64). Synthesis of these proteins has been observed among some *Xenorhabdus* bacteria when they enter stationary phase in complex, nutrient rich media and these proteins were determined to take up one-third of the cell volume (62, 63). Furthermore, deletion of *pixA* modestly alters colonization and persistence dynamics of *X. nematophila* during *S. carpocapsae* colonization, which is generally considered a nutritionally-restricted host niche (62). If PixA is truly an amino acid reserve, then we would hypothesize that it would be degraded during environmental transitions between

amino acid rich environments (e.g. LB) to amino acid deficient ones (e.g. GMM). We indirectly tested this possibility by inoculating LB-grown, exponential and stationary phase *X. nematophila* cells in GMM (**Supplemental Figure 2.14)**. Despite our prediction, we saw no significant difference in the lag phase of GMM cultures inoculated with LB-grown, exponential and stationary phase cells. Of the three predictors identified, PixA is the strongest predictor of a prolonged lag phase among *Xenorhabdus* bacteria but may not fully explain the observed lag physiology.

The results of our study provide strong evidence demonstrating physiological diversity among *Xenorhabdus* bacteria during growth in amino acid-limiting environments. Paired with our comparative genomics data, we provide possible sources of genomic variation that correlate with our physiological data which serve as possible predictors of lag length in *Xenorhabdus*. These results offer future research areas of exploration in *Xenorhabdus* and draw attention to the dearth of information available regarding the general physiology of this bacterial clade. Finally, our data also highlight an association between *Xenorhabdus* lag length and their nematode-associated lifestyles. This suggests that specific *Steinernema* nematode host niches may select for physiological traits that enhance or reduce the length of *Xenorhabdus* lag time *in vitro*.

REFERENCES

1. Bertrand RL. 2019. Lag Phase Is a Dynamic, Organized, Adaptive, and Evolvable Period That Prepares Bacteria for Cell Division. J Bacteriol 201.
2. Madar D, Dekel E, Bren A, Zimmer A, Porat Z, Alon U. 2013. Promoter activity dynamics in the lag phase of Escherichia coli. BMC Syst Biol 7:136.
3. Chu D, Barnes DJ. 2016. The lag-phase during diauxic growth is a trade-off between fast adaptation and high growth rate. Scientific Reports 6:25191.
4. Basan M, Honda T, Christodoulou D, Hörl M, Chang YF, Leoncini E, Mukherjee A, Okano H, Taylor BR, Silverman JM, Sanchez C, Williamson JR, Paulsson J, Hwa T, Sauer U. 2020. A universal trade-off between growth and lag in fluctuating environments. Nature 584:470-474.
5. Wu C, Mori M, Abele M, Banaei-Esfahani A, Zhang Z, Okano H, Aebersold R, Ludwig C, Hwa T. 2023. Enzyme expression kinetics by Escherichia coli during transition from rich to minimal media depends on proteome reserves. Nature Microbiology 8:347-359.
6. Hosono R, Kuno S. 1974. Mechanism of inhibition of bacterial growth by adenine. J Biochem 75:215-20.
7. Moreno-Gámez S, Kiviet DJ, Vulin C, Schlegel S, Schlegel K, van Doorn GS, Ackermann M. 2020. Wide lag time distributions break a trade-off between reproduction and survival in bacteria. Proceedings of the National Academy of Sciences 117:18729-18736.

8. Fridman O, Goldberg A, Ronin I, Shoresh N, Balaban NQ. 2014. Optimization of lag time underlies antibiotic tolerance in evolved bacterial populations. Nature 513:418-21.

9. Robinson TP, Aboaba OO, Kaloti A, Ocio MJ, Baranyi J, Mackey BM. 2001. The effect of inoculum size on the lag phase of Listeria monocytogenes. International Journal of Food Microbiology 70:163-173.

10. Finkel SE. 2006. Long-term survival during stationary phase: evolution and the GASP phenotype. Nature Reviews Microbiology 4:113-120.

11. Bättig P, Hathaway LJ, Hofer S, Mühlemann K. 2006. Serotype-specific invasiveness and colonization prevalence in Streptococcus pneumoniae correlate with the lag phase during in vitro growth. Microbes Infect 8:2612-7.

12. Hathaway LJ, Brugger SD, Morand B, Bangert M, Rotzetter JU, Hauser C, Graber WA, Gore S, Kadioglu A, Mühlemann K. 2012. Capsule type of Streptococcus pneumoniae determines growth phenotype. PLoS Pathog 8:e1002574.

13. Sperfeld M, Narváez-Barragán DA, Malitsky S, Frydman V, Yuda L, Rocha J, Segev E. 2024. Algal methylated compounds shorten the lag phase of Phaeobacter inhibens bacteria. Nature Microbiology 9:2006-2021.

14. Goodrich-Blair H, Clarke DJ. 2007. Mutualism and pathogenesis in Xenorhabdus and Photorhabdus: two roads to the same destination. Molecular Microbiology 64:260-268.

15. Soutar CD, Stavrinides J. 2020. Phylogenetic analysis supporting the taxonomic revision of eight genera within the bacterial order Enterobacterales. Int J Syst Evol Microbiol 70:6524-6530.

16. Murfin KE, Lee MM, Klassen JL, McDonald BR, Larget B, Forst S, Stock SP, Currie CR, Goodrich-Blair H. 2015. Xenorhabdus bovienii Strain Diversity Impacts Coevolution and Symbiotic Maintenance with Steinernema spp. Nematode Hosts. mBio 6:e00076.

17. Chaston JM, Murfin KE, Heath-Heckman EA, Goodrich-Blair H. 2013. Previously unrecognized stages of species-specific colonization in the mutualism between Xenorhabdus bacteria and Steinernema nematodes. Cellular microbiology 15:1545-1559.

18. Martens EC, Heungens K, Goodrich-Blair H. 2003. Early colonization events in the mutualistic association between Steinernema carpocapsae nematodes and Xenorhabdus nematophila bacteria. J Bacteriol 185:3147-54.

19. Cowles CE, Goodrich-Blair H. 2008. The Xenorhabdus nematophila nilABC genes confer the ability of Xenorhabdus spp. to colonize Steinernema carpocapsae nematodes. J Bacteriol 190:4121-8.

20. Snyder H, Stock SP, Kim SK, Flores-Lara Y, Forst S. 2007. New insights into the colonization and release processes of Xenorhabdus nematophila and the morphology and ultrastructure of the bacterial receptacle of its nematode host, Steinernema carpocapsae. Appl Environ Microbiol 73:5338-46.

21. Stilwell MD, Cao M, Goodrich-Blair H, Weibel DB. 2018. Studying the Symbiotic Bacterium Xenorhabdus nematophila in Individual, Living Steinernema carpocapsae Nematodes Using Microfluidic Systems. mSphere 3.

22. Flores-Lara Y, Renneckar D, Forst S, Goodrich-Blair H, Stock P. 2007. Influence of nematode age and culture conditions on morphological and physiological parameters in the bacterial vesicle of Steinernema carpocapsae (Nematoda: Steinernematidae). J Invertebr Pathol 95:110-8.

23. Martens EC, Russell FM, Goodrich-Blair H. 2005. Analysis of Xenorhabdus nematophila metabolic mutants yields insight into stages of Steinernema carpocapsae nematode intestinal colonization. Mol Microbiol 58:28-45.

24. Orchard SS, Goodrich-Blair H. 2005. Pyrimidine nucleoside salvage confers an advantage to Xenorhabdus nematophila in its host interactions. Appl Environ Microbiol 71:6254-9.

25. Mucci NC, Jones KA, Cao M, Wyatt MR, 2nd, Foye S, Kauffman SJ, Richards GR, Taufer M, Chikaraishi Y, Steffan SA, Campagna SR, Goodrich-Blair H. 2022. Apex Predator Nematodes and Meso-Predator Bacteria Consume Their Basal Insect Prey through Discrete Stages of Chemical Transformations. mSystems 7:e0031222.

26. Hussa EA, Casanova-Torres AM, Goodrich-Blair H. 2015. The Global Transcription Factor Lrp Controls Virulence Modulation in Xenorhabdus nematophila. J Bacteriol 197:3015-25.

27. Cowles KN, Cowles CE, Richards GR, Martens EC, Goodrich-Blair H. 2007. The global regulator Lrp contributes to mutualism, pathogenesis and phenotypic variation in the bacterium Xenorhabdus nematophila. Cell Microbiol 9:1311-23.

28. Orchard SS, Goodrich-Blair H. 2004. Identification and Functional Characterization of a Xenorhabdus nematophila Oligopeptide Permease. Applied and Environmental Microbiology 70:5621-5627.

29. Holdbrook R, Randall JL, Reavey CE, Tummala Y, Andongma AA, Rice A, Smith JA, Simpson SJ, Cotter SC, Wilson K. 2025. Nutribloods: Novel synthetic lepidopteran haemolymphs for understanding insect–microbe nutritional interactions in vitro. Physiological Entomology 50:264-276.

30. Richards Gregory R, Herbert Erin E, Park Y, Goodrich-Blair H. 2008. Xenorhabdus nematophila lrhA Is Necessary for Motility, Lipase Activity, Toxin Expression, and Virulence in Manduca sexta Insects. Journal of Bacteriology 190:4870-4879.

31. Richards Gregory R, Goodrich-Blair H. 2010. Examination of Xenorhabdus nematophila Lipases in Pathogenic and Mutualistic Host Interactions Reveals a Role for xlpA in Nematode Progeny Production. Applied and Environmental Microbiology 76:221-229.

32. Park D, Forst S. 2006. Co-regulation of motility, exoenzyme and antibiotic production by the EnvZ-OmpR-FlhDC-FliA pathway in Xenorhabdus nematophila. Mol Microbiol 61:1397-412.

33. Cowles KN, Goodrich-Blair H. 2005. Expression and activity of a Xenorhabdus nematophila haemolysin required for full virulence towards Manduca sexta insects. Cell Microbiol 7:209-19.

34. Chaston JM, Suen G, Tucker SL, Andersen AW, Bhasin A, Bode E, Bode HB, Brachmann AO, Cowles CE, Cowles KN, Darby C, de Léon L, Drace K, Du Z, Givaudan A, Herbert Tran EE, Jewell KA, Knack JJ, Krasomil-Osterfeld KC, Kukor R, Lanois A, Latreille P, Leimgruber NK, Lipke CM, Liu R, Lu X, Martens EC, Marri PR, Médigue C, Menard ML, Miller NM, Morales-Soto N, Norton S, Ogier JC, Orchard SS, Park D, Park Y, Qurollo BA, Sugar DR, Richards GR, Rouy Z, Slominski B, Slominski K, Snyder H, Tjaden BC, van der Hoeven R, Welch RD, Wheeler C, Xiang B, Barbazuk B, et al. 2011. The entomopathogenic bacterial endosymbionts Xenorhabdus and Photorhabdus: convergent lifestyles from divergent genomes. PLoS One 6:e27909.

35. Bhasin A, Chaston JM, Goodrich-Blair H. 2012. Mutational analyses reveal overall topology and functional regions of NilB, a bacterial outer membrane protein required for host association in a model of animal-microbe mutualism. J Bacteriol 194:1763-76.

36. Miller JH. 1972. Experiments in molecular genetics. (No Title).

37. Harris CL. 1981. Cysteine and growth inhibition of Escherichia coli: threonine deaminase as the target enzyme. J Bacteriol 145:1031-5.

38. Imlay KRC, Korshunov S, Imlay JA. 2015. Physiological Roles and Adverse Effects of the Two Cystine Importers of Escherichia coli. Journal of Bacteriology 197:3629-3644.

39. Mosteller RD, Goldstein RV. 1975. Unusual sensitivity of Escherichia coli to adenine or adenine plus histidine. J Bacteriol 123:750-1.

40. Davis BD. 1951. Inhibition of Escherichia coli by p-aminobenzoic acid and its reversal by p-hydroxybenzoic acid. J Exp Med 94:243-54.

41. Reitzer L. 2004. Biosynthesis of Glutamate, Aspartate, Asparagine, L-Alanine, and D-Alanine. EcoSal Plus 1:10.1128/ecosalplus.3.6.1.3.

42. Kikuchi Y, Kojima H, Tanaka T. 1999. Mutational analysis of the feedback sites of lysine-sensitive aspartokinase of Escherichia coli. FEMS Microbiol Lett 173:211-5.

43. Boy E, Patte JC. 1972. Multivalent repression of aspartic semialdehyde dehydrogenase in Escherichia coli K-12. J Bacteriol 112:84-92.

44. Hondorp ER, Matthews RG. 2006. Methionine. EcoSal Plus 2.

45. Patte J. 1996. Biosynthesis of Threonin and Lysine, Chap. 32 (1) in Escherichia coli and Salmonella, Cellular and Molecular Biology. 1996.

46. Zdych E, Peist R, Reidl J, Boos W. 1995. MalY of Escherichia coli is an enzyme with the activity of a beta C-S lyase (cystathionase). J Bacteriol 177:5035-9.

47. González JC, Peariso K, Penner-Hahn JE, Matthews RG. 1996. Cobalamin-independent methionine synthase from Escherichia coli: a zinc metalloenzyme. Biochemistry 35:12228-34.

48. Kooliyottil R, Inman F, 3rd, Mandjiny S, Holmes L. 2014. Physiological Constants of the Entomopathogenic Bacterium Xenorhabdus nematophila Determined by Microbial Growth Kinetics. ISRN Microbiol 2014:834054.

49. Givaudan A, Baghdiguian S, Lanois A, Boemare N. 1995. Swarming and Swimming Changes Concomitant with Phase Variation in Xenorhabdus nematophilus. Appl Environ Microbiol 61:1408-13.

50. Smigielski AJ, Akhurst RJ, Boemare NE. 1994. Phase Variation in Xenorhabdus nematophilus and Photorhabdus luminescens: Differences in Respiratory Activity and Membrane Energization. Appl Environ Microbiol 60:120-5.

51. Grossman AS, Mauer TJ, Forest KT, Goodrich-Blair H. 2021. A Widespread Bacterial Secretion System with Diverse Substrates. mBio 12:e0195621.

52. Lal PB, Schneider BL, Vu K, Reitzer L. 2014. The redundant aminotransferases in lysine and arginine synthesis and the extent of aminotransferase redundancy in Escherichia coli. Mol Microbiol 94:843-56.

53. Gophna U, Bapteste E, Doolittle WF, Biran D, Ron EZ. 2005. Evolutionary plasticity of methionine biosynthesis. Gene 355:48-57.

54. Seiflein TA, Lawrence JG. 2006. Two transsulfurylation pathways in Klebsiella pneumoniae. J Bacteriol 188:5762-74.

55. Hasebe F. 2021. MetW regulates the enzymatic activity of MetX in Pseudomonas. Biosci Biotechnol Biochem 85:351-358.

56. Foglino M, Borne F, Bally M, Ball G, Patte JC. 1995. A direct sulfhydrylation pathway is used for methionine biosynthesis in Pseudomonas aeruginosa. Microbiology (Reading) 141 (Pt 2):431-9.

57. Bastard K, Perret A, Mariage A, Bessonnet T, Pinet-Turpault A, Petit J-L, Darii E, Bazire P, Vergne-Vaxelaire C, Brewee C, Debard A, Pellouin V, Besnard-Gonnet M, Artiguenave F, Médigue C, Vallenet D, Danchin A, Zaparucha A, Weissenbach J, Salanoubat M, de Berardinis V. 2017. Parallel evolution of non-homologous isofunctional enzymes in methionine biosynthesis. Nature Chemical Biology 13:858-866.

58. Yamamoto K, Nonaka G, Ozawa T, Takumi K, Ishihama A. 2015. Induction of the Escherichia coli yijE gene expression by cystine. Biosci Biotechnol Biochem 79:218-22.

59. Soutourina J, Blanquet S, Plateau P. 2001. Role of d-Cysteine Desulfhydrase in the Adaptation of Escherichia coli to d-Cysteine *. Journal of Biological Chemistry 276:40864-40872.

60. Nagasawa T, Ishii T, Kumagai H, Yamada H. 1985. D-Cysteine desulfhydrase of Escherichia coli. Purification and characterization. Eur J Biochem 153:541-51.

61. Mahmoud SA, Chien P. 2018. Regulated Proteolysis in Bacteria. Annu Rev Biochem 87:677-696.

62. Goetsch M, Owen H, Goldman B, Forst S. 2006. Analysis of the PixA inclusion body protein of Xenorhabdus nematophila. J Bacteriol 188:2706-10.

63. Lucas J, Goetsch M, Fischer M, Forst S. 2018. Characterization of the pixB gene in Xenorhabdus nematophila and discovery of a new gene family. Microbiology (Reading) 164:495-508.

64. Couche GA, Gregson RP. 1987. Protein inclusions produced by the entomopathogenic bacterium Xenorhabdus nematophilus subsp. nematophilus. J Bacteriol 169:5279-88.

65. Aussel L, Ezraty B. 2021. Methionine Redox Homeostasis in Protein Quality Control. Front Mol Biosci 8:665492.

66. Schubert C, Zedler S, Strecker A, Unden G. 2021. L-Aspartate as a high-quality nitrogen source in Escherichia coli: Regulation of L-aspartase by the nitrogen regulatory system and interaction of L-aspartase with GlnB. Molecular Microbiology 115:526-538.

67. Strecker A, Schubert C, Zedler S, Steinmetz P, Unden G. 2018. DcuA of aerobically grown Escherichia coli serves as a nitrogen shuttle (L-aspartate/fumarate) for nitrogen uptake. Molecular Microbiology 109:801-811.

68. San-Blas E, Gowen SR, Pembroke B. 2008. Steinernemafeltiae: Ammonia triggers the emergence of their infective juveniles. Experimental Parasitology 119:180-185.

69. Bouvet OM, Grimont PA. 1987. Diversity of the phosphoenolpyruvate/glucose phosphotransferase system in the Enterobacteriaceae. Ann Inst Pasteur Microbiol 138:3-13.

70. Liang Q, Zhang F, Li Y, Zhang X, Li J, Yang P, Qi Q. 2015. Comparison of individual component deletions in a glucose-specific phosphotransferase system revealed their different applications. Sci Rep 5:13200.

71. Horler RS, Vanderpool CK. 2009. Homologs of the small RNA SgrS are broadly distributed in enteric bacteria but have diverged in size and sequence. Nucleic Acids Res 37:5465-76.

72. Richards GR, Vivas EI, Andersen AW, Rivera-Santos D, Gilmore S, Suen G, Goodrich-Blair H. 2009. Isolation and characterization of Xenorhabdus nematophila transposon insertion mutants defective in lipase activity against Tween. J Bacteriol 191:5325-31.

73. Jubelin G, Pagès S, Lanois A, Boyer MH, Gaudriault S, Ferdy JB, Givaudan A. 2011. Studies of the dynamic expression of the Xenorhabdus FliAZ regulon reveal atypical iron-dependent regulation of the flagellin and haemolysin genes during insect infection. Environ Microbiol 13:1271-84.

74. Grossman AS, Escobar CA, Mans EJ, Mucci NC, Mauer TJ, Jones KA, Moore CC, Abraham PE, Hettich RL, Schneider L, Campagna SR, Forest KT, Goodrich-Blair H. 2022. A Surface Exposed, Two-Domain Lipoprotein Cargo of a Type XI Secretion System Promotes Colonization of Host Intestinal Epithelia Expressing Glycans. Frontiers in microbiology 13:800366-800366.

75. An R, Grewal PS. 2016. Comparative Analysis of Xenorhabdus koppenhoeferi Gene Expression during Symbiotic Persistence in the Host Nematode. PLOS ONE 11:e0145739.

76. Shoeman R, Coleman T, Redfield B, Greene RC, Smith AA, Saint-Girons I, Brot N, Weissbach H. 1985. Regulation of methionine synthesis in Escherichia coli: effect of metJ gene product and S-adenosylmethionine on the in vitro expression of the metB, metL and metJ genes. Biochem Biophys Res Commun 133:731-9.

77. Born TL, Blanchard JS. 1999. Enzyme-catalyzed acylation of homoserine: mechanistic characterization of the Escherichia coli metA-encoded homoserine transsuccinylase. Biochemistry 38:14416-23.

78. Patte JC, Le Bras G, Cohen GN. 1967. Regulation by methionine of the synthesis of a third aspartokinase and of a second homoserine dehydrogenase in Escherichia coli K 12. Biochim Biophys Acta 136:245-7.

79. Pearson WR. 2013. An introduction to sequence similarity ("homology") searching. Curr Protoc Bioinformatics Chapter 3:3.1.1-3.1.8.

80. Xu J, Lohrke S, Hurlbert IM, Hurlbert RE. 1989. Transformation of Xenorhabdus nematophilus. Appl Environ Microbiol 55:806-12.

81. Neidhardt FC, Bloch PL, Smith DF. 1974. Culture medium for enterobacteria. J Bacteriol 119:736-47.

82. Christopherson MR, Lambrecht JA, Downs D, Downs DM. 2012. Suppressor analyses identify threonine as a modulator of ridA mutant phenotypes in Salmonella enterica. PLoS One 7:e43082.

83. Camacho C, Coulouris G, Avagyan V, Ma N, Papadopoulos J, Bealer K, Madden TL. 2009. BLAST+: architecture and applications. BMC Bioinformatics 10:421.

84. Vallenet D, Calteau A, Cruveiller S, Gachet M, Lajus A, Josso A, Mercier J, Renaux A, Rollin J, Rouy Z, Roche D, Scarpelli C, Médigue C. 2017. MicroScope in 2017: an expanding and evolving integrated resource for community expertise of microbial genomes. Nucleic Acids Res 45:D517-d528.

85. Community TG. 2024. The Galaxy platform for accessible, reproducible, and collaborative data analyses: 2024 update. Nucleic Acids Research 52:W83-W94.

86. Katoh K, Standley DM. 2013. MAFFT Multiple Sequence Alignment Software Version 7: Improvements in Performance and Usability. Molecular Biology and Evolution 30:772-780.

87. Katoh K, Misawa K, Kuma K, Miyata T. 2002. MAFFT: a novel method for rapid multiple sequence alignment based on fast Fourier transform. Nucleic Acids Res 30:3059-66.

88. Vaidya G, Lohman DJ, Meier R. 2011. SequenceMatrix: concatenation software for the fast assembly of multi-gene datasets with character set and codon information. Cladistics 27:171-180.

89. Capella-Gutiérrez S, Silla-Martínez JM, Gabaldón T. 2009. trimAl: a tool for automated alignment trimming in large-scale phylogenetic analyses. Bioinformatics 25:1972-3.

90. Edgar RC. 2022. Muscle5: High-accuracy alignment ensembles enable unbiased assessments of sequence homology and phylogeny. Nature Communications 13:6968.

91. Minh BQ, Schmidt HA, Chernomor O, Schrempf D, Woodhams MD, von Haeseler A, Lanfear R. 2020. IQ-TREE 2: New Models and Efficient Methods for Phylogenetic Inference in the Genomic Era. Mol Biol Evol 37:1530-1534.

92. Hoang DT, Chernomor O, von Haeseler A, Minh BQ, Vinh LS. 2018. UFBoot2: Improving the Ultrafast Bootstrap Approximation. Mol Biol Evol 35:518-522.

93. Kalyaanamoorthy S, Minh BQ, Wong TKF, von Haeseler A, Jermiin LS. 2017. ModelFinder: fast model selection for accurate phylogenetic estimates. Nat Methods 14:587-589.

94. Letunic I, Bork P. 2024. Interactive Tree of Life (iTOL) v6: recent updates to the phylogenetic tree display and annotation tool. Nucleic Acids Res 52:W78-w82.

APPENDIX

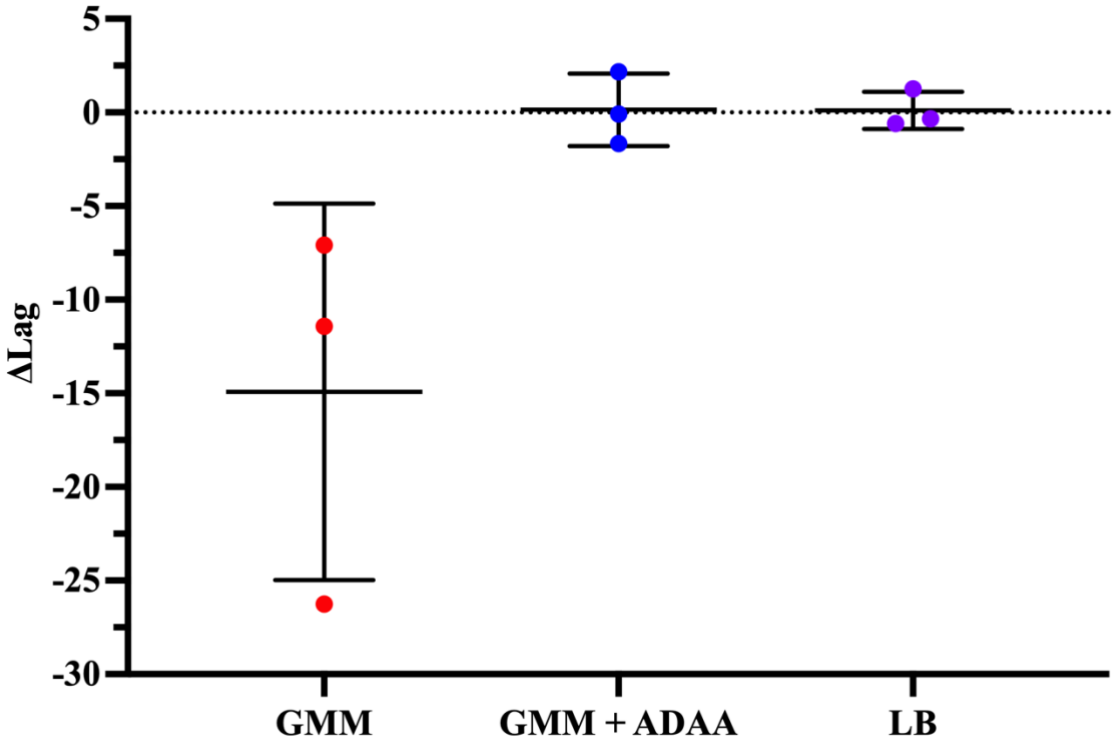


Figure 2.8: *X. nematophila* growth in GMM is not due to eventual accumulation of a minority population adapted to growth in this condition.

The change in lag time between passaged and unpassaged *X. nematophila* in LB (purple), GMM (red), and GMM+ADAA (blue). Data points represent three biological replicates (each representing 3 technical replicates). Error bars indicate ±1 SD. Data points above a *Δ*lag of 0 would indicate that passaged strains are adapted to growth in the tested medium, while those equal to or less than 0 indicate that passaged strains are no more adapted to growth in the condition than are the initial inoculum.

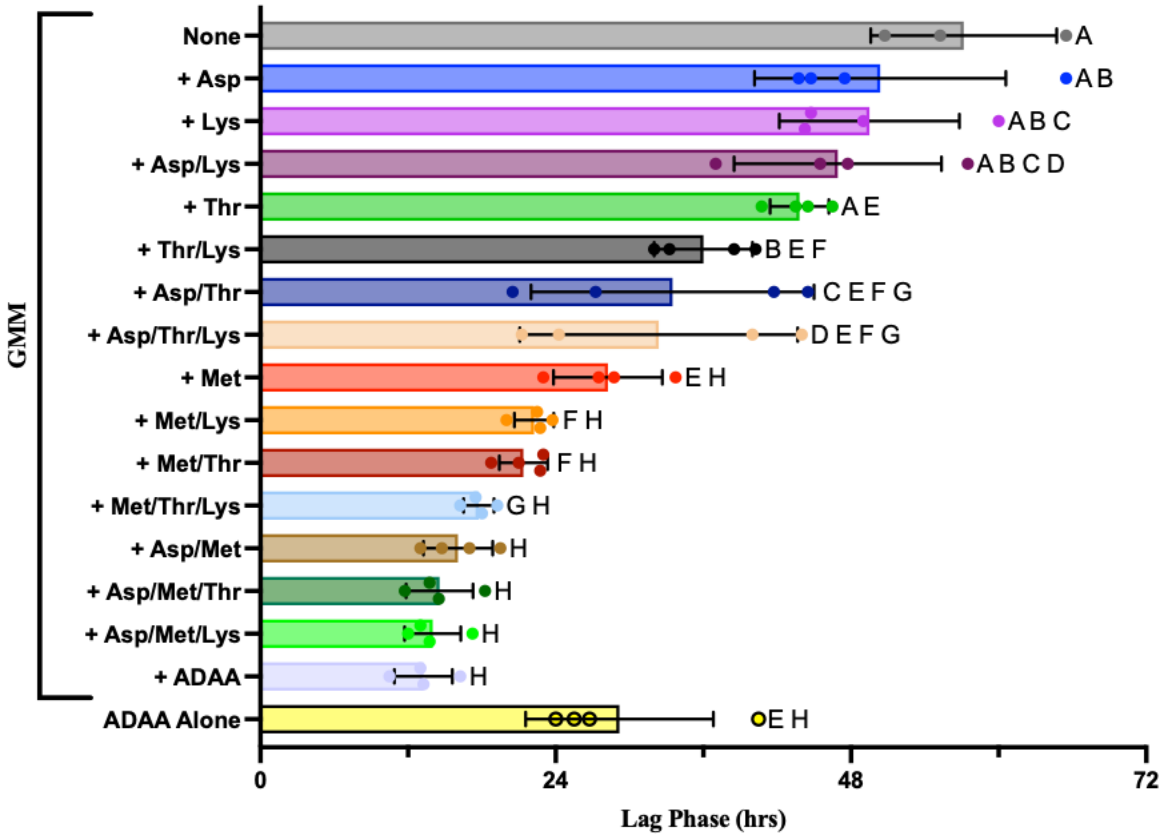


Figure 2.9: The lag time of X. nematophila in GMM is primarily responsive to methionine.

Extended figure of the average lag time of *X. nematophila* (3-4 biological replicates, ±1SD) in GMM alone (none) or supplemented (+) with different combinations of the ADAA. The data was analyzed via a One-way ANOVA and significance is shown using letter designations (A-H).

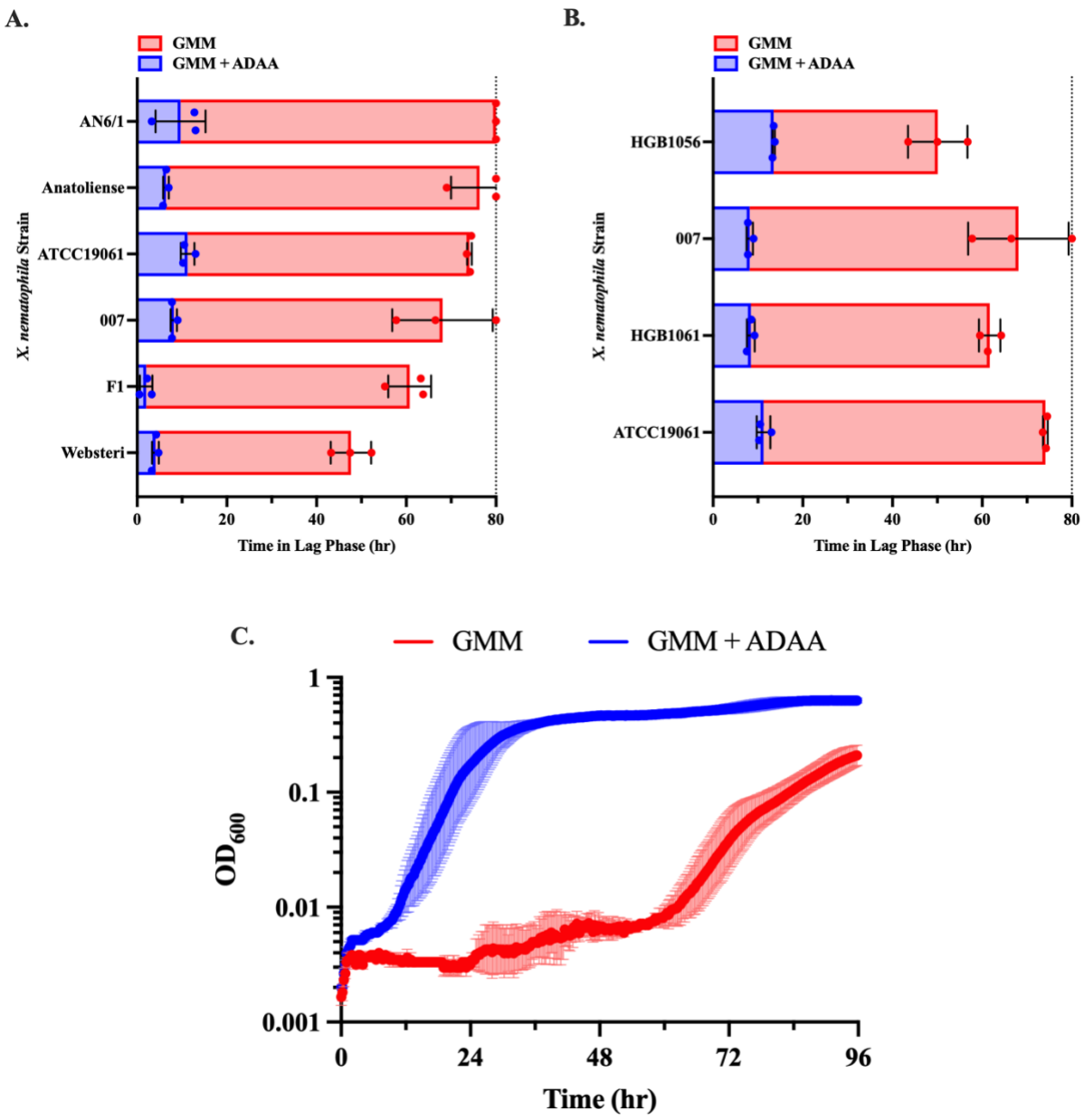


Figure 2.10: *X. nematophila* lag in GMM is minimally influenced by intraspecific variation.

A) The average lag times of *X. nematophila* isolates (3 biological replicates) in GMM (red) or GMM+ADAA (blue). Error bars indicate ±1 SD. **B)** Comparison of the average lag times of *X. nematophila* primary and secondary form variants in GMM or GMM+ADAA among two distinct isolates HGB800 and HGB007. **C)** Growth curve of *X. nematophila* AN6/1 in GMM to confirm eventual growth in GMM (3 biological replicates, ±1 SD).

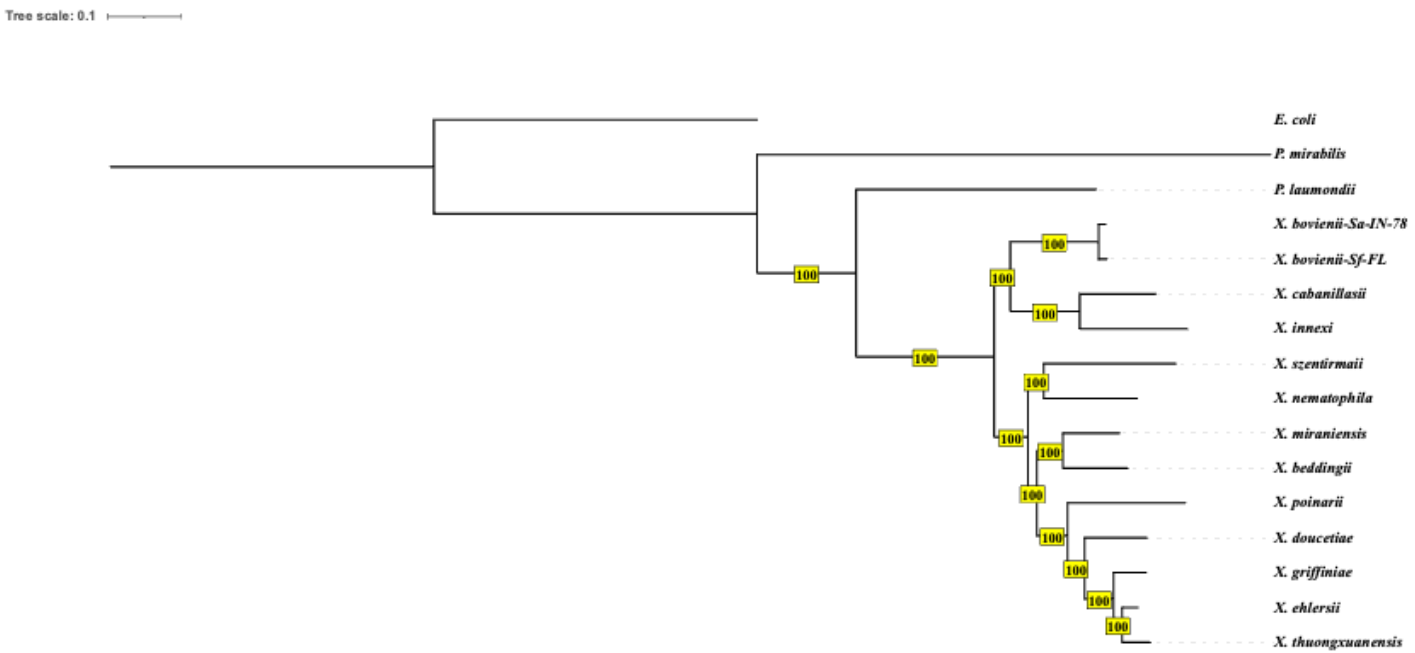


Figure 2.11: Phylogenetic tree of tested *Xenorhabdus* species (and other selected Enterobacterales).

Numbers on the branches indicated bootstrap support values. Only bootstraps greater than 80% are shown.

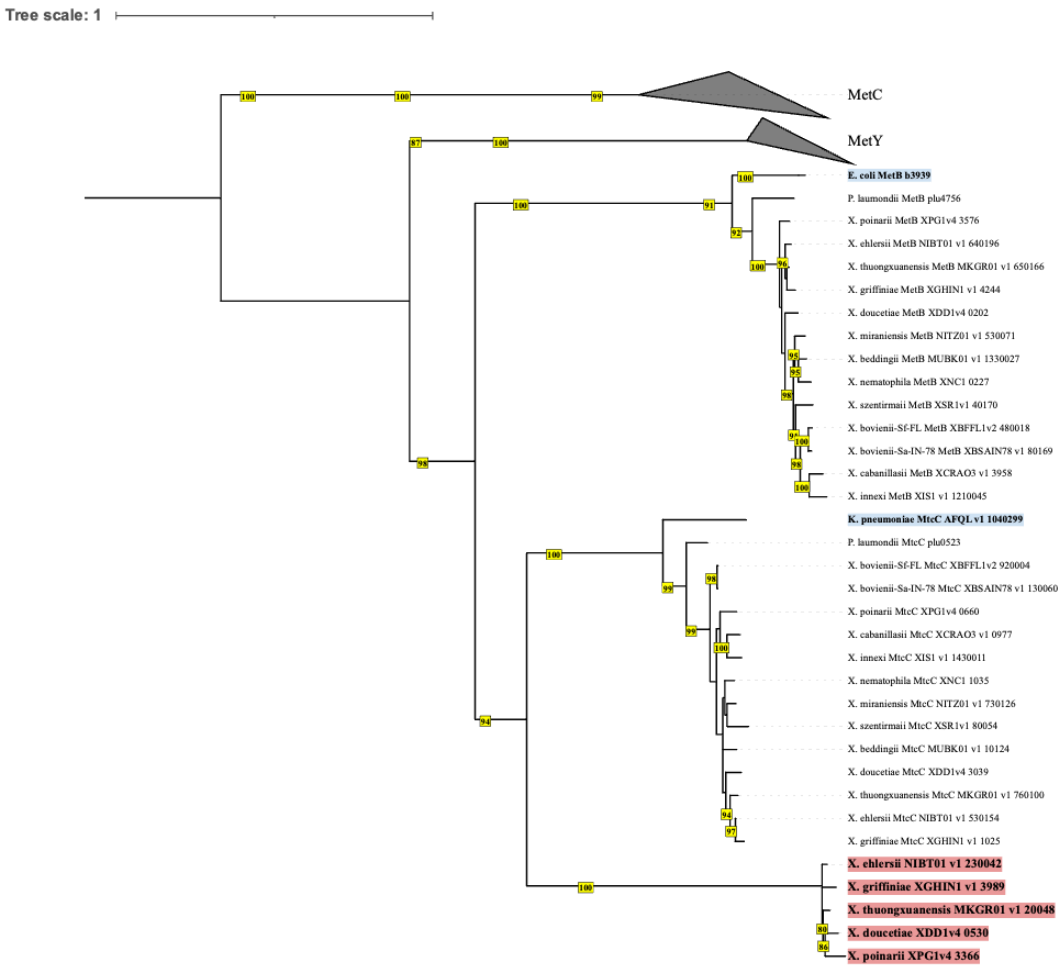


Figure 2.12: Phylogenetic tree of MetB, MetC, MetY, MtcC, and MtcC-like proteins encoded in the genomes of *Xenorhabdus* species (and other selected *Enterobacterales*).

The MetY and MetC clades are collapsed for easier visualization of the MetB, MtcC, and MtcC-like protein phylogenetic relationships Numbers on the branches indicated bootstrap support values. Only bootstraps greater than 80% are shown.

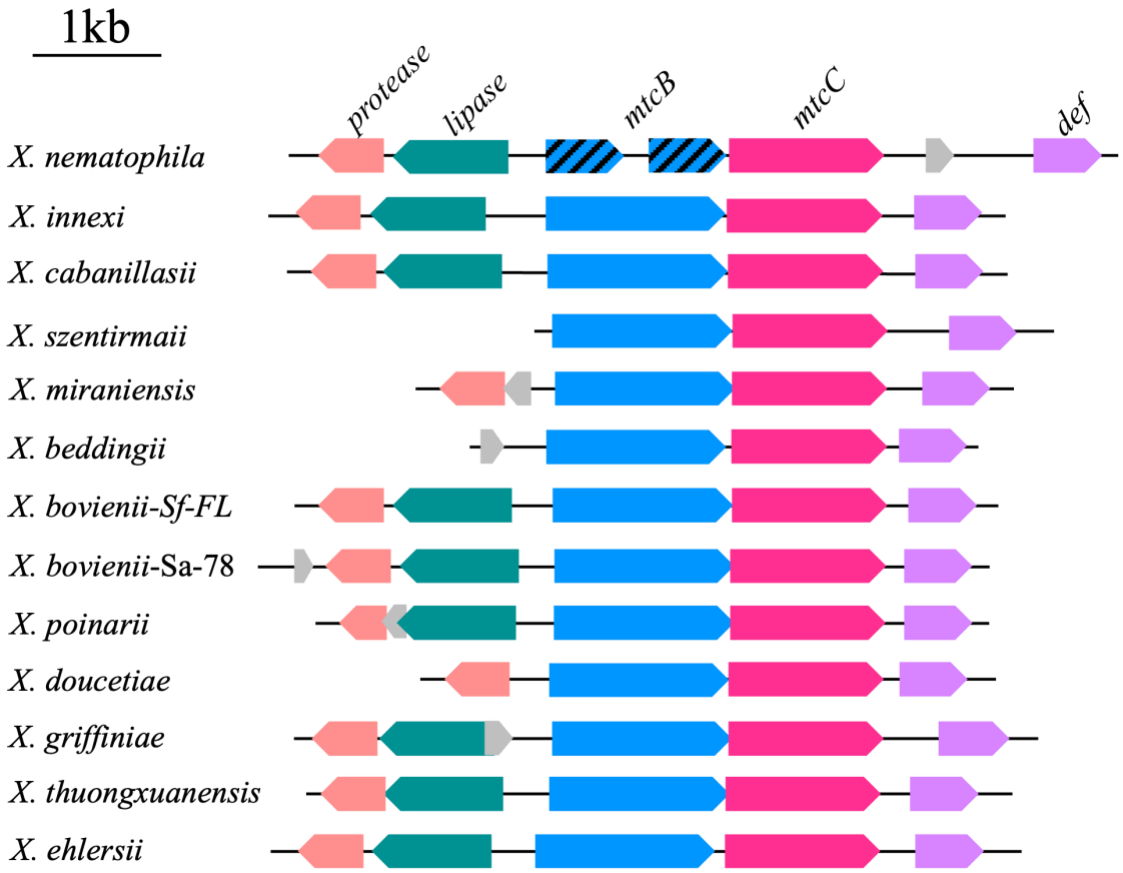


Figure 2.13: Genomic neighborhood of *Xenorhabdus* mtcC locus. Predicted ORFs with lines through them indicate if the sequence is not contiguous.

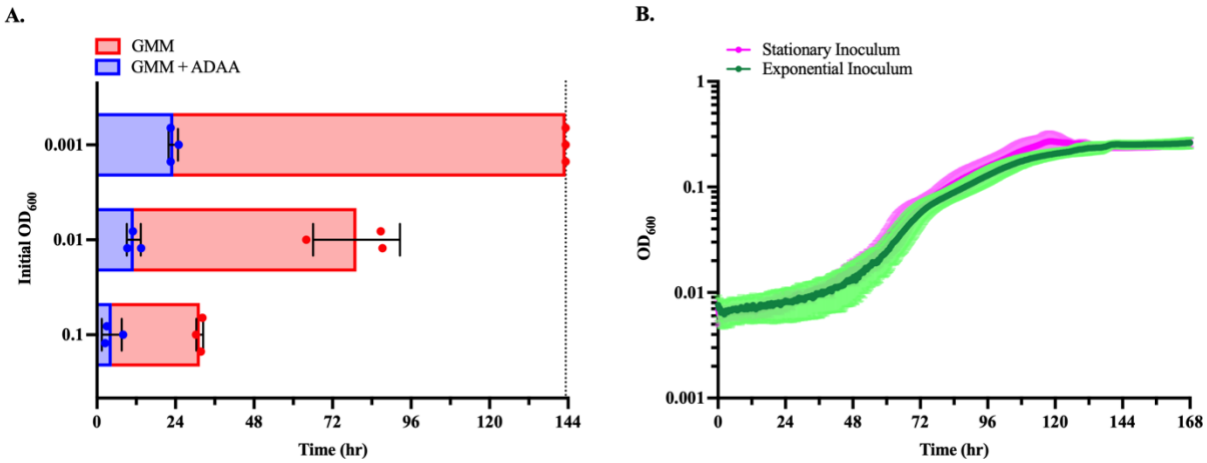


Figure 2.14: Inoculum density but not growth phase alters *X. nematophila* lag phase length.

A) The impact of initial inoculum size on *X. nematophila* lag time in GMM with (blue) or without (red) the ADAA over a 144h experiment. Data points represent biological replications and error bars indicate ±1 SD. **B)** Growth of X. *nematophila* exponential (green) and stationary phase (pink) cells when grown in GMM. Curves are the average of three biological replicates and error bars indicate ±1 SD.

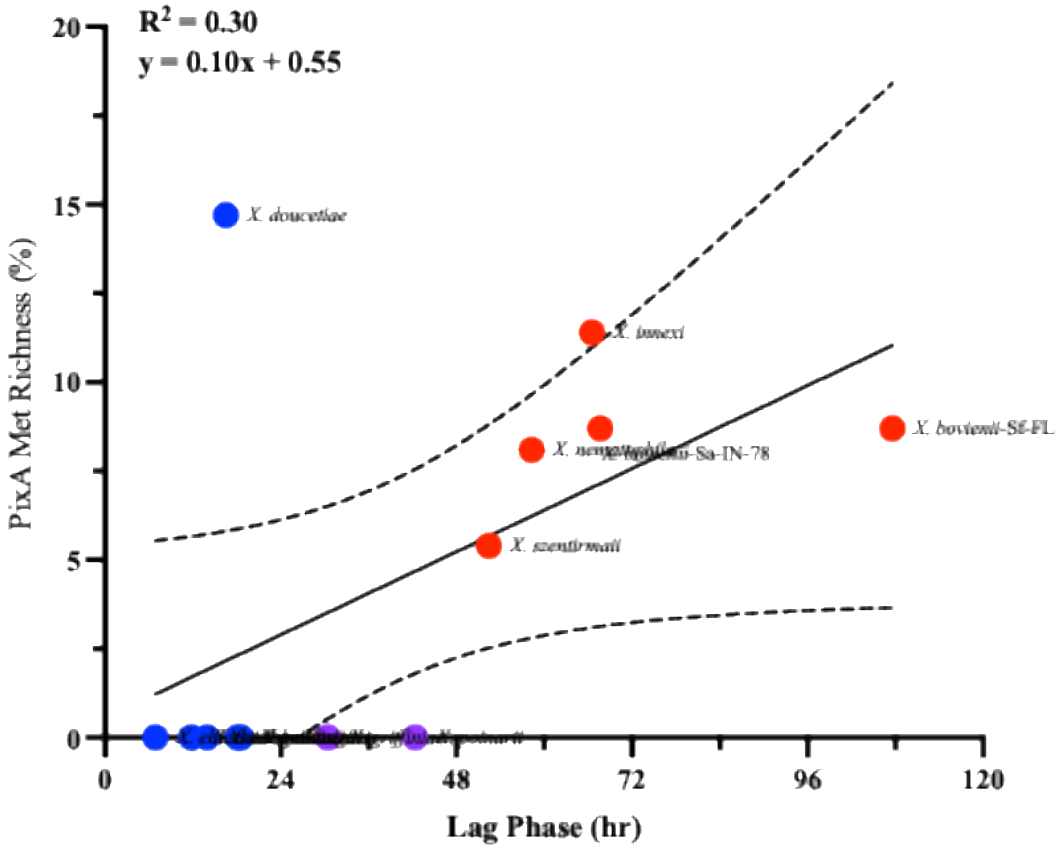


Figure 2.15: Correlation between PixA Met richness and *Xenorhabdus* lag length.

The average lag time of each tested *Xenorhabdus* species (x-axis) in GMM from Figure 5 plotted against the Met Richness of their PixA ortholog if it is encoded. Data points are color coated based on their short (blue), intermediate (purple), and long (red) lag phenotypes determined in Figure 5. These data were analyzed via a simple linear regression with the line of best fit being represented by the solid black line ($y = 0.10x + 0.55$, $R^2 = 0.30$) Dashed lines represent ±1 CI.

CHAPTER 3: SYMBIONT METHIONINE BIOSYNTHESIS POSITIVELY INFLUENCES MUTUALISTIC ASSOCIATIONS WITH *S. FELTIAE* NEMATODES BY OPTIMIZING INTESTINAL COLONIZATION AND SUPPORTING FECUNDITY.

Authors: Cameron Moore and Heidi Goodrich-Blair

Author Contributions

I developed the methodology and performed all experimental analyses presented in this chapter. I also contributed to project conceptualization, statistical analysis, and wrote the initial manuscript.

Heidi Goodrich-Blair secured funding and contributed to project conceptualization, manuscript editing, and writing

ABSTRACT

Animals are auxotrophs for multiple amino acids including L-methionine and must acquire them from digestion of dietary protein, degradation of endogenous protein reserves, or from amino acid prototrophic constituents of their microbiome. In entomopathogenic nematodes of the *Steinernema* clade, derivation of essential amino acids is facilitated by consumption of their obligate *Xenorhabdus* symbionts for which they form specific, co-adapting, and co-evolving mutualisms. In this study we investigate how L-methionine biosynthesis in *X. bovienii*-Sf-FL contributes to aspects of its mutualistic partnership with *S. feltiae*-FL nematodes. Deletion of the *metE* gene in *X. bovienii*-Sf-FL inhibits bacterial outgrowth within the receptacle of *S. feltiae*-FL infective juvenile nematodes resulting in a colonization defect. Furthermore, the *metE* deficient *X. bovienii*-Sf-FL symbiont suppresses nematode reproduction *in vitro* and *in vivo* resulting in significant reduction in *S. feltiae*-FL infective juvenile emergence phenotypes. These findings suggest that Met prototrophy in the *X. bovienii*-Sf-FL symbiont is essential for maintaining its mutualistic association with its cognate nematode host.

INTRODUCTION

Amino acids are essential metabolites for all living organisms as they are required for the synthesis of proteins [1]. Many organisms like bacteria, archaea, plants, and fungi can synthesize amino acids *de novo* provided sufficient levels of carbon, nitrogen, and sulfur are available [2-4]. Unlike these organisms, all forms of animal life are auxotrophic for certain amino acids, hereafter called essential amino acids (EAAs), the identities of which vary by clade [1, 5, 6]. Dietary dependence for amino acids among animals is thought to coincide with the Cambrian explosion, and it has been speculated that the loss of amino acid prototrophy may have contributed to the evolutionary success of animals during this era [7]. Animals acquire EAAs primarily from dietary sources or from members of their microbiomes [8]. The contributions of microbial symbionts varies considerably based on the animal host's diet. For example, animals with diets rich in amino acids (e.g., carnivores and omnivores) are less dependent on microbial amino acid synthesis than those with amino acid limited diets (e.g., herbivores) [8, 9]. Indeed, acquisition of nutrients like amino acids from microbial symbionts appears to allow certain animal species to expand their dietary range and succeed on seemingly nutrient-poor food sources [9]. To this end, microbial provisioning of amino acids is likely a pervasive aspect of animal biology; however, it is unclear as to how dependent certain animal species are on their microbial symbionts for EAA relative to dietary EAA acquisition.

Entomopathogenic nematodes (EPNs) of the *Steinernema* clade present a distinctive opportunity by which to study how microorganisms provision nutrients to an animal host's diet. Most, if not all, *Steinernema* are obligately associated with mutualistic

Xenorhabdus bacteria throughout their lifecycle where together they infect and kill naïve insect hosts [10-12]. Within the insect cadaver *Xenorhabdus* degrade insect host tissue and utilize the liberated nutrients to support bacterial population growth [13-15]. Consequently, the *Steinernema* nematode host feeds on the growing *Xenorhabdus* population as its primary food source which supports nematode growth, reproduction, and development [15]. This trophic relationship has been best characterized in the *X. nematophila* - *S. carpocapsae* mutualism where myriad bacterial factors (e.g, exoenzymes, competition factors, transcriptional regulation, etc.) have been shown to positively influence nematode fitness in natural (e.g. insect) and synthetic (e.g. laboratory) environments [16-18]. In addition to their role in their nematode host's diet, *Xenorhabdus* also colonize and proliferate within the anterior intestine of migratory, infective juvenile (IJ) stage *Steinernema* nematodes in the luminal space of their receptacle tissue [19, 20]. In *X. nematophila,* disruption of specific amino acid and B vitamin biosynthesis pathways (e.g. Thr, Met, pyroxidine, *p*-aminobenzoic acid) can reduce or even abolish outgrowth and colonization within the receptacle of its nematode host *S. carpocapsae* during its IJ life stage suggesting that in this environment these nutrients are growth-limiting [21, 22]. Other biosynthetic disruptions, however, do not negatively influence *X. nematophila* colonization dynamics suggesting that these bacteria may have access to these nutrients within the nematode receptacle [21, 22]. As the only free-living stage of the *Steinernema* lifecycle, IJ fitness is critical to the evolutionary success of this animal. The IJ must persist in soil environments long enough to identify and infect a new insect host, or the lineage will perish. *Xenorhabdus* colonization and outgrowth reduces IJ longevity under certain

environmental conditions, yet the absence of these symbionts reduces nematode fitness, due to their role in insect virulence and bioconversion [11, 23, 24]. Given that *Steinernema* nematodes are auxotrophic for many nutrients including the EAAs, it has been largely inferred that they acquire these nutrients from their *Xenorhabdus* symbionts, which are predicted to be prototrophic for all 20 of the common amino acids ([6, 25], Chapter 2).

In their natural context, *Steinernema* and their *Xenorhabdus* symbionts, compete with other EPNs as well as saprophytic microbes, for competitive dominance within the insect cadaver [18, 26]. When EPN coinfections occur, *Steinernema* nematodes are exposed to non-cognate *Xenorhabdus* bacteria, yet choose to preferentially feed and reproduce upon their cognate symbiont [10, 27, 28]. This species or strain-level dietary specificity is imperative for *Steinernema* fitness as feeding on a non-cognate *Xenorhabdus* can negatively impact nematode development, reproduction, insect infectivity, and in some cases survival [10, 28]. For example, *S. feltiae*-FL associates and feeds upon its cognate symbiont *X. bovienii*-Sf-FL but is killed when reared on *X. bovienii* symbionts derived from *S. intermedium* or *S. affine*-IN-78 nematodes *in vitro* [11, 28]. This suggests that evolutionary success for *Steinernema* nematodes hinges on their ability to recognize and reproduce upon their cognate *Xenorhabdus* symbiont while evading competitor *Xenorhabdus* symbionts. Across the *Xenorhabdus* clade, intra-and inter-specific genomic variation is contained largely within the mobilome of these bacteria thus suggesting that these organisms were physiologically similar [26, 29]. However in Chapter 2 of this dissertation, we demonstrated that *Xenorhabdus* species are physiologically diverse particularly in regard to their metabolic demand for the EAA L-methionine (Met). Certain

Xenorhabdus species, including *X. nematophila*, exhibit a high biosynthetic demand for Met that manifest in the form of a prolonged lag phase when cultivated in Met-deficient growth media (Chapter 2). However, this phenotype is not universally conserved among *Xenorhabdus* strains and is not linked to their evolutionary lineage, suggesting that a high metabolic demand for Met may reflect niche-specific adaptation. This is supported by evidence from *X. nematophila* demonstrating that prototrophy for Met is required for optimal colonization and persistence within the intestine of its *S. carpocapsae* host [21]. Given that *Xenorhabdus-Steinernema* associations are highly specific, co-adapting, and co-evolving, we hypothesize that this elevated demand for Met *in vitro* may be linked to the unique metabolic demands these bacteria may face in their nematode host niches.

Met is required for many biological phenomena across domains of life [3, 30]. Most notably, Met is critical for protein translation initiation and is a precursor for the essential metabolite S-adenosylmethionine (AdoMet) which serves as the primary methyl donor in many essential biochemical processes [3, 31]. Met biosynthetic pathways among prototrophic organisms like bacteria can vary mechanistically, and these diverse biosynthetic strategies can be adaptive under specific environmental conditions [30, 32-34]. Both Met prototrophy and auxotrophy exist among animal-associated microbes, with auxotrophy forming in microbes that have regular access to Met within their animal host niche [35-37]. Further, metabolic activity within Met biosynthetic pathways can be positively or negatively impacted by environmental parameters such as the availability of exogenous co-factors, temperature, and reactive oxygen stress which can vary depending on conditions within an animal host [38-41]. Finally, Met synthesis is also energetically

costly as it incorporates metabolites from aspartate-derived amino acid biosynthesis, cysteine biosynthesis, and the folate cycle [42-44]. Consistent with these observations, a balance of Met foraging and biosynthetic strategies are employed by animal-associated microbes and these activities can positively and negatively impact animal host fitness [21, 45-47].

In this study, we investigate the impact of Met biosynthesis on the mutualistic associations between the EPN *S. feltiae*-FL and its symbiont *X. bovienii*-Sf-FL. Here we demonstrate that disruption of Met biosynthesis in *X. bovienii*-Sf-FL reduces the bacterium's ability to colonize and support the fecundity of *S. feltiae*-FL nematodes *in vitro*. We also observe that prolonged association with a Met auxotrophic *X. bovienii*-Sf-FL symbiont reduces *S. feltiae*-FL fecundity of during infections of *Galleria mellonella,* suggesting that Met prototrophy is critical for the evolutionary success of the *X. bovienii* - *S. feltiae*-FL symbiotic association.

MATERIALS AND METHODS

Bacterial Strains and Cultivation Conditions

All Xenorhabdus bacteria used in this study were cryopreserved in 20% glycerol stocks at -80˚C. Strains were revived by streaking on Luria-Bertani (LB) agar plates supplemented with 0.1% sodium pyruvate and grown for 16-24 h at 30˚C [48]. Bacterial overnight cultures were non-clonal to ensure representation of all potential natural variants in the assays [49, 50]. Where appropriate the growth medium was supplemented with kanamycin (Kan, 50 µg/mL), ampicillin (Amp, 150 µg/mL), and erythromycin (Erm, 200 µg/mL), diaminopimelic acid (DAP, 0.3 mM), and L-methionine (Met, 0.2 mM, Sigma Aldrich). A

filter-sterilized (0.22 µm pore, Avantor), MOPS-based (40 mM, 3-(N-morpholino)-propanesulfonic acid, MP Biomedicals) glucose minimal medium (11 mM, GMM, Fisher Scientific) was used to cultivate X. bovienii-Sf-FL strains (Chapter 2, [51]). Nematode-bacterial co-cultures were conducted on lipid agar (LA) which contains 8 g/L of nutrient broth powder (Oxoid), 5 g/L of yeast extract (Research Products International), 2 mg/mL of MgCl2·6H2O (Acros Organic), 0.7% corn syrup (MP Biomedical) and 0.4% corn oil (Crisco), and 15 g/L of agar (Fisher Scientific) [52]. Overnight cultures were normalized to an OD600 of 1.0, before 600 µL of bacterial culture were seeded onto the lipid agar medium. For competition experiments, 300 µL of wild-type and mutant bacteria (both cultures at an OD600 of 1.0) were seeded onto lipid agar. To generate confluent bacterial lawns, the lipid agar was incubated at 25˚C for 48 h.

***Xenorhabdus metE* Deletion and Complement Generation**

X. bovienii-Sf-FL *metE* deletion was generated following a similar approach to that described previously [21]. Briefly, genomic DNA from *X. bovienii*-Sf-FL was extracted using a PureLink™ Genomic DNA Mini Kit (Invitrogen) per the manufacturer's instructions and used as template for PCR amplification using Q5 DNA Polymerase (New England BioLabs). The 1000-bp regions flanking *metE* were amplified using the XbFL_metEUp_pKR100_F, XbFL_metEUp_KanR_R, XbFL_metEDown_KanR_F, and XbFL_metEDown_pKR100_R primers (Invitrogen). The *kanR* resistance gene was amplified using primers KanF and KanR from pEVS107 plasmid DNA template isolated using the Wizard® Plus SV Minipreps DNA Purification system (Promega, Table 2). Amplified DNA fragments were then purified using the Zymo Cleaning and Concentrating

Table 3.1: Bacterial Strains and Plasmids

Parental Background	HGB #	Genotype/Description	Antibiotic Resistance	Source or Reference
X. bovienii – Sf - FL	1699	Symbiont of *Steinernema feltiae* - FL	Amp	[53]
	2777	*ΔmetE*	Amp, Kan	This study
	2779	*ΔmetE attTn7::metE*$_{X.\ nematophila}$	Amp, Kan, Erm	This study
X. nematophila	800	Symbiont of *Steinernema carpocapsae*	Amp	[25]
E. coli S17 λ pir	180	pKR100	Chlor	[17]
	280	pEVS107	Kan, Erm	[17]
E. coli (BW29427 DAP dependent)	2778	pKR100 – *ΔmetE*$_{X.\ bovienii}$	Chlor, Kan	This study
	2780	pEVS107 - *metE*$_{X.\ nematophila}$	Kan, Erm	This study
	1284	pUX-BF13	Amp	[54]

Kit (Zymo Research) and were assembled into a *Sal*I (Fast Digest, ThermoFisher) and *Sac*I (Fast Digest, ThermoFisher) digested plasmid pKR100 via HiFi assembly (New England BioLabs). The HIFI assembly mixture was transformed into (DAP)-dependent *E. coli* BW29427 and successful transformants were selected on LBP supplemented with DAP, Kan, and Chlr. Candidate plasmids were screened for proper assembly using *Xba*I (Fast Digest, ThermoFisher) and *Hpa*I (Fast Digest, ThermoFisher) restriction enzyme digestion. To generate deletion strains, the resulting pKR100-*ΔmetE*$_{X.\ bovienii}$ plasmid was conjugated from *E. coli* BW29427 into *X. bovienii*-Sf-FL using previously established protocols [55]. *Xenorhabdus* exconjugants were selected on LB supplemented with Amp and Kan, screened for the absence of catalase activity to confirm the absence of the donor *E. coli* strain, and patched onto LB+Kan and LB+Chlr to assess loss of the pKR100-*metE* plasmid via chloramphenicol sensitivity. Deletion of the *metE* gene was confirmed by amplifying the *metE* locus (1000 bp upstream of the start codon to 1000 bp downstream of the stop codon using primers XbFL_metEUp_pKR100_F and XbFL_metEDown_pKR100_R) and assessing for size differences via 1% agarose gel electrophoresis. Met auxotrophy was assessed in GMM via 96-well growth assays as described above.

The *X. bovienii*-Sf-FL *metE* mutant was complemented with *X. nematophila metE*. The complement construct was created by amplification of the *metE* locus (1000 bp upstream of the start codon to 1000 bp downstream of the stop codon) from *X. nematophila* genomic DNA using Q5 DNA Polymerase and the primers: pEVS107_metE_locus_F and pEVS107_metE_locus_R. The pEVS107 plasmid was isolated as described above and

digested with *Apa*I (FastDigest, ThermoFisher) and *Kpn*I (FastDigest, ThermoFisher) restriction enzymes. Amplified and digested DNA were purified using a Zymo Cleaning and Concentrating Kit, HiFi assembled, and transformed into DAP-dependent *E. coli* BW29427. Successful transformants were selected on LBP supplemented with DAP, Kan and Erm and plasmids from the resulting colonies were screened via *Age*I (New England Biolabs) and *Xho*I (New England Biolabs) restriction digest for those with the desired plasmid assembly product, pEVS107-*metE*$_{X.\ nematophila}$ (*metE*$_{Xn}$). This plasmid was tri-parentally conjugated into the *X. bovienii*-Sf-FL *metE* mutant. Exconjugants were selected on LB supplemented with Amp and Erm, assessed for the absence of catalase activity (to confirm *Xenorhabdus*) and for restored Met prototrophy (to confirm presence of a functional *metE*).

Growth Curve and Survival Assays

The OD_{600} of overnight LB cultures were measured on a Genesys 50 spectrophotometer (Thermo Fisher) and were then normalized to an OD_{600} of 1.0. Cells were washed three times with 1X PBS and diluted to an OD_{600} of 0.01 into sterile media. Growth curves were carried out in 96-well plates with double orbital shaking (282 cycles per minute) at a total volume of 250 µL of media in a Synergy H1 plate reader (Agilent). The plate reader was programmed to measure OD_{600} every 0.25h. Growth curve data were blanked using OD_{600} from a media blank and data were visualized logarithmically in GraphPad Prism v10.6.1.

Table 3.2: Primers used in this study

Primer name	Primer Sequence (5'to 3')	PCR target (underline)	Overlap
XbFL_metEUp_pKR100_F	aatttgtggaattcccgggaCGCTTTACAAGCGGCAAATTG	1000 bp fragment upstream of XbSfFL *metE*	pKR100 – upstream of the *Sac*I restriction enzyme site
XbFL_metEUp_KanR_R	gctcgatgagtttttctaatGTTGTCACCCGCAAATTTTAGC	1000 bp fragment upstream of XbSfFL *metE*	The *kanR* gene from pEVS107
XbFL_metEDown_KanR_F	gattttgagacacaacgtggTGAAAACGCCCGCTACAG	1000 bp fragment downstream of XbSfFL *metE*	The *kanR* gene from pEVS107
XbFL_metEDown_pKR100_R	tccgtcacaggtactgcagGCCAGATGAACGGGGTTATC	1000 bp fragment downstream of XbSfFL *metE*	pKR100 – downstream of the *Sal*I restriction enzyme site
KanF	GCCGTTTCTGTAATGAAGGAG	*kanR* cassette from pEVS107	n/a
KanR	CCACGTTGTGTCTCAAAATC	*kanR* cassette from pEVS107	n/a
pEVS107_metE_locus_F	ccttccagtctagttctagaAATGTATCAATGGCAGGTTG	*X. nematophila metE* locus	pEVS107 – upstream of the X restriction enzyme site
pEVS107_metE_locus_R	agagatctactagtggccaaTCATAAAACCCCATTTCAATCTG	*X. nematophila metE* locus	pEVS107 – upstream of the X restriction enzyme site

We assessed bacterial survival on lipid agar as previously described [56]. Briefly, five 13-mm MCE filter membranes (3.0 µm pore size, Millipore) were sterilized and placed on the surface of sterile LA plates. Plates were treated with bacterial cultures and incubated as described above. Every 5 d, one filter was removed from the lipid agar lawn and the overlayed bacterial lawn was resuspended in 1 mL of 1X PBS. The bacterial suspension was serial diluted in 1X PBS and plated on LBP (in technical triplicate) to enumerate colony forming units (CFU). For competition assays, dilutions were plated on permissive LBP and LBP+Kan to differentiate between mutant and wild-type *X. bovienii* strains.

Nematode Husbandry and Aposymbiotic J1 Nematode Isolation

S. feltiae - FL nematodes were propagated every 3 months in *Galleria mellonella* larvae and collected using modified white traps as described previously [52]. Emerged IJs were collected in sterile water and stored in tissue culture flasks that were kept in the dark at 25˚C. Aposymbiotic J1 nematodes were isolated using a modified version of a previously described protocol [12]. Briefly, *S. feltiae* IJs were seeded onto lawns of *X. bovienii*-Sf-FL and incubated for 72 h at 25˚C. Nematode-bacterium co-cultures were flooded with sterile water and the nematodes were collected in a 50 mL conical tube, washed once with sterile water, and collected again via sedimentation. The mixed population of nematodes, including juvenile and adult stages, were resuspended in a 1.98% bleach and 0.25 M KOH solution and mixed via gentle inversion for 10 min. Aposymbiotic *S. feltiae* eggs were isolated via centrifugation at 1,811 x g for 5 min, washed in the bleach and KOH solution, and immediately centrifuged. The bleached eggs were washed in sterile, LB broth four times, collected via centrifugation, and incubated in LB broth in a 60 mm x 15 mm petri

dish overnight at room temperature. The number of hatched J1 nematodes were enumerated the next day and added to bacterial lawns on lipid agar at approximately 5000 J1 juveniles per plate.

Immature *S. feltiae* IJ Isolation and Enumeration

Aposymbiotic *S. feltiae* J1 nematodes were incubated on lipid agar lawns of *X. bovienii* strains for 6 d at 25˚C. Plates were flooded with sterile water and isolated mixed-stage nematodes were collected into conical tubes. Nematodes were collected via centrifugation (1000 x g for 10 min) and washed once with sterile water. Collected nematodes were re-suspended in a 1% SDS solution and incubated for 20 min at room temperature with occasional inversion. Immature IJs survive SDS treatment, but the remaining nematode stages will not. The SDS-treated worms were then washed thrice in sterile water. At this stage, immature IJs were differentiated from SDS-killed nematodes and counted in each condition.

Assessment of Mature *S. feltiae* IJ Emergence and Collection

Aposymbiotic *S. feltiae* J1 nematodes were incubated on lipid agar lawns of *X. bovienii* strains for 7 d at 25˚C and then the co-cultures were water trapped in 25 mL of sterile water. To enumerate the numbers of emerged mature IJs, at the times indicated for each experiment, all water was removed and collected from the water traps and replenished with nematode-free, sterile water. The collected water samples were mixed gently, and 3 x 10 mL aliquots were pipetted onto glass slides for nematode counting using an Olympus SZH-ILLD stereomicroscope. If no nematodes were counted initially, a secondary sampling of 3 x 100 m L aliquots was used. The average number of emerged IJs per mL of

sample was calculated and used to estimate total IJ emergence of that collection day. The total numbers of each subsequent collection day were added together for each biological replicate. Nematodes were collected for colonization assays in tissue culture flasks and stored at 25˚C until the assay (0-90 d post collection). Early emerged IJs were collected between 0 and 3-days post water trap, while late emerged IJs were collected between 5 and 7-days post water trap.

***S. feltiae* IJ Colonization Assays**

Collected *S. feltiae* IJs (mature or immature) were sampled in 1 mL aliquots from tissue culture flasks and centrifuged twice at 21,130 g for 6 sec each. To surface sterilize, each sample was treated with a 1% bleach solution for 2 min before the samples were centrifuged and washed thrice with sterile water. Approximately 200 surface sterilized *S. feltiae* IJs were then transferred to a sterile microcentrifuge tube containing 250 mL of sterile LB. Samples were ground with a hand-held homogenizer for 2 min to release bacteria from the IJ intestinal receptacle. After addition of 750 mL of sterile LB the nematode homogenate was serially diluted onto LBP agar. Plates were incubated at 30˚C overnight and CFU were counted. For competitive colonization assays, wild-type and mutant bacterial strains in the nematode-homogenate were distinguished from each other by plating on LBP and LBP + Kan. The number of Kan-resistant colonies was subtracted from the total number of colonies counted on LBP. The competitive index of the mutant was calculated as previously described [57]. Briefly, the output ratio (e.g., the proportion of mutant CFU to wild-type CFU derived from nematode homogenate) was divided by the

input ratio (e.g., proportion of mutant CFU to wild-type CFU determined from LA survival assays).

Natural Infection Assay and Infection Productivity

Sand trap assays were conducted in 12-well plates (Thermo Fisher) using a protocol modified from previously described approaches [11]. Individual wells were filled with 1 g of sand (Fisher Scientific) and inoculated with mature *S. feltiae* IJs that had been reared on and collected from LA lawns of wild type, *ΔmetE*, or *ΔmetE att*Tn*7::metEXn* (50 IJs in 100µL of sterile water, 4 biological replicates per strain). We treated sand with unaged (1-3 d in tissue culture) and aged IJs (30 d in tissue culture) to account for variations in bacterial load within the IJ receptacle. IJ-treated sand was incubated at 25˚C for 2 h before *G. mellonella* larvae (Grubco) were added to the wells (one insect per well). Twenty-four insects were assessed per strain (six per biological replicate). Insect death was assessed every 12 h over 2 d and following this time course, insect cadavers were water trapped to assess IJ nematode emergence for 24 d post water trap as described above.

RESULTS

A *X. bovienii metE* mutant is auxotrophic for L-methionine but can persist on lipid agar medium in the absence of competition with wild type

To assess the importance of methionine biosynthesis in *X. bovienii* symbiotic fitness, we disrupted the pathway by deleting via allelic exchange with a kanamycin resistance cassette the *metE* gene, predicted to encode a cobalamin-independent methionine synthase enzyme that catalyzes the conversion of L-homocysteine into L-methionine. While some bacteria encode multiple enzymes (*e.g.*, MetH and MmuM) capable of

synthesizing methionine, MetE appears to be the only such enzyme encoded by *Xenorhabdus* species (Chapter 2). The *X. bovienii ΔmetE* mutant did not grow in amino-acid-deficient glucose minimal media over a 168-h time course, in contrast to the wild-type parent and complement strain (*ΔmetE* Tn*7::metEXn*) which started growing after 96 h of incubation, reaching a max OD_{600} of 0.11 (**Fig 3.1C**). Supplementation of methionine at 0.2 mM was sufficient to restore *metE* mutant growth in GMM, consistent with the predicted function of *X. bovienii* MetE in methionine biosynthesis (**Fig 3.1D**). On LA, which is an amino-acid-replete nutrient broth agar medium, *ΔmetE* survived as well as wild type over a 20-d incubation at 25˚C, indicating that this medium contains sufficient methionine to support *X. bovienii ΔmetE* proliferation and persistence (**Fig 3.1B**). In co-culture, we observed that fewer viable cells of the *ΔmetE* strain were isolated relative to wild-type, suggesting that Met prototrophy engenders a competitive advantage for *X. bovienii*-Sf-FL on LA (**Table 3.3).**

***S. feltiae* infective juvenile emergence and colonization by *X. bovienii* is reduced after cultivation with the *X. bovienii ΔmetE* mutant relative to wild type**

To assess the role of *metE* in *X. bovienii* mutualism with its *S. feltiae* nematode host, *in vitro* lipid agar co-cultivations were initiated by inoculating aposymbiotic *S. feltiae* J1-stage juveniles onto lawns of wild type and *X. bovienii ΔmetE*. Under these conditions, IJs are expected to start developing around 6 d post inoculation and to start migrating off the plate (emergence) after 7 d of incubation at 25˚C. By placing the agar plates into a water trap, the emerging IJs can be collected over time. Emerged nematodes were collected daily for 23 d and populations were enumerated to assess daily (**Figure 3.2A**) and total

(**Figure 3.1B**) emergence. *S. feltiae* IJ emergence was delayed by 1 d and significantly fewer IJs emerged over time in co-cultivations with *X. bovienii ΔmetE* compared to wild-type ($p < 0.05$, unpaired student's t-test, **Figure 3.2A.** and **B**). At 0-3 d post water trap and 7-10 d post water trap, two emerged *S. feltiae* IJ populations, early (**Figure 3.2C**) and late emerged (**Figure 3.2D**), respectively, were separately stored in water and sampled over a 90-d time course to assess the average colony forming units (CFU) of *X. bovienii* per IJ. In early emerged IJs, there was a significant difference in initial colonization levels between nematodes reared on the wild-type and *ΔmetE* lawns ($p < 0.05$, unpaired student's t-test). This trend continued, but was not significant, after storage in water for 30, 60, and 90 d. A similar trend was observed for the late emerged IJs, but only the 30-d post collection time point was significantly different for wild type versus *ΔmetE* colonization levels.

The role of *metE* in the phenotypes observed above was verified by complementation of the *X. bovienii ΔmetE* mutant with the *metE* gene locus from *X. nematophila* (*metE*$_{Xn}$). Given the sequence similarly observed between *Xenorhabdus* MetE orthologs, we hypothesized that complementation with *metEXn* would be sufficient to restore mutualistic associations with *S. feltiae*-FL (Chapter 2). This gene was placed *in trans* at the *X. bovienii att*Tn*7* site downstream of *glmS*. The *X. bovienii ΔmetE att*Tn*7*::*metEXn* strain supported *S. feltiae* emergence similar to wild type (**Figure 3.3A**), and partially rescued the colonization defect observed in early emerged IJs (**Figure 3.3B**). Overall, these data suggest that loss of Met biosynthesis negatively impacts the mutualism between *X. bovienii* and its *S. feltiae*-FL host.

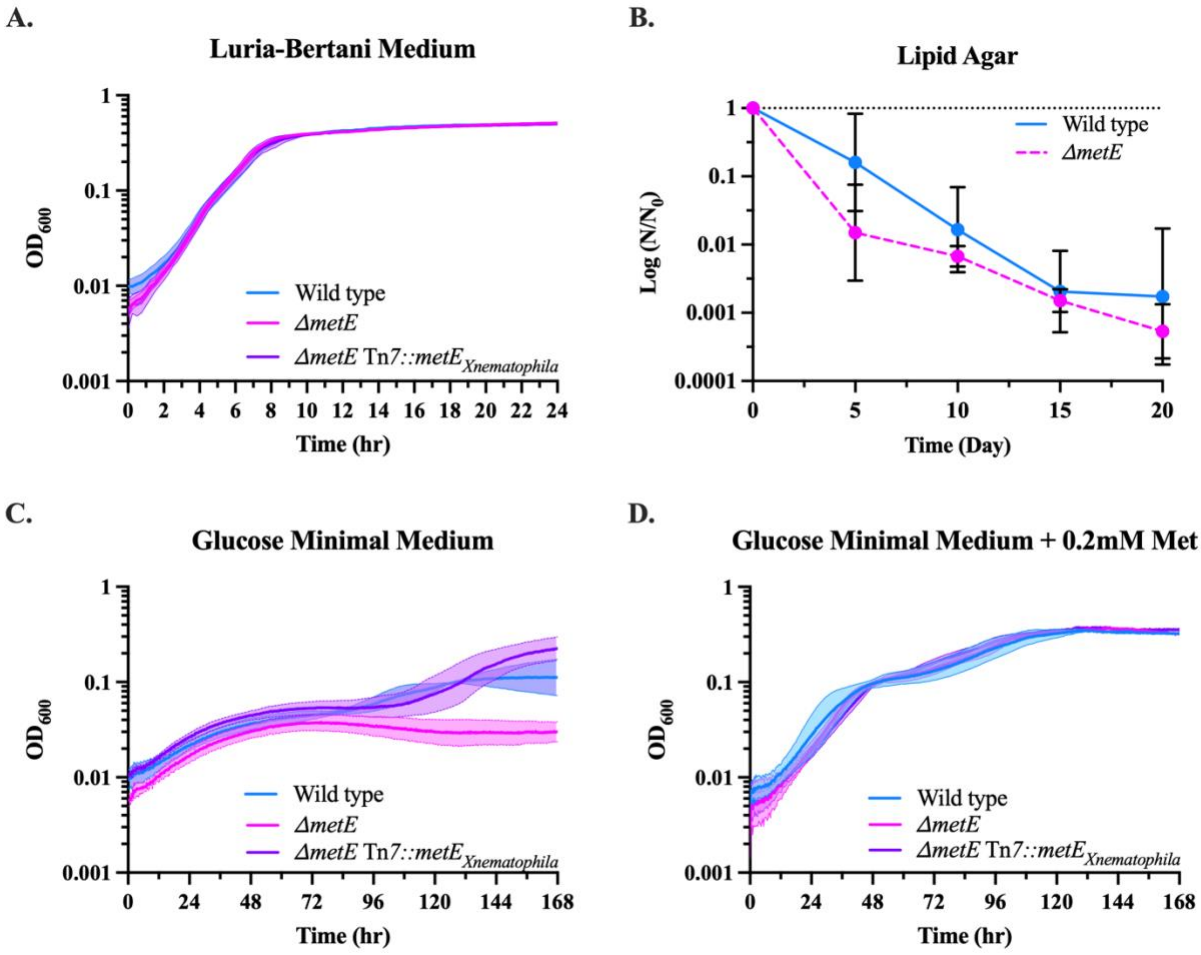


Figure 3.1: Deletion of the *X. bovienii*-Sf-FL *metE* gene does not alter wild-type growth and survival characteristics on Met-replete media.

Growth over 168 h (**A, C, D**) and survival over 20 d (**B**) of wild type (blue), *ΔmetE* (pink), or *ΔmetE* Tn*7::metEXn* in LB (**A**), LA (B), GMM (**C**), and GMM + 0.2 mM Met (**D**). For each strain three biological replicates were tested and shading (A, C, and D) or error bars (B) indicate ±1 SD. Curves in A, C, and D represent the average OD_{600} of the three biological replicates.

Table 3.3: **Proportions of wild-type and *ΔmetE X. bovienii*-Sf-FL strain on LA at 0 and 10 d post inoculation.**

The average CFU, ±1 SD, and the percentage of total CFU are shown.

Bacterial Strain	Days on Lipid Agar					
	0			10		
	Average CFU	SD	% of Total CFU	Average CFU	SD	% of Total CFU
Wild Type	$5.55x10^7$	$5.70x10^7$	75.6	$1.08x10^5$	$5.83x10^4$	92.3
ΔmetE	$1.79\ x10^7$	$1.27\ x10^7$	24.4	$9.09\ x10^3$	$7.15\ x10^3$	7.7

Methionine supplementation enhances *S. feltiae* IJ emergence after *in vitro* co-cultivation on wild-type and *ΔmetE* lawns

The data described above indicate that during *in vitro* cultivation, bacterial symbionts synthesize and provide Met that is necessary to support the nematode lifecycle. To determine if environmental supplementation of methionine can replace bacterial biosynthesis, we monitored *S. feltiae* IJ emergence over 14 d when co-cultivated with *X. bovienii* wild-type or *ΔmetE* on LA supplemented either with a sterile water vehicle or 0.2 mM Met. Consistent with the observations described above, more IJs emerged from the wild type relative to *ΔmetE* co-cultivations, but only in the absence of Met supplementation. When methionine was added, *S. feltiae* emergence from *X. bovienii ΔmetE* co-cultivations phenocopied the emergence pattern of nematodes cultivated with wild type in the absence of Met. Although not statistically significant, we noted an elevated level of nematode emergence from wild-type lawns supplemented with Met, relative to un-supplemented lawns (**Figure 3.4A**). Colonization levels of neither the wild type nor the *ΔmetE* mutant were impacted by methionine supplementation; we observed, as before, a *ΔmetE* colonization defect (**Figure 3.4B**). Overall, these data indicate that both bacterial and environmental Met pools can positively impact *S. feltiae* emergence and suggest that Met is a limiting resource for some aspect of IJ development or behavior.

Wild-type *X. bovienii* outcompetes a *metE* mutant for colonization but cannot rescue *metE*-dependent IJ emergence.

Given that the wild-type *X. bovienii* strain was able to outcompete the *metE* mutant on LA, we hypothesized that a mixed culture of both wild-type and mutant bacteria

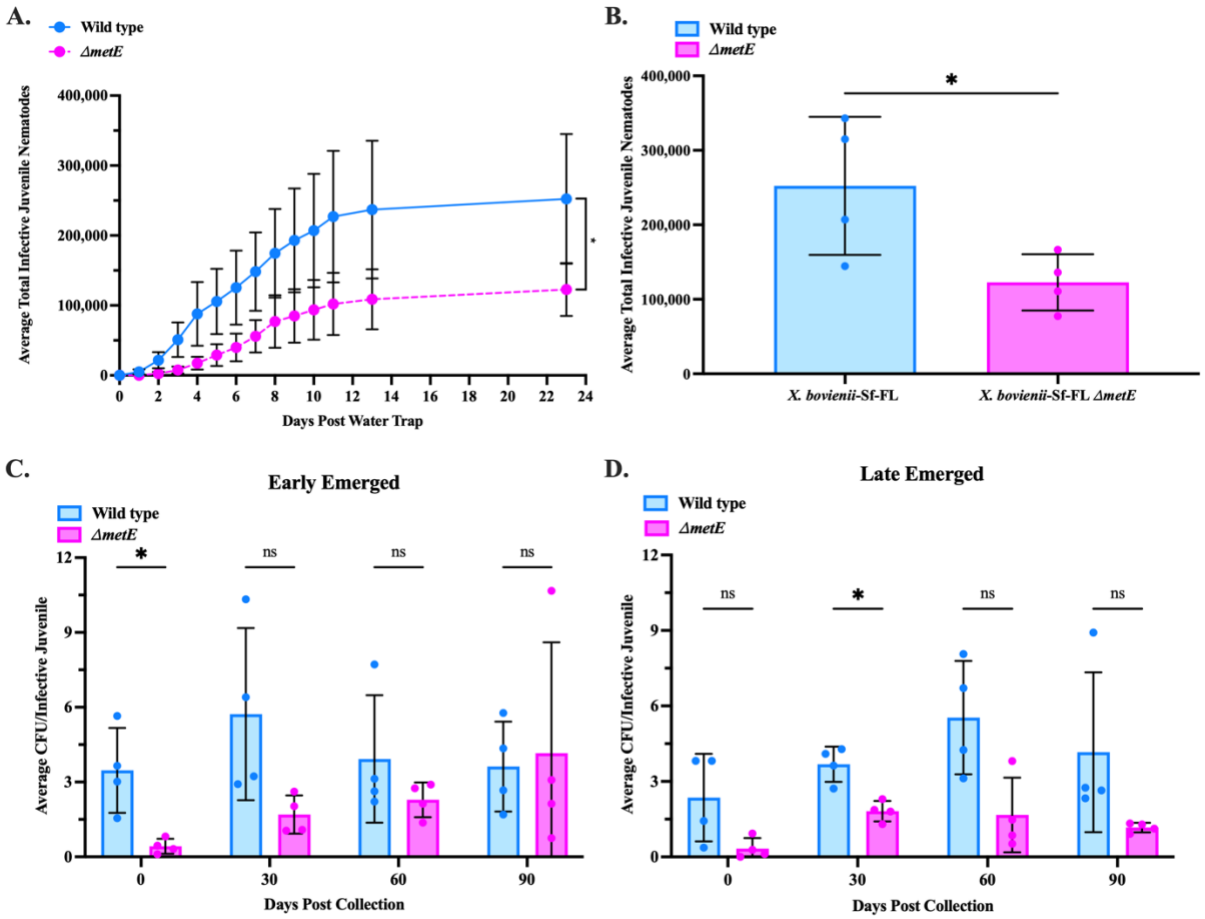


Figure 3.2: Fewer mature, *S. feltiae*-FL IJs emerge from lipid agar plates and are colonized by fewer bacterial cells when reared on methionine auxotrophic *X. bovienii*-Sf-FL.

Aposymbiotic J1-stage nematodes were inoculated onto lipid agar lawns of *X. bovienii*-SF-FL wild-type (blue) or *ΔmetE* (pink) and allowed to develop before being placed in a water trap to collect infective juveniles (IJs) to **A)** quantify numbers of IJs emerging over time after water trapping, **B)** quantify the total number of IJs emerged at 24 d post-water trap, and to determine the average *X. bovienii* CFU/IJ over time of storage (days post collection) of IJ populations collected at early (**C**) or late (**D**) water trapping time points (see materials and methods for details). Four biological replicates were tested for each condition and error bars indicate ±1 SD. Statistical significance was tested via an unpaired, student's t-test.

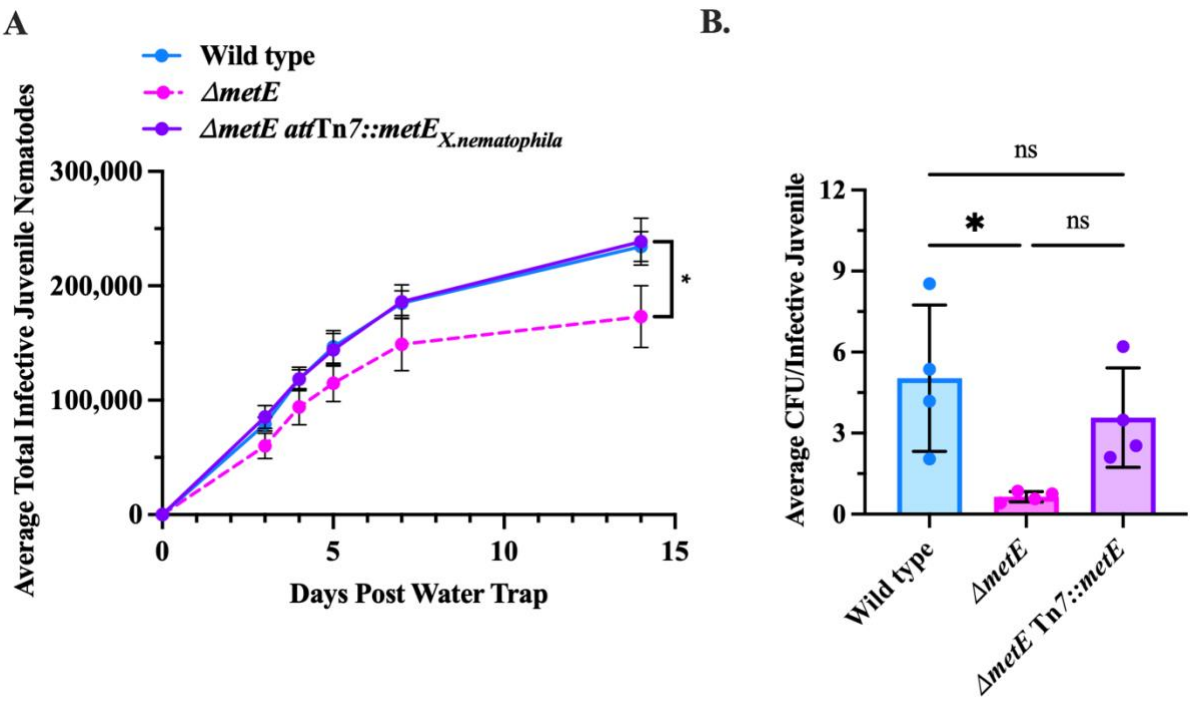


Figure 3.3: Complementation with the *metE* ortholog of *X. nematophila* fully and partially restores *S. feltiae*-FL IJ emergence and *X. bovienii*-Sf-FL colonization, respectively.

S. feltiae FL infective juvenile nematode emergence into water traps over 14 d (**A**) and colonization by *X. bovienii* (average CFU/IJ, **B**) at early emergence were measured after co-cultivation with *X. bovienii* SF FL wild type (blue), *ΔmetE* (pink), and *ΔmetE attTn7::metE*$_{Xn}$ (purple). Four biological replicates were tested for each condition and error bars indicate ±1 SD. Statistical significance was tested via a One-way ANOVA.

would support wild-type levels of IJ nematode emergence. However, IJ emergence levels from the mixed culture were comparable to those observed from co-cultivation with *ΔmetE* alone, suggesting the presence of a *metE* deficient strain in a wild-type population is sufficient to limit nematode emergence (**Figure 3.5**). We next assessed the colonization of the IJs-reared on the mixed cultures. We predicted that the wild-type strain would have a competitive advantage over the *metE* mutant strain based on our previous colonization and co-culture observations. Wild-type and *metE* mutant strains were distinguished from each other by antibiotic resistance and the data are summarized in **Table 3.4**. Consistent with our previous results, the average wild-type *X. bovienii* CFU derived from *S. feltiae* IJs significantly outnumbered those of the *metE* mutant, and the competitive index of the *metE* mutant was 0.03 (±0.04) and 0.17 (±0.25) using input ratios from 0 and 10 d post inoculation, respectively, indicating a competitive disadvantage compared to the wild type. This is consistent with our earlier observation that there were fewer colony forming units of the *ΔmetE* strain derived from mixed culture on LA when in competition with the wild-type parental strain at both 0 and 10 d timepoints (**Table 3.3**).

Symbiont Met biosynthesis improves bacterial outgrowth *in vivo* and *S. feltiae* host fecundity

The observation that significantly fewer *S. feltiae* IJs emerge from *ΔmetE* lawns compared to the wild-type and *ΔmetE attTn7::metE*$_{Xn}$ strains suggested that symbiont Met prototrophy positively impacts nematode fecundity (e.g., reproduction, development, growth) or nematode migratory behavior. To address this question, we determined if the number of pre-migratory, immature IJs differed between symbiont genotypes (**Figure**

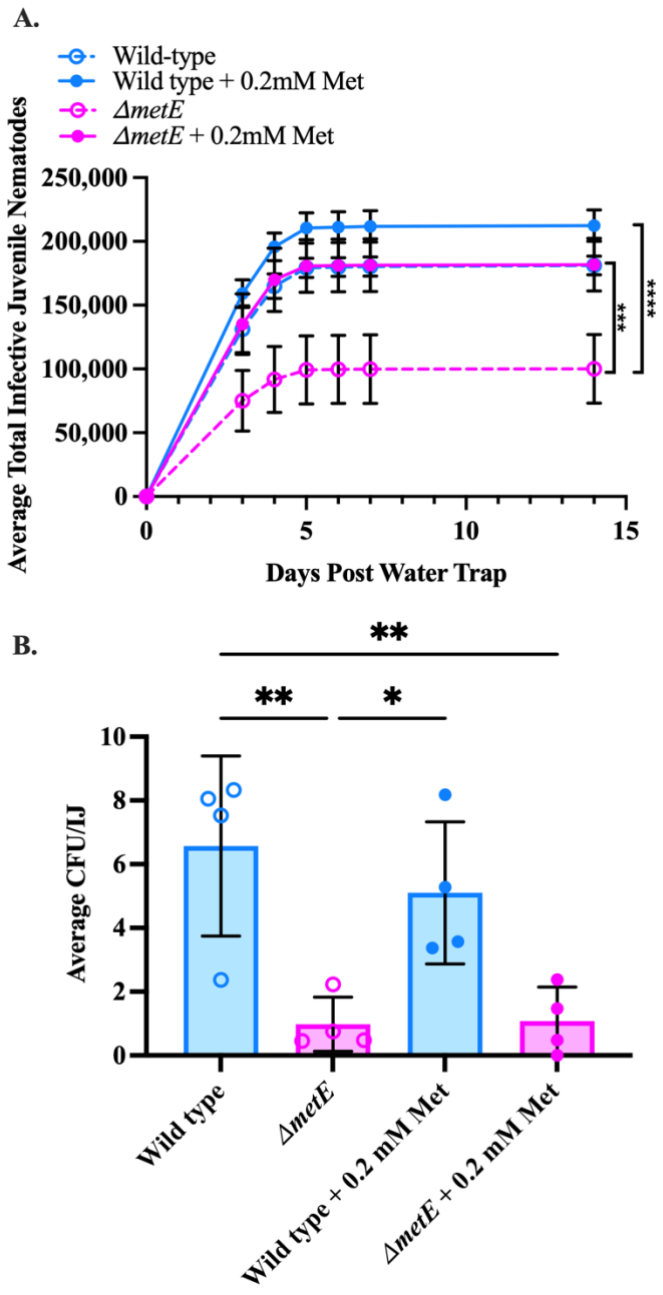


Figure 3.4: Increased levels of exogenous Met restores the emergence defect but not attenuated colonization of *ΔmetE*-reared *S. feltiae*-FL IJs.

S. feltiae-FL IJs were reared on lawns of wild-type (blue) and *ΔmetE X. bovienii*-Sf-FL on lipid agar supplemented with (closed circles) or without (open circles) 0.2 mM Met. Emergence of *S. feltiae*-FL IJs was assessed daily over a 14-d time course (**A**), while colonization was assessed in early emerged *S. feltiae*-FL IJs (**B**). Four biological replicates were tested for each condition and error bars indicate ±1 SD. Statistical significance was tested via a One-way ANOVA.

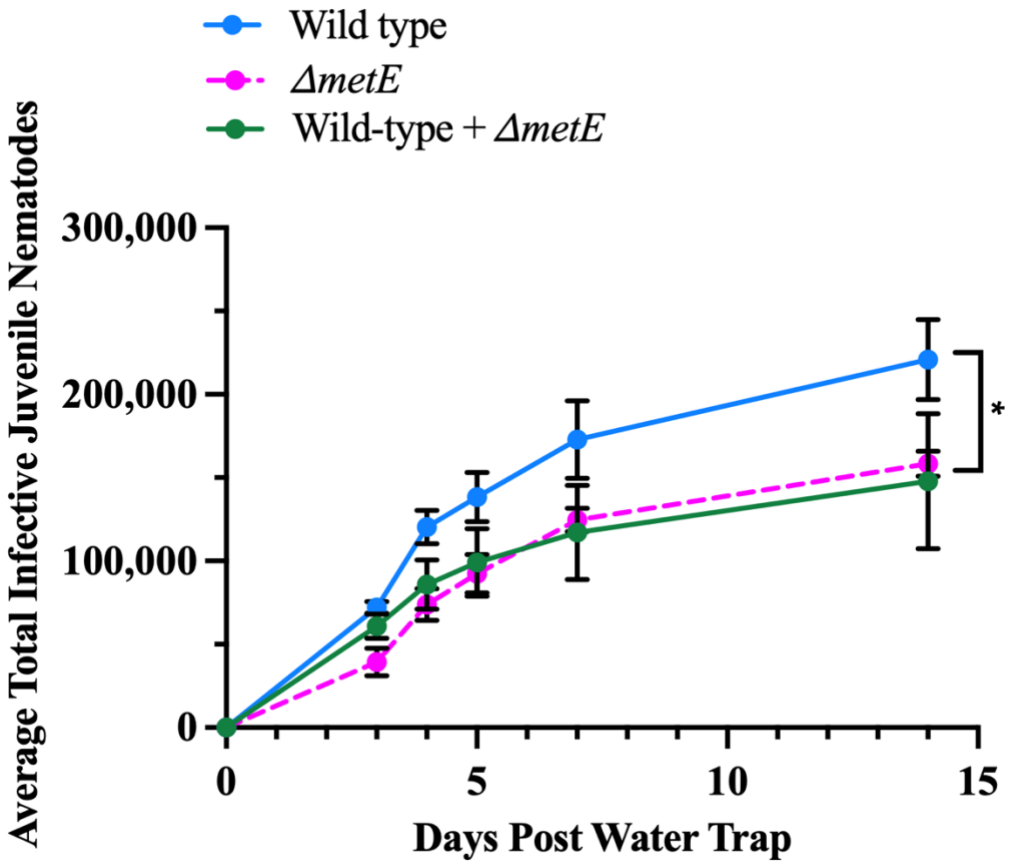


Figure 3.5: Average emergence of *S. feltiae*-FL IJs reared on mixed culture populations (green) phenocopies IJ emergence from a *ΔmetE* monoculture (pink) instead of wild type (blue).

Four biological replicates were tested for each condition and error bars indicate ±1 SD. Statistical significance was tested via a One-way ANOVA.

3.6A). We observed significantly fewer immature IJs were isolated from the *ΔmetE* condition ($p < 0.05$, 26,667 ± 15,154) than from wild type (61,667 ± 19,341) and *ΔmetE attTn7::metE*$_{Xn}$ (72,500 ± 16,415). This suggests that the reduced emergence phenotype is likely caused by reduced *S. feltiae* fecundity rather than failure of IJs to emerge from LA plates.

The colonization defect of the *ΔmetE* strain in early-emerged *S. feltiae* IJs was observed at 0 d post collection, but not at 30, 60, or 90 d. Based on these observations, we hypothesized that *ΔmetE* strains may have a delay in their ability to replicate within the nematode receptacle, which we term an *in vivo* outgrowth defect. We tested this by measuring bacterial burden in mature *S. feltiae* IJs stored over a 6-d time course (**Figure 3.6B**). As anticipated, wild-type *X. bovienii* exhibited an increase in population size over the 6-d experiment starting with 1.97 CFU/IJ (± 0.53) and reaching 5.76 CFU/IJ (± 1.72, $p < 0.01$) by 4 d post collection. By the end of the experiment, *S. feltiae* IJs were only colonized by 3.35 CFU/IJ (± 1.17) suggesting that there is periodical growth and death phases within the receptacle. Over the course of the experiment, the *ΔmetE* strain maintained a bacterial burden between 0.52 CFU/IJ (± 0.12, d = 0) and 0.87 CFU/IJ (± 0.61, d = 6). At five of the seven timepoints (0, 2, 3, 4, and 5 d post collection), colonization of *S. feltiae* IJs by the *ΔmetE* strain was significantly different from wild type. At 1- and 6-d post collection, the *ΔmetE* strain was not significantly different. Together these data suggest that, like the wild type, the *ΔmetE* strain can proliferate within *S. feltiae* IJs but to a much lower carrying capacity.

At 0 d post collection the *ΔmetE attTn7::metE*$_{Xn}$ strain colonized *S. feltiae* IJs similar to the wild-type strain and was significantly different from *ΔmetE* ($p < 0.01$). From 1- to 4-d post collection, the *ΔmetE attTn7:: metE*$_{Xn}$ strain was not significantly different from wild-type or the *ΔmetE* strain consistent with our previous observation that the complementation only partially restored the colonization phenotype. At 5-d post collection, *ΔmetE attTn7::metE*$_{Xn\ colonized}$ at significantly lower levels compared to wild type ($p < 0.01$), while at 6 d it colonized to similar levels. These data suggest that the presence of a non-native *metE* locus can partially restore aspects of *X. bovienii* outgrowth during nematode colonization but is not sufficient for all outgrowth stages.

Mature *S. feltiae* IJs can infect, kill, and reproduce within insects regardless of the Met biosynthetic capability of their symbiont.

Met prototrophy in *X. bovienii* significantly impacts the reproduction of *S. feltiae* and is further required for optimal colonization of the IJ receptacle when reared on LA medium. Given that a Met deficient symbiont impeded early colonization and nematode fecundity, we hypothesized that *ΔmetE* reared IJs would be less fit during insect infection compared to wild-type reared IJs. To test this, we raised IJs on bacterial lawns of wild type, *ΔmetE, ΔmetE* attTn*7::metEXn* in two independent propagations. The first propagation we collected mature, early emerged IJs from each condition and aged them for 30 d at 25˚C. In the second experiment, we collected early emerged IJs but did not age them and used both sets of nematodes to perform natural infection assays. We chose to test aged and unaged IJs to account for possible disparities in the number of CFU per IJ (**Figure 3.2C**). We assessed IJ colonization prior to insect infection and noted that the *metE* mutant

Table 3.4: Met auxotrophy confers a competitive disadvantage to *X. bovienii*-Sf-FL during *S. feltiae*-FL nematode colonization.

***X. bovienii* Strain**	CFU/IJ		Competitive Index (Output Ratio/Input Ratio)			
			Input Ratio Day 0		Input Ratio Day 10	
	Mean	SD	Mean	SD	Mean	SD
Wild type	4.68	1.70	n/a	n/a	n/a	n/a
ΔmetE	0.75	0.59	0.03	0.04	0.17	0.25

had significantly lower bacterial burden in both the unaged and aged IJs in contrast to our previous observations (**Figure 3.7)**.

We assessed virulence of the aged and unaged IJs via using a natural infection assay in which the nematodes were inoculated into sand traps and later baited with *G. mellonella* larvae. Unaged IJs, regardless of the Met biosynthesis status of the symbiont they cultivated on, killed 100% of the insect larvae within 36 h (**Figure 3.8A).** The same observation was made for the aged IJs raised wild-type and *ΔmetE* lawns (**Figure 3.8B**). Uninfected *G. mellonella* larvae, which were baited on sand treated with sterile water, survived the entire 48 h experiment. Altogether, our data suggest that the ability of *S. feltiae* IJs to infect and kill insects is not significantly impacted by the Met biosynthetic status of the symbiont they were reared upon or their colonization status by that symbiont. We next collected the insect cadavers and water trapped them to determine the reproductive productivity of the unaged and aged IJs. After 10-11 d post water trap, we observed emergence from *G. mellonella* infected by both populations of nematodes. Over the 24-d experiment, we observed no significant differences in emergence patterns for unaged *S. feltiae* IJs reared on wild type, *ΔmetE*, and *⊿metE* attTn*7::metEXn* lawns (**Fig. 6C)**. This suggests that Met levels *in insecta* are sufficient to support both the outgrowth of *X. bovienii* and the growth, development, and reproduction of *S. feltiae* nematodes. In the aged population, we noted a significant difference in emergence between the *ΔmetE* and *⊿metE* attTn*7::metE*$_{Xn}$ reared IJs ($p < 0.05$, One-Way ANOVA, Tukey's HSD) but not between *ΔmetE* and wild type although the mutant did trend lower in overall emergence. Furthermore, the average total emergence of *ΔmetE*-reared, unaged (290,420 ± 43,092) and aged IJs (133, 915 ± 37, 021)

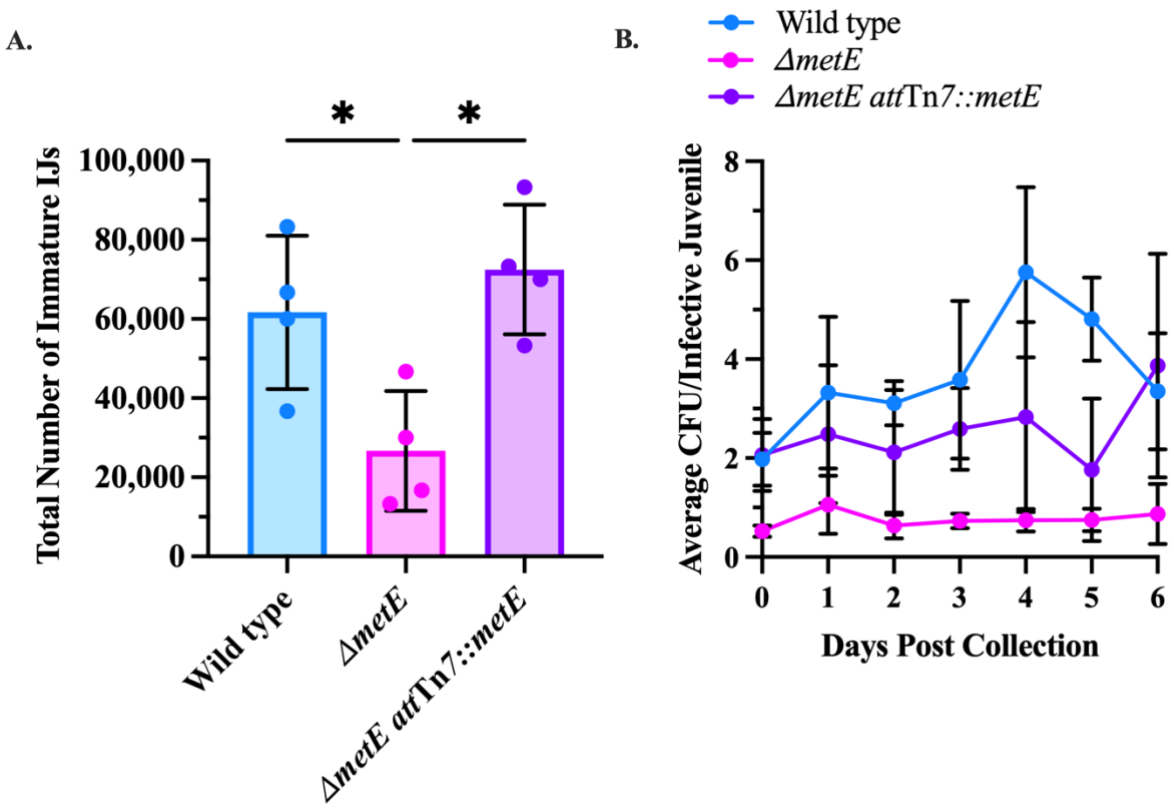


Figure 3.6: A) *S. feltiae* nematodes exhibit decreased reproduction when reared on a *ΔmetE* (pink) *X. bovienii* symbiont than when reared on wild type (blue) or *ΔmetE attTn7::metE*$_{Xn}$ (purple) symbionts after 6 d.

B) Met auxotrophic *X. bovienii* (pink) does not exhibit similar *in vivo* growth dynamics to wild-type (blue) or *ΔmetE attTn7::metE*$_{X. nematophila}$ (purple) when colonizing the receptacle of mature *S. feltiae* IJs. Four biological replicates were tested for each condition and error bars indicate ±1 SD. Statistical significance was tested via a One-way ANOVA.

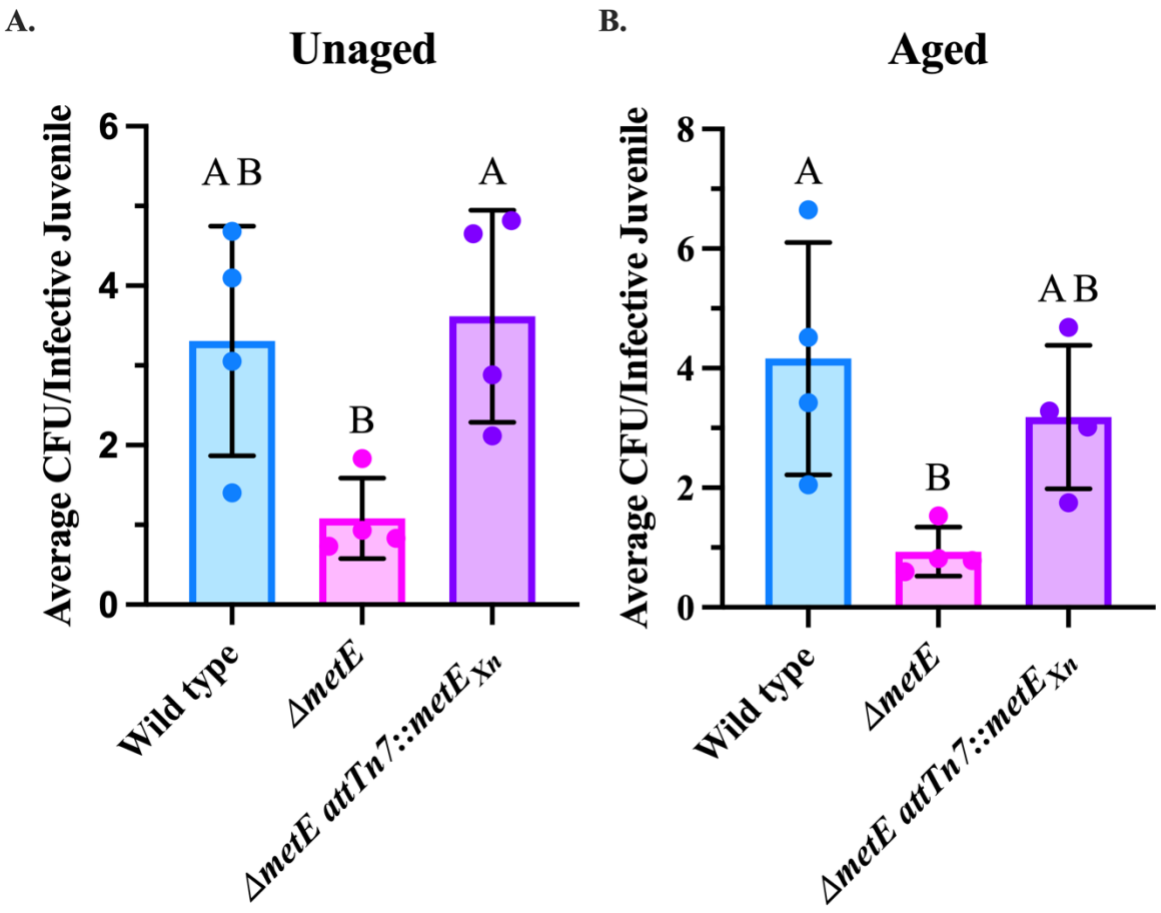


Figure 3.7: Bacterial burden of unaged (A) and aged (B) *S. feltiae* IJs prior to natural infection assays when reared on wild type (blue), *ΔmetE* (pink), and *ΔmetE attTn7::metE*$_{Xn}$ (purple) strains.

Four biological replicates were tested per bacterial strain and Error bars indicate ±1 SD. Letters indicate statistical significance groups based on a One-Way ANOVA with Tukey's HSD.

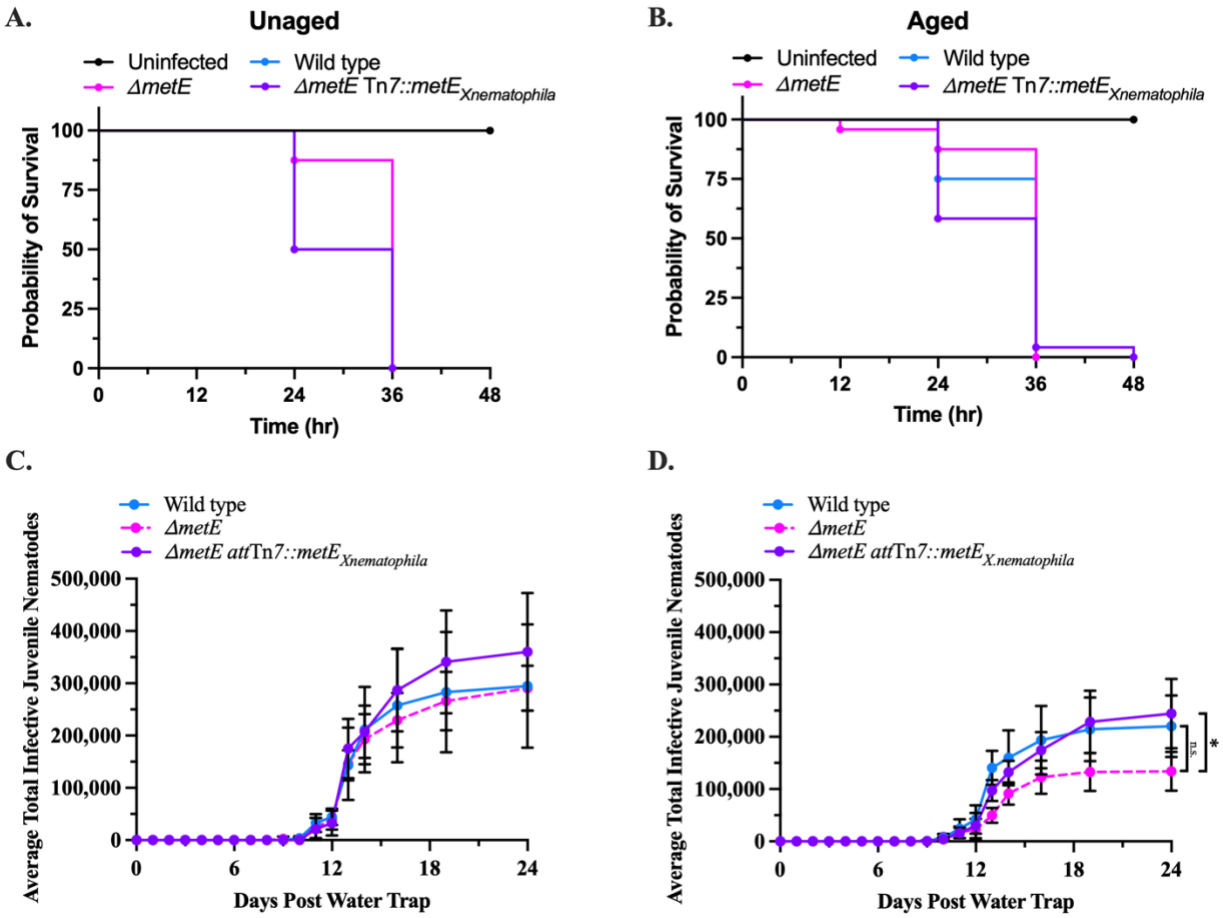


Figure 3.8: Unaged (A and C) and Aged (B and D) *S. feltiae* IJs reared on a *ΔmetE* mutant (pink) exhibited similar virulence and emergence phenotypes to IJs reared on wild-type (blue) and *ΔmetE attTn7::metE*$_{Xn}$ (purple) strains when infecting *G. mellonella.*

Four biological replicates were tested per bacterial strain and were infected into six insect larvae. Error bars indicate ±1 SD.

were significantly different ($p = 0.0016$, student's t-test). These data suggests that mature, aged *S. feltiae* IJs and their exhibit increased demands for Met within insect hosts if they are colonized by a Met auxotrophic *X. bovienii* symbiont.

DISCUSSION

We establish in this study that *X. bovienii* biosynthesis of the essential amino acid Met contributes to the fecundity of its symbiotic nematode host, *S. feltiae*. Our data revealed that the number of emerged (mature) and unemerged (immature) IJs is dependent upon the *X. bovienii* symbiont's ability to produce Met endogenously suggesting that some aspect of nematode growth, development, and/or reproduction is being affected. In the well-studied bacterivorous nematode *Caenorhabditis elegans,* inhibition of folate and Met metabolism in the common laboratory food source, *E. coli* OP50, induces caloric restriction which in turn improves nematode longevity while reducing reproductive behaviors [58-60]. These changes in nematode reproduction led to a reduction in viable progeny due to altered egg laying behavior in adults and decreased production of yolk proteins in the oocytes [58, 59]. Tetrahydrofolate-derivatives from the folate cycle are used to methylate L-homocysteine which ultimately generates Met [3]. Increasing the exogenous Met pool was sufficient to ameliorate these reduced fecundity phenotypes and had no effect on the increased longevity of *C. elegans* suggesting that Met influences fecundity, while dietary folate levels, but not Met, influence lifespan [59, 60]. While the reproductive strategies employed in *C. elegans* and *S. feltiae* are distinct from each other, the *C. elegans* findings suggest that the fecundity defects that we observed, measured as IJ progeny production, of the *ΔmetE*-reared *S. feltiae* may be caused by reduced egg laying and progeny longevity or

viability. Like *C. elegans*, the reduced fecundity of the *S. feltiae-X. bovienii ΔmetE* association was restored by Met supplementation in the media or, in the case of unaged IJs, by natural infection in *G. mellonella* insects. Curiously, *G. mellonella* infection did not rescue the fecundity of aged *S. feltiae-X. bovienii ΔmetE* IJs, which exhibited significantly lower reproduction than their unaged counterparts. This suggests that prolonged colonization of *S. feltiae* with a Met-deficient symbiont may increase the nematode's Met demand to support reproduction within the insect environment.

In the wild-type *S. feltiae-X. bovienii* association, the bacterium can provision both itself and its nematode host with methionine assuming there is the availability of other nutrients. However, in the *S. feltiae-X. bovienii ΔmetE* association, both the bacterium and the nematode rely on exogenous sources of methionine. In this case, not only does the bacterium fail to provide Met to its host, but it also serves as a potential sink for Met to support its own growth. This suggests that a Met-deficient *X. bovienii* symbiont may not only fail to provision Met to its host but may in fact sequester Met due to reduced availability. Supporting the idea that competition for exogenous Met reduces *S. feltiae* fecundity, nematodes reared with both *X. bovienii* wild type and the *ΔmetE* mutant had reduced fecundity, despite the dominance of the wild type strain in the population. This suggests that the *ΔmetE* strain successfully scavenges Met and reduces its availability for the nematode host. Taken together, our data add support for the model that bacterially derived Met is important for reproduction of bacterivorous nematodes, including in a co-evolved mutualistic symbiosis.

Xenorhabdus colonization initiation, outgrowth, and persistence within the non-feeding *Steinernema* IJ receptacle is critical to the mutualism, as it ensures the evolutionary success and continuation of both organisms. This aspect of the mutualism is also highly specific as only cognate *Xenorhabdus* symbionts can colonize their *Steinenema* host [12, 61]. In the *X. nematophila*-*S. carpocapsae* symbiosis, bacterial colonization factors have been identified that function in all three aspects of IJ colonization. Factors like the NilB and C type 11 secretion system and the sigma factor RpoS, were characterized as initiation factors in *X. nematophila* as disruption of the genes encoding these proteins abolished most if not all colonization within the receptacle of S. *carpocapsae* IJs [56, 61, 62]. Disruption of factors involved in outgrowth often result in an abortive colonization phenotype (i.e., colonization followed by eventual cell death) or reduced bacterial carriage within the receptacle of *S. carpocapsae* nematodes [22, 56, 61]. Both types of outgrowth factors have been identified in *X. nematophila* and include genes involved in amino acid and vitamin biosynthetic processes: *thrC, pabA,* and *metE* [21, 22]. The *X. nematophila metE* and *pabA* mutants display modest reductions in population size within the receptacle, while a *thrC* mutant displays an abortive phenotype, in which colonizing receptacle cells appear to die and get cleared [21, 22]. Here we report the first known *X. bovienii* colonization-defective mutant, *ΔmetE*, which displays a phenotype like that of *X. nematophila metE:* reduced population size within the receptacle. That the *X. bovienii ΔmetE* mutant can colonize and persist within the *S. feltiae* IJ receptacle, even if at reduced levels, indicates that it has some source of Met, either from endogenous protein reserves or from the nematode. However, reduced population size of the *X. bovienii ΔmetE* mutant relative to wild type indicates that

these sources of Met are insufficient for demand. Over a 90-d time course of *S. feltiae* nematode aging, the *X. bovienii ΔmetE* strain consistently colonized at lower levels than wild type up to 30 d of aging. After 30 d, the *ΔmetE* defect was variable; in one set of experiments the mutant reached wild type levels of colonization, whereas in another the mutant remained lower. One caveat to *X. bovienii* colonization measurements is that this symbiont colonizes at very low levels (~6 cfu/IJ) relative to *X. nematophila* (~100 cfu/IJ), which complicates discernment of statistically significant fluctuations [19, 20]. Regardless, our data demonstrate that the *ΔmetE* mutant consistently exhibits lower, populations sizes relative to wild type, indicating a role for *metE* in outgrowth and persistence of *X. bovienii* in the nematode IJ receptacle.

Our data indicate that *X. bovienii* Met biosynthesis is critical for multiple aspects of its mutualism with *S. feltiae* including bacterial colonization and nematode fecundity *in vitro* and *in vivo*. This is, to our knowledge, the first report of any *Xenorhabdus* metabolic factor contributing to both colonization and fecundity phenotypes of their *Steinernema* host. Previous co-phylogenetic analyses conducted on isolates of *X. bovienii,* and their cognate nematode hosts suggested that *X. bovienii*-Sf-FL shares evolutionary history with *S. feltiae* and is not subject to host-switching events as has been suggested for other *X. bovienii* isolates [11]. Our data support these findings as the fitness of *S. feltiae* is dependent upon the Met proficiency of its cognate symbiont indicating metabolic interconnectedness between both organisms. Similarly, *X. bovienii* fitness within the receptacle of *S. feltiae* is reduced if the bacterium cannot synthesize Met *de novo*, suggesting that there is limited bioavailable Met in this niche. Together, this suggests that

Met is a limiting resource for *X. bovienii* and *S. feltiae* in their natural environments and that maintenance of bacterial Met prototrophy is adaptive for the fitness of both organisms.

REFERENCES

1. Chandel, N.S., *Amino Acid Metabolism.* Cold Spring Harb Perspect Biol, 2021. **13**(4).
2. Chiaiese, P., et al., *Sulphur and nitrogen nutrition influence the response of chickpea seeds to an added, transgenic sink for organic sulphur.* Journal of Experimental Botany, 2004. **55**(404): p. 1889-1901.
3. Hondorp, E.R. and R.G. Matthews, *Methionine.* EcoSal Plus, 2006. **2**(1).
4. Boer, V.M., et al., *Growth-limiting Intracellular Metabolites in Yeast Growing under Diverse Nutrient Limitations.* Molecular Biology of the Cell, 2010. **21**(1): p. 198-211.
5. Wu, G., *Amino acids: biochemistry and nutrition*. 2021: CRC press.
6. Hou, Y. and G. Wu, *Nutritionally Essential Amino Acids.* Advances in Nutrition, 2018. **9**(6): p. 849-851.
7. Pickard, B.S., *Five hundred million years of hunger: how animals evolved to survive essential amino acid scarcity.* Emerg Top Life Sci, 2025. **9**(6).
8. Mertz, C.M., et al., *Microbially derived essential amino acids compensate for dietary deficiencies in an ecologically relevant mammalian host.* Isme j, 2026. **20**(1).
9. Cornwallis, C.K., et al., *Symbioses shape feeding niches and diversification across insects.* Nat Ecol Evol, 2023. **7**(7): p. 1022-1044.
10. McMullen, J.G., 2nd, et al., *Fitness costs of symbiont switching using entomopathogenic nematodes as a model.* BMC Evol Biol, 2017. **17**(1): p. 100.

11. Murfin, K.E., et al., *Xenorhabdus bovienii Strain Diversity Impacts Coevolution and Symbiotic Maintenance with Steinernema spp. Nematode Hosts.* mBio, 2015. **6**(3): p. e00076.

12. Chaston, J.M., et al., *Previously unrecognized stages of species-specific colonization in the mutualism between Xenorhabdus bacteria and Steinernema nematodes.* Cellular microbiology, 2013. **15**(9): p. 1545-1559.

13. Jubelin, G., et al., *Studies of the dynamic expression of the Xenorhabdus FliAZ regulon reveal atypical iron-dependent regulation of the flagellin and haemolysin genes during insect infection.* Environ Microbiol, 2011. **13**(5): p. 1271-84.

14. Park, D. and S. Forst, *Co-regulation of motility, exoenzyme and antibiotic production by the EnvZ-OmpR-FlhDC-FliA pathway in Xenorhabdus nematophila.* Mol Microbiol, 2006. **61**(6): p. 1397-412.

15. Mucci, N.C., et al., *Apex Predator Nematodes and Meso-Predator Bacteria Consume Their Basal Insect Prey through Discrete Stages of Chemical Transformations.* mSystems, 2022. **7**(3): p. e0031222.

16. Richards Gregory, R., et al., *Xenorhabdus nematophila lrhA Is Necessary for Motility, Lipase Activity, Toxin Expression, and Virulence in Manduca sexta Insects.* Journal of Bacteriology, 2008. **190**(14): p. 4870-4879.

17. Richards Gregory, R. and H. Goodrich-Blair, *Examination of Xenorhabdus nematophila Lipases in Pathogenic and Mutualistic Host Interactions Reveals a Role for xlpA in Nematode Progeny Production.* Applied and Environmental Microbiology, 2010. **76**(1): p. 221-229.

18. Singh, S., et al., *Role of secondary metabolites in establishment of the mutualistic partnership between Xenorhabdus nematophila and the entomopathogenic nematode Steinernema carpocapsae.* Appl Environ Microbiol, 2015. **81**(2): p. 754-64.

19. Martens, E.C., K. Heungens, and H. Goodrich-Blair, *Early colonization events in the mutualistic association between Steinernema carpocapsae nematodes and Xenorhabdus nematophila bacteria.* J Bacteriol, 2003. **185**(10): p. 3147-54.

20. Stilwell, M.D., et al., *Studying the Symbiotic Bacterium Xenorhabdus nematophila in Individual, Living Steinernema carpocapsae Nematodes Using Microfluidic Systems.* mSphere, 2018. **3**(1).

21. Flores-Lara, Y., et al., *Influence of nematode age and culture conditions on morphological and physiological parameters in the bacterial vesicle of Steinernema carpocapsae (Nematoda: Steinernematidae).* J Invertebr Pathol, 2007. **95**(2): p. 110-8.

22. Martens, E.C., F.M. Russell, and H. Goodrich-Blair, *Analysis of Xenorhabdus nematophila metabolic mutants yields insight into stages of Steinernema carpocapsae nematode intestinal colonization.* Mol Microbiol, 2005. **58**(1): p. 28-45.

23. Mitani, D.K., H.K. Kaya, and H. Goodrich-Blair, *Comparative study of the entomopathogenic nematode, Steinernema carpocapsae, reared on mutant and wild-type Xenorhabdus nematophila.* Biological Control, 2004. **29**(3): p. 382-391.

24. Sicard, M., et al., *Stages of infection during the tripartite interaction between Xenorhabdus nematophila, its nematode vector, and insect hosts.* Appl Environ Microbiol, 2004. **70**(11): p. 6473-80.

25. Chaston, J.M., et al., *The entomopathogenic bacterial endosymbionts Xenorhabdus and Photorhabdus: convergent lifestyles from divergent genomes.* PLoS One, 2011. **6**(11): p. e27909.

26. Kauffman, S.J., et al., *Genomic Diversification and Tailocin-Mediated Competition in Animal-Associated Xenorhabdus Bacteria.* ISME Communications, 2026.

27. Bashey, F., H. Hawlena, and C.M. Lively, *Alternative paths to success in a parasite community: within-host competition can favor higher virulence or direct interference.* Evolution, 2013. **67**(3): p. 900-7.

28. Murfin, K.E., et al., *Symbiont-mediated competition: Xenorhabdus bovienii confer an advantage to their nematode host Steinernema affine by killing competitor Steinernema feltiae.* Environ Microbiol, 2018.

29. Heppert, J.K., et al., *Analyses of Xenorhabdus griffiniae genomes reveal two distinct sub-species that display intra-species variation due to prophages.* BMC Genomics, 2024. **25**(1): p. 1087.

30. Gophna, U., et al., *Evolutionary plasticity of methionine biosynthesis.* Gene, 2005. **355**: p. 48-57.

31. Parungao, G.G., et al., *Complementation of a metK-deficient E. coli strain with heterologous AdoMet synthetase genes.* Microbiology (Reading), 2017. **163**(12): p. 1812-1821.

32. Hasebe, F., *MetW regulates the enzymatic activity of MetX in Pseudomonas.* Biosci Biotechnol Biochem, 2021. **85**(2): p. 351-358.

33. Cherest, H., F. Eichler, and H. de Robichon-Szulmajster, *Genetic and Regulatory Aspects of Methionine Biosynthesis in Saccharomyces cerevisiae.* Journal of Bacteriology, 1969. **97**(1): p. 328-336.

34. Ravanel, S., et al., *The specific features of methionine biosynthesis and metabolism in plants.* Proc Natl Acad Sci U S A, 1998. **95**(13): p. 7805-12.

35. Starke, S., et al., *Amino acid auxotrophies in human gut bacteria are linked to higher microbiome diversity and long-term stability.* The ISME Journal, 2023. **17**(12): p. 2370-2380.

36. Chong, R.A., H. Park, and N.A. Moran, *Genome Evolution of the Obligate Endosymbiont Buchnera aphidicola.* Molecular Biology and Evolution, 2019. **36**(7): p. 1481-1489.

37. Barth, A.L. and T.L. Pitt, *Auxotrophic variants of Pseudomonas aeruginosa are selected from prototrophic wild-type strains in respiratory infections in patients with cystic fibrosis.* J Clin Microbiol, 1995. **33**(1): p. 37-40.

38. Mordukhova, E.A. and J.G. Pan, *Evolved cobalamin-independent methionine synthase (MetE) improves the acetate and thermal tolerance of Escherichia coli.* Appl Environ Microbiol, 2013. **79**(24): p. 7905-15.

39. González, J.C., et al., *Cobalamin-independent methionine synthase from Escherichia coli: a zinc metalloenzyme.* Biochemistry, 1996. **35**(38): p. 12228-34.

40. Schink, S.J., et al., *MetA is a "thermal fuse" that inhibits growth and protects Escherichia coli at elevated temperatures.* Cell Rep, 2025. **44**(1): p. 115257.

41. Hondorp, E.R. and R.G. Matthews, *Oxidative Stress Inactivates Cobalamin-Independent Methionine Synthase (MetE) in Escherichia coli.* PLOS Biology, 2004. **2**(11): p. e336.

42. Kaleta, C., et al., *Metabolic costs of amino acid and protein production in Escherichia coli.* Biotechnology Journal, 2013. **8**(9): p. 1105-1114.

43. Harris, C.L., *Cysteine and growth inhibition of Escherichia coli: threonine deaminase as the target enzyme.* J Bacteriol, 1981. **145**(2): p. 1031-5.

44. Tuite, N.L., K.R. Fraser, and P. O'Byrne C, *Homocysteine toxicity in Escherichia coli is caused by a perturbation of branched-chain amino acid biosynthesis.* J Bacteriol, 2005. **187**(13): p. 4362-71.

45. Vanhove, A.S., et al., *Methionine Availability in the Arthropod Intestine Is Elucidated through Identification of Vibrio cholerae Methionine Acquisition Systems.* Appl Environ Microbiol, 2020. **86**(11).

46. Husna, A.U., et al., *Methionine biosynthesis and transport are functionally redundant for the growth and virulence of Salmonella Typhimurium.* J Biol Chem, 2018. **293**(24): p. 9506-9519.

47. Graf, J. and E.G. Ruby, *Host-derived amino acids support the proliferation of symbiotic bacteria.* Proc Natl Acad Sci U S A, 1998. **95**(4): p. 1818-22.

48. Xu, J., et al., *Transformation of Xenorhabdus nematophilus.* Appl Environ Microbiol, 1989. **55**(4): p. 806-12.

49. Sugar, D.R., et al., *Phenotypic variation and host interactions of Xenorhabdus bovienii SS-2004, the entomopathogenic symbiont of Steinernema jollieti nematodes.* Environ Microbiol, 2012. **14**(4): p. 924-39.

50. Park, Y., et al., *Clonal variation in Xenorhabdus nematophila virulence and suppression of Manduca sexta immunity.* Cellular Microbiology, 2007. **9**(3): p. 645-656.

51. Neidhardt, F.C., P.L. Bloch, and D.F. Smith, *Culture medium for enterobacteria.* J Bacteriol, 1974. **119**(3): p. 736-47.

52. McMullen, J.G., 2nd and S.P. Stock, *In vivo and in vitro rearing of entomopathogenic nematodes (Steinernematidae and Heterorhabditidae).* J Vis Exp, 2014(91): p. 52096.

53. Lee, M.M. and S.P. Stock, *A multilocus approach to assessing co-evolutionary relationships between Steinernema spp. (Nematoda: Steinernematidae) and their bacterial symbionts Xenorhabdus spp. (gamma-Proteobacteria: Enterobacteriaceae).* Syst Parasitol, 2010. **77**(1): p. 1-12.

54. Bao, Y., et al., *An improved Tn7-based system for the single-copy insertion of cloned genes into chromosomes of gram-negative bacteria.* Gene, 1991. **109**(1): p. 167-168.

55. Alani, O.S., et al., *Conjugation and transposon mutagenesis of Xenorhabdus griffiniae HGB2511, the bacterial symbiont of the nematode Steinernema hermaphroditum (India).* MicroPubl Biol, 2023. **2023**.

56. Vivas, E.I. and H. Goodrich-Blair, *Xenorhabdus nematophilus as a model for host-bacterium interactions: rpoS is necessary for mutualism with nematodes.* J Bacteriol, 2001. **183**(16): p. 4687-93.

57. Orchard, S.S. and H. Goodrich-Blair, *Pyrimidine nucleoside salvage confers an advantage to Xenorhabdus nematophila in its host interactions.* Appl Environ Microbiol, 2005. **71**(10): p. 6254-9.

58. Cabreiro, F., et al., *Metformin Retards Aging in C. elegans by Altering Microbial Folate and Methionine Metabolism.* Cell, 2013. **153**(1): p. 228-239.

59. Zhou, G., et al., *Methionine increases yolk production to offset the negative effect of caloric restriction on reproduction without affecting longevity in C. elegans.* Aging (Albany NY), 2020. **12**(3): p. 2680-2697.

60. Virk, B., et al., *Excessive folate synthesis limits lifespan in the C. elegans: E. coli aging model.* BMC Biol, 2012. **10**: p. 67.

61. Cowles, C.E. and H. Goodrich-Blair, *The Xenorhabdus nematophila nilABC genes confer the ability of Xenorhabdus spp. to colonize Steinernema carpocapsae nematodes.* J Bacteriol, 2008. **190**(12): p. 4121-8.

62. Grossman, A.S., et al., *A Surface Exposed, Two-Domain Lipoprotein Cargo of a Type XI Secretion System Promotes Colonization of Host Intestinal Epithelia Expressing Glycans.* Frontiers in microbiology, 2022. **13**: p. 800366-800366.

CHAPTER 4: FIXED LRP EXPRESSION IN XENORHABDUS NEMATOPHILA IS DETRIMENTAL FOR SURVIVAL IN NUTRIENT-LIMITED NICHES.

Authors: Cameron Moore, Jennifer Heppert, Mengyi Cao and Heidi Goodrich-Blair

Author Contributions

I developed the methodology and performed all experimental analyses presented in this chapter excluding the RNA-seq and the *X. nematophila* cell yield experiment. I performed gene ontology analyses of the RNA-seq data set and analyzed the data. I also contributed to project conceptualization, manuscript writing, and editing.

Jennifer Heppert contributed to the generation of the RNA-seq dataset presented in this chapter by securing funding, developing the methodology, collecting the samples, submitting the data for sequencing, and the statistical analysis of the sequencing data.

Mengyi Cao conducted the cell yield experiment (Figure 7) detailed in the discussion and analyzed the data from that experiment. She also contributed to project conceptualization.

Heidi Goodrich-Blair secured funding, contributed to project conceptualization, manuscript editing, and writing.

ABSTRACT

Phenotypic heterogeneity is a strategy bacteria within an isogenic population u adapt to changes in their environments and is commonly observed in the context of microbial interactions with hosts. *X. nematophila* is symbiotic bacterium that obligately engages in mutualistic and antagonistic symbioses with *Steinernema* nematodes and insects, respectively, repetitively alternating between both host environments over its lifecycle. Phenotypic heterogeneity in *X. nematophila* is controlled in part by the global transcription factor Lrp, a mediator of host-specific adaptation whose differential expression leads to distinct host outcomes. Generally, elevated *lrp* expression in *X. nematophila* better supports the mutualistic association with *Steinernema* nematodes, while lower *lrp* expression improves *X. nematophila* virulence during insect infection. We demonstrate here that *X. nematophila* cells expressing constitutively high levels of *lrp* fail to persist during prolonged colonization of *S. carpocapsae* infective juvenile (IJ) nematodes, suggesting that the environment within the receptacle of aging IJs selects against this physiological state. *In vitro* growth assays conducted in chemically defined media reveal that a *X. nematophila* strain expressing fixed high *lrp* exhibits reduced fitness compared to cells expressing fixed low-*lrp* levels across conditions. Furthermore in amino acid-deficient conditions, the fixed high-*lrp* cells are unable to grow over a 168-h experiment unless exogenous methionine is present. By evaluating the influence of Lrp on the *X. nematophila* transcriptome, we uncover Lrp-regulated genes that were not observed in previously transcriptomic analyses that are essential for cellular growth including those involved in central carbon metabolism, amino acid metabolism, and protein synthesis. Our

data suggest that changes in Lrp activity or fulfillment of cellular demands for Met may influence population-wide shifts in *X. nematophila* during IJ colonization.

INTRODUCTION

Bacteria occupy diverse ecological niches that present biological, chemical, and physical changes. To survive and adapt to dynamic environmental conditions, bacteria must recognize how their environment is changing and alter their cellular physiology in response. Although adaptive responses can vary depending on the organism and environment, most, if not all, responses are linked to changes in an organism's genetic content and/or variation in gene expression [1]. Within clonal populations of bacteria, natural variation in gene expression at the cell-to-cell level has been observed and is hypothesized as a basis for biological bet-hedging in which sub-populations vary in their adaptive fitness under specific environments [1, 2]. The mechanisms driving cell-to-cell variation are diverse but are generally associated with reversible changes in genomic structure, epigenetic modification, or changes in transcriptional profile [1, 3, 4]. Much of our understanding of phenotypic heterogeneity comes from studies of human pathogenic microbes in which phenotypic heterogeneity can impact antimicrobial tolerance [5], immune system evasion [6], and niche expansion [7]. For example, metabolically dormant, persister cells within *Salmonella enterica* populations arise in response to a variety of environmental changes experienced during infection such as acidification or nutrient deprivation [7]. Upon treatment with antibacterial agents, this persister cell state is adaptive for survival in the host as it allows the bacterium to survive the treatment and proliferate once the environmental insult has cleared [7]. However, this phenomenon has been observed broadly in many non-pathogenic bacterial species suggesting that the utility of this strategy is not niche-specific [8-10]. As such, it is imperative to understand more

broadly among bacterial species how phenotypic variation arises and the environmental contexts for which specific variant sub-populations are better adapted.

The bacterium *Xenorhabdus nematophila* displays a type of phenotypic heterogeneity termed virulence modulation (VMO) that includes distinct adaptive states for associations with two invertebrate animal hosts [11, 12]. In its natural lifecycle, *X. nematophila* mutualistically associates with entomopathogenic *S. carpocapsae* nematodes. The nematode host vectors *X. nematophila* to and from susceptible insect hosts that are killed and consumed by the bacterium [13-15]. VMO was first observed in the context of insect virulence where *X. nematophila* wild-type clones derived from an isogenic population exhibited variability in their ability to kill insect hosts [12, 16]. In clones where virulence was attenuated, it was observed that expression and production of leucine-responsive regulatory protein (Lrp) was elevated compared to virulent clones [16]. Disruption of *lrp* in *X. nematophila* abrogated VMO as the clonal isolates derived from this population were exhibited attenuated virulence phenotypes [16]. Interestingly, complementation of the *X. nematophila lrp-2::kan* mutant with constructs that fixed *lrp* expression at high or low levels resulted in two distinct VMO states: attenuated and virulent, respectively [16-20]. This suggested that VMO in *X. nematophila* was driven by variability in Lrp levels within clonal populations.

Lrp is a global transcription factor in *X. nematophila* that is required for both mutualistic and antagonistic host interactions [21, 22]. Microarray-based transcriptomic analyses indicated that Lrp regulates ~7% of genes encoded within the *X. nematophila* genome [14, 16, 23] In *Escherichia coli* recent work revealed that the Lrp exerts regulatory

control over one-third of the genome in a context-dependent manner suggesting the *X. nematophila* Lrp regulon may be larger than revealed by microarray under a single growth condition [24]. Disruption of *lrp* significantly alters various aspects of *X. nematophila* physiology including flagellar biosynthesis, toxin production, secondary metabolite biosynthesis, and growth [21, 23]. Promoter-fusion experiments demonstrated that expression of genes known to fall within the Lrp regulon, such as *fliC*, are heterogeneously expressed over the course of insect infection and that clones with homogeneous *fliC* expression exhibit attenuated virulence unlike their heterogenous counterparts [18, 25]. In the context of *X. nematophila* mutualism with *S. carpocapsae* nematodes fixed high-*lrp* expressing *X. nematophila* better supports nematode fecundity and the colonization frequency of IJ nematodes relative to fixed low-*lrp* expressing strains [17, 19]. However, as *S. carpocapsae* IJs age in culture, *X. nematophila* populations shift from a homogenously high Lrp expression state (measured indirectly via P_{fliC}-*gfp* activity) to heterogenous high and low *lrp* expression states [17]. This suggests that conditions within aging *S. carpocapsae* IJ nematodes may select against cells expressing *lrp* at high levels in *X. nematophila* and select for a low-*lrp* expressing cells.

In this study, we report that fixed expression of *lrp* within *X. nematophila* populations is sufficient to abrogate temporal shifts in P_{fliC}-*gfp* expression during colonization of *S. carpocapsae* IJs. Furthermore, our data demonstrate that fixed high-*lrp* expression is not adapted for persistence within *S. carpocapsae* IJs nor is it adapted for growth in amino acid deficient growth conditions, particularly environments where methionine is absent. Conversely, strains with low levels of *lrp* are capable of growing and

persisting in these conditions suggesting that amino acid limitation is a likely driver of Lrp-dependent heterogeneity in *X. nematophila*. Re-evaluation of the *X. nematophila* Lrp regulon suggests that the maladaptation of the high-*lrp* strain to *in vivo* and *in vitro* conditions may be associated with dysregulation of genes predicted to be essential for growth. These data support a model that Lrp-dependent heterogeneity is modulated by fluctuations in environmental nutrients during the association between *X. nematophila* and *S. carpocapsae* IJs and is adaptive for survival within this host niche.

MATERIALS AND METHODS

Bacterial Growth Conditions

All *Xenorhabdus* bacteria used in this study were cryopreserved in 20% glycerol stocks at -80˚C. Strains were revived onto Luria-Bertani (LB) agar plates supplemented with 0.1% sodium pyruvate and grown for 16-24 h at 30˚C [26]. Bacterial overnight cultures were non-clonal to ensure representation of wild-type phenotypic variant sub-populations during each experiment [12]. A filter-sterilized (0.22 µm pore, Avantor), MOPS-based (40mM, 3-(N-morpholino)- propanesulfonic acid, MP Biomedicals) defined medium was used to grow *X. nematophila* strains [27]. The rich, defined permutation of the medium used in this study was described in Chapter 2 and contains glucose (11mM, Fisher Scientific), all 20 of the proteinogenic amino acids, nucleobases (adenine, uracil, guanine, and cytosine), and vitamins (thiamine, pantothenate, *p*-aminobenzoic acid, *p*-hydrxoybenzoic acid, 2, 3 – hydroxybenzoic acid, Chapter 2, [27]). For cultivations in minimal medium (MM), glucose (GMM), amino acids (AA), aspartate-derived amino acids (Asp, Thr, Lys 0.4 mM, ADAA), and methionine (Met, 0.2 mM, Sigma Aldrich)

were filter sterilized and added to the media as supplements. Nematode-bacterial co-cultures were conducted on lipid agar (LA) which contains 8 g/L of nutrient broth powder (Oxoid), 5 g/L of yeast extract (Research Products International), 2 mg/mL of $MgCl_2 \cdot 6H_2O$ (Acros Organic), 0.7% corn syrup (MP Biomedical) and 0.4% corn oil (Crisco), and 15 g/L of agar (Fisher Scientific) [28].

Growth Curve Assays

The OD_{600} of overnight LB cultures were measured on a Genesys 50 spectrophotometer (Thermo Fisher) and were then normalized to an OD_{600} of 1.0. Cells were washed three times with 1X PBS and diluted to an OD_{600} of 0.01 into sterile media. Growth curves were carried out in 96- well plates or in 17x100 mm, disposable culture tubes (hereafter, test tubes). For 96-well plate assays cultures were grown with double orbital shaking (282 cycles per minute) at a total volume of 250 µL of media in a Synergy H1 plate reader (Agilent). The plate reader was programmed to measure OD_{600} every 0.25h. For test tube assays, bacteria were grown in 5 mL of sterile media and grown in a cell rotator (New Brunswick Scientific) at 56 rpm. To assess viable cell counts during growth, samples were taken from test tube cultures, serial diluted in 1X PBS and plated on LB agar for colony counts. A Keyence epifluorescence microscope was utilized to assess P_{fliC}-*gfp* fluorescence phenotypes in colonies isolated from each growth condition. Growth curve data were blanked using OD_{600} from media only conditions and data were visualized logarithmically in GraphPad Prism v10.6.1. The growth dynamics for these cultures were determined as described previously in Chapter 2.

Table 4.1: Bacterial Strains and Growth Conditions

Strain Genotype	HGB #	Description	Antibiotic Resistance	Reference
X. nematophila ATCC19061	800	Symbiont of *Steinernema carpocapsae*	Amp	[29]
	1979	HGB800 with *att*Tn*7 ::*P_{fliC}-*gfp*/ Pl_{acUV5}-*rfp*	Amp, Erm, Chl	[19]
	2264	*X. nematophila att*Tn*7 ::*P_{fliC}-*gfp*/ Pl_{acUV5}-*rfp* that exhibits heterogenous P_{fliC}-*gfp* expression.	Amp, Erm, Chl	[17]
	2265	*X. nematophila att*Tn*7 ::*P_{fliC}-*gfp*/ Pl_{acUV5}-*rfp* that exhibits homogenously high P_{fliC}-*gfp* expression.	Amp, Erm, Chl	[17]
X. nematophila lrp-2::kan	1059	*X. nematophila lrp* null mutant	Amp, Kan	[21]
	2261	HGB1059 with *att*Tn*7 ::*P_{fliC}-*gfp*/ Pl_{acUV5}-*rfp*	Amp, Kan, Erm, Chl	[19]
	2262	HGB2261 with *kefA::* Pl_{acUV5}-*lrp* (Stop → Start); Low-*lrp*	Amp, Kan, Erm, Chl, Tet	[19]
	2263	HGB2261 with *kefA::* Pl_{acUV5}-*lrp* (Start → Stop); High-*lrp*	Amp, Kan, Erm, Chl, Tet	[19]

Spot Dilution Assays from Glycerol Stocks

The wild-type, *lrp-2::kan,* low, and high-*lrp X. nematophila* strains were revived from their original freezer stocks in the Goodrich-Blair Lab strain collection onto LB agar and grown for 24 h 30˚C. Overnight cultures for each strain were prepared in biological triplicate and grown for ~16 h at 30˚C. The OD_{600} of each culture was taken and they were normalized to an OD_{600} of 1.0 and prepared as glycerol stocks as described above. Samples were stored in -80˚C freezer for 7 d before strains were sampled into 1.5 mL Eppendorf using wooden applicator sticks. 100 µL of each sample was collected and serially diluted in sterile 1X PBS. The dilution series was plated on LB agar and monitored for growth. Spots were imaged on a Keyence epifluorescence microscope to assess P_{fliC}-*gfp* expression phenotypes in each strain and qualitatively assessed.

Aposymbiotic *S. carpocapsae* J1 Nematode Isolation and IJ Colonization Assay

Aposymbiotic *S. carpocapsae* nematodes eggs were isolated using a modified version of a describe previously protocol [30]. Briefly, *S. carpocapsae* IJs were seeded onto lawns of *X. nematophila* and incubated for 72 h at 25˚C. Nematode-bacterium co-cultures were collected via sedimentation, were resuspended in a 1.98% bleach and 0.25 M KOH solution, and mixed via gentle inversion for 10 min. Aposymbiotic eggs were isolated via centrifugation at 1,811 x g for 5 min, washed again in the bleach and KOH solution, and centrifuged. To remove the bleach solution, *S. carpocapsae* eggs were washed in sterile, LB broth, collected via centrifugation, enumerated, and added to bacterial lawns on lipid agar at approximately 5000 eggs per plate.

Aposymbiotic *S. carpocapsae* eggs were incubated on lipid agar lawns of *X. nematophila* strains for 7 d at 25˚C and then the co-cultures were water trapped in 25 mL of sterile water. Nematodes were collected for colonization assays in tissue culture flasks after 1-3 days post emergence and incubated at 25˚C. Collected *S. carpocapsae* IJs were sampled and centrifuged twice at maximum speed for 6 sec. Samples were treated with a 1% bleach solution for 2 min before the samples were centrifuged and washed with sterile water. Approximately 200 IJs were transferred to microcentrifuge tubes containing 250 mL of sterile LB. Samples were ground with a hand-held homogenizer for 2 min to release bacteria from the IJ receptacle. After addition of 750 mL of sterile LB, the nematode homogenate was serial diluted onto LBP agar. Plates were incubated at room temperature for 2 d before enumerating colony forming units and imaging on an epifluorescence microscope (Keyence). Microscopy images were analyzed via ImageJ [31] and the corrected total colony fluorescence was calculated for each colony imaged [32].

RNA Isolation, cDNA synthesis, and RNA-seq

Four biological replicates of *Xenorhabdus* wild-type and *lrp-2::kan* (HGB800 and HGB1059) were sub-cultured into fresh LB broth at starting OD_{600} of 0.05 and grown into early stationary phase (OD_{600} of 1.0). The cultures were pelleted, resuspended in 600 µL of Bacterial RNA Protect Reagent (Qiagen), pelleted again, and stored at -80˚C. RNA was isolated using a standard Trizol/Chloroform extraction protocol. Briefly, cells were lysed by multiple freeze thaw cycles into lysozyme (10 mg/mL, ThermoFisher). Trizol (Thermofisher) was added, samples were vortexed for 30 sec, and then incubated for 5 min at room temperature. Samples were then centrifuged at 12,000 x g for 10 min at 4˚C. The

supernatant was transferred and mixed with 100 µL of chloroform for 15 sec then incubated for 3 min at room temperature. After centrifugation at 12,000 x g for 10 min at 4˚C, the aqueous phase was transferred, and RNA was precipitated with isopropanol. The precipitate was washed twice with 70% ethanol before being solubilized in nuclease free water. The RNA concentration and quality was assessed using an Agilent TapeStation. Samples were next run on an Illumina NextSeq platform with 150 bp paired-end reads, resulting in an average of 18 million reads per sample (~600x coverage). The Galaxy server and following packages were used to analyze the reads and determine differential expression [33]. FastQC was used to assess read quality, Trim Galore! was used to autodetect and trim adapter sequences (trimming was confirmed by rerunning FastQC, SortMeRNA was used to deplete rRNA and tRNA sequences using a custom database generated for *X. nematophila*, HiSAT2 was used for read mapping, followed by FeatureCounts and DESeq2 to quantitate differential gene expression. Significance cutoffs were established at an adjusted p-value of 0.05, and fold change of 1.5 and were based on those used previously to determine the Lrp regulon *E. coli* [24]. The locus tags corresponding to the differentially expressed genes were submitted to ShinyGO v. 0.85.1 [34] and KEGG Mapper [35] for assignment of biological and metabolic functions.

RESULTS

Selection against *X. nematophila* high *lrp* expression occurs within the receptacle of *S. carpocapsae* IJ nematodes

Wild-type populations of *X. nematophila* exhibit a shift from homogenously high P*fliC*-*gfp* expression to heterogenous P*fliC*-*gfp* expression during colonization of aging *S.*

carpocapsae IJs [17]. The *X. nematophila* transcription factor, Lrp, is required for expression of *fliC* and both *lrp* and *fliC* are variably expressed within *X. nematophila* populations [16, 21, 25]. We hypothesized that variable *lrp* expression drives a population-wide shift in *X. nematophila fliC* expression. To test this hypothesis, we reared *S. carpocapsae* IJs on lawns of wild-type, *lrp-2::kan,* fixed low, and fixed high *lrp* strains engineered with a P_{fliC}-*gfp*/P_{lacUV5}-*rfp* reporter and assessed their fluorescence phenotypes over time (**Fig 4.1A** and **C**). We initially observed that very few *S. carpocapsae* IJs emerged from lawns of the *X. nematophila lrp-2::kan* mutant into water traps. Furthermore, when assessing bacterial colonization on the few emerged nematodes from this condition, few *lrp-2::kan* colonies could be derived from the IJs. Both observations were consistent with previous findings that *lrp* is required for the development and colonization of *S. carpocapsae* IJs [17, 19, 21]. Based on these observations, we chose not to assess this condition further.

Over our 60-d experiment, wild-type *X. nematophila* exhibited an overall decrease in PfliC-*gfp* expression during *S. carpocapsae* IJ colonization. At 0 d post emergence (dpe), 94% of wild-type *X. nematophila* colonies derived from IJs exhibited high P_{fliC}-*gfp* intensity with the remaining 6% exhibiting an intermediate P_{fliC}-*gfp* intensity. These data are consistent with previous studies from our group demonstrating that high *lrp* expression in *X. nematophila* is adaptive for colonization initiation with *S. carpocapsae* IJs [17, 19]. By 60 dpe, 80% of the colonies derived from *S. carpocapsae* IJs had an intermediate P_{fliC}-*gfp* intensity. Across the 60-d experiment, colonies derived from the fixed low-*lrp* associated *S. carpocapsae* IJs had predominantly (87-96%) little to no expression of P_{fliC}-

gfp, consistent with previous observations that the low-*lrp* strain expresses *fliC* at lower levels and is less motile than wild-type *X. nematophila* [16, 19]. We had predicted that only high P*fliC*-*gfp* expressing colonies could be liberated from *S. carpocapsae* IJs reared on a *X. nematophila* fixed high-*lrp* strain; however, at 0 dpe that 41% of the population had high P*fliC*-*gfp* expression, 14% of the population had intermediate P*fliC*-*gfp* expression, and 44% of the population had little to no P*fliC*-*gfp* expression. By the end of the 60-d experiment, we noted that the majority colonies derived from the high-*lrp* reared nematodes (62%) had little to no P*fliC*-*gfp* expression, while 37% of the population had intermediate P*fliC*-*gfp* expression, and no colonies exhibited high P*fliC*-*gfp* expression.

Heterogeneity in regard to P*fliC*-*gfp* expression in *X. nematophila* has not been reported previously during early stages of *S. carpocapsae* IJ colonization [17]. Given that CFUs derived from high-*lrp* reared IJs exhibited high, intermediate, and no P*fliC*-*gfp* expression at 0 dpe, we considered that the conditions stimulating this variation could be specific to the IJ receptacle environment as this strain was previously characterized to have homogenously high P*fliC*-*gfp* expression at the colony-level [19]. We tested this possibility by examining the fluorescence phenotypes of the high-*lrp* strain during *in vitro* culture to determine if this strain exhibited homogenous or heterogenous P*fliC*-*gfp* expression. Spot-dilution assays of the high-*lrp* strain revealed that P*fliC*-*gfp* heterogeneity was observable at the colony-level when the strain was revived from cryopreserved glycerol stocks (**Figure 4.2**). This suggested that induction of heterogeneity in the high-*lrp* strain was not specific to the conditions found within the receptacle of *S. carpocapsae* IJs. Heterogenous P*fliC*-*gfp* expression in the *X. nematophila* high-*lrp* strain could be caused by multiple possibilities,

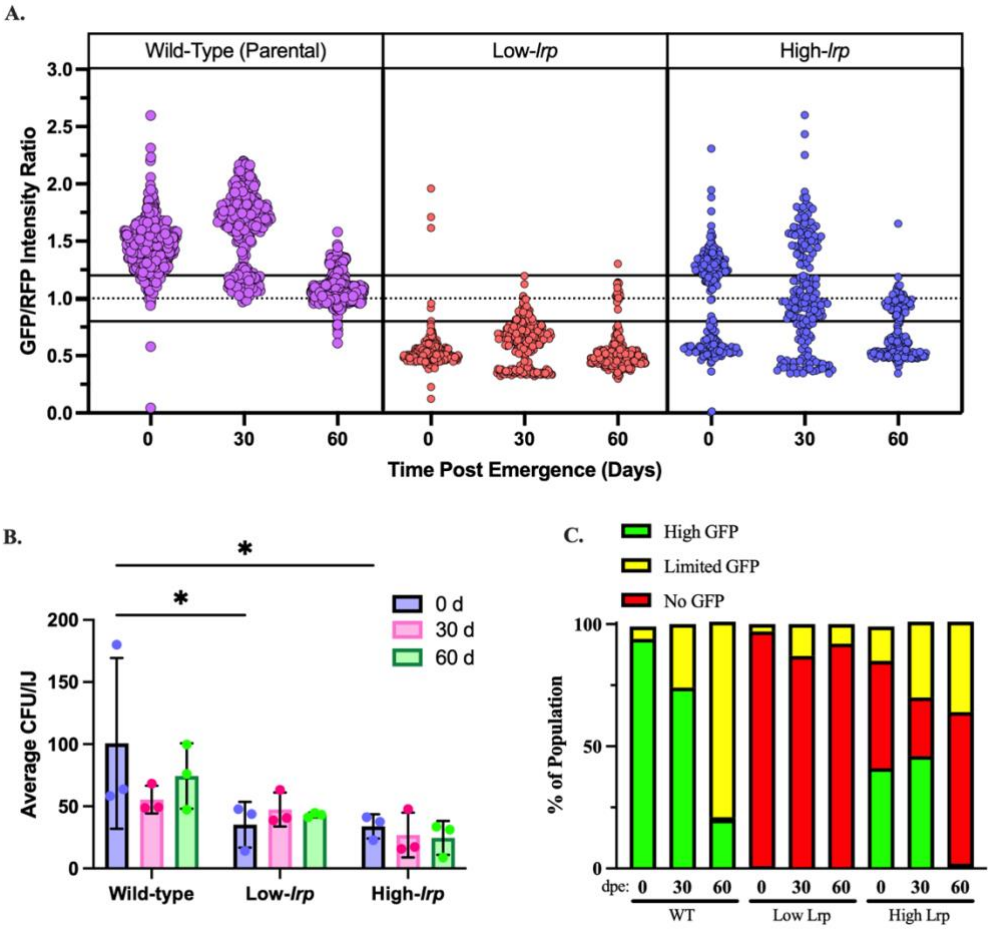


Figure 4.1: Constitutive *lrp* expression is detrimental for *X. nematophila* persistence within *S. carpocapsae* IJs.

A) Fluorescence intensity of P_{fliC}-*gfp* (relative to constitutive *rfp* expression) in CFUs of *X. nematophila* wild-type (purple), fixed-low (red), and fixed-high *lrp* (blue) expression strain when liberated from unaged (0 d) and aged (30 and 60 d) *S. carpocapsae* IJs. Dots represent individual, imaged CFUs from 3 biological and 3 technical replicates. Solid lines at y = 1.2 and y = 0.8 denote thresholds for fluorescence phenotype determination, while the dashed line at y = 1.0 indicates where equal GFP/RFP intensity would be expected. **B)** Bacterial burden of strains in *S. carpocapsae* IJs over time (0 d– blue, 30 d – pink, 60 d – green; 3 biological replicates per strain). Statistical analyses were conducted via a Two-Way ANOVA with a Tukey's HSD *post hoc* analysis and error bars are shown for ±1 SD. **C)** Proportion of CFUs from Fig 1A, exhibiting high (green), limited (yellow), and no (red) P_{fliC}-*gfp* expression over time. Data points represent individual CFUs liberated from the IJs of unaged (0 d) and aged (30-60 d) *S. carpocapsae* IJs. Each strain is engineered with a P_{fliC}-*gfp*/P_{lacUV5}-*rfp* at the *att*Tn*7* site and fluorescence phenotypes of the colonies were imaged on a Keyence epifluorescence microscope. GFP and RFP intensity were analyzed via ImageJ to determine the GFP/RFP intensity ratio.

such as alternative gene expression regulatory pathways, epigenetic modifications, or variation in genomic content. We first examined if P*fliC*-*gfp* variation was caused by genomic differences between cells comprising the high-*lrp* strain. We isolated variants of the high-*lrp* strain that exhibited either P*fliC*-*gfp* positive and negative phenotypes and sequenced their genomes. This analysis revealed that the P*fliC*-*gfp* positive isolate contained both the P*fliC*-*gfp* and high-*lrp* genomic insertion, while the P*fliC*-*gfp* negative isolate contained only the P*fliC*-*gfp* insertion. From this we reasoned that the high-*lrp* P*fliC*-*gfp* negative isolate had lost the constitutive *lrp* genomic insert and reverted to the *lrp-2::kan* P*fliC*-*gfp* null phenotype (**Figure 4.2**). In the context of the *S. carpocapsae* IJ colonization assay described above, the appearance of P*fliC*-*gfp* negative colonies derived from high-*lrp* reared *S. carpocapsae* IJs suggests that there is *in vivo* selection against *X. nematophila* cells expressing high levels of *lrp*.

***X. nematophila* cells expressing high levels of *lrp* are better adapted for growth in amino acid replete environments but grow poorly in amino acid limiting conditions.**

We hypothesized that the persistence defect of the *X. nematophila* high-*lrp* strain in the receptacle of aging *S. carpocapsae* IJs was associated with the strain's inability to grow or persist in nutrient-limited environment. To test this, we sought to perform growth assays of *X. nematophila* wild-type, *lrp-2::kan,* fixed low, and fixed high *lrp* strains in media conditions varying in their nutrient richness. We assessed growth dynamics (length of lag phase, growth rate, and maximum OD_{600}) to determine relative fitness under each condition. Strains were pre-grown in LB broth and sub-cultured into either rich, defined medium (RDM), glucose minimal medium with all 20 amino acids (GMM + AA), MM +

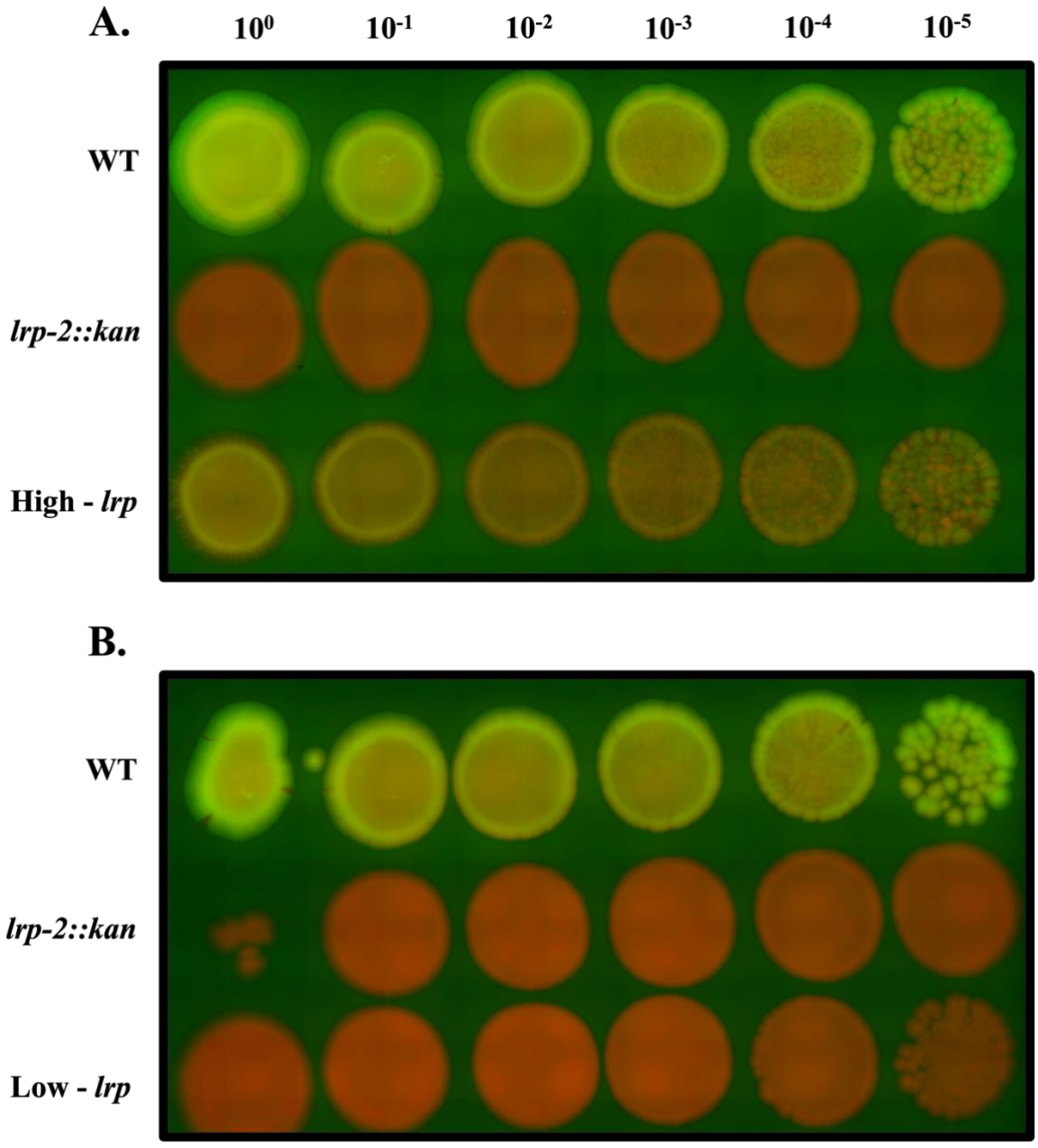


Figure 4.2: Spot dilution assay of *X. nematophila* wild-type, *lrp-2::kan*, low-*lrp*, and high-*lrp* strains on LB when revived from glycerol stocks stored at -80°C for 7 d.

Spot dilution assay of *X. nematophila* wild-type, *lrp-2::kan*, low-*lrp*, and high-*lrp* strains on LB when revived from glycerol stocks stored at -80°C for 7 d.
Spot dilution assays were conducted in biological triplicate and representative images are shown for the high-*lrp* strain (**A**) and the low-*lrp* strain (**B**). Images were taken on a Keyence epifluorescence microscope and are overlays of the green and red fluorescence channels.

AA, GMM + methionine (Met), or GMM. Prior to these experiments, we investigated if the high-*lrp* strain (i.e., the P_{fliC}-*gfp* positive high-*lrp* isolate) could maintain homogenous P_{fliC}-*gfp* expression (a proxy for high *lrp* expression) and determined that this strain maintained stable P_{fliC}-*gfp* expression during cultivation in LB broth (**Table 4.2**). This was done to ensure that the inoculum used for growth assays in defined media was truly representative of the high-*lrp* phenotype.

When transitioning from growth in LB to growth in RDM (**Figure 4.3A, Figure 4.4ABC**), we observed no significant differences among the tested strains in regard to lag phase and maximum OD_{600}; however, we did note differences in regard to growth rate. The wild-type had a significantly higher growth rate (0.45 ± 0.09, One-Way ANOVA) compared to the *lrp-2::kan* (0.27 ± 0.04, $p < 0.05$), fixed low (0.27 ± 0.04, $p < 0.05$), and fixed high *lrp* (0.13 ± 0.02, $p < 0.001$) strains (One-Way ANOVA). Furthermore, the fixed high *lrp* strain exhibited a significantly lower growth rate than the *lrp-2::kan* and fixed low *lrp* strain ($p < 0.05$). These data suggest that variability in Lrp levels has little to no impact on the ability of *X. nematophila* to adapt and reach an optimal growth yield when transitioning between nutrient replete media. The lower growth rate observed in the fixed high *lrp* strain compared to the low and no *lrp* conditions suggests that *X. nematophila* populations with homogenously high *lrp* may incur a slight fitness cost when grown in nutrient replete conditions. We observed a similar trend in growth rate when the tested strains were transitioned from LB to GMM+AA (**Figure 4.3B, Figure 4.4DEF**), which lacks nucleobases and vitamins. This suggested to us that nucleobases and vitamins contribute very little to the differences in *X. nematophila* growth rates in any of the tested

strains. We did observe differences in regard to lag phase and maximum OD_{600} in GMM+AA. The wild-type (1.5 ± 0.00) and fixed high *lrp* (1.42 ± 0.14) strains had significantly longer lag times than the *lrp-2::kan* strain (0.5± 0.00, $p < 0.05$, One-Way ANOVA) while the fixed low *lrp* strain (0.83 ± 0.58) exhibited a non-significant intermediate phenotype. Second, both the *lrp-2::kan* (0.54 ± 0.03) and fixed low *lrp* (0.55 ± 0.02) strains reached a significantly lower OD_{600} than the wild-type (0.64 ± 0.01, $p <0.01$) and fixed high *lrp* strain (0.66 ± 0.02, $p < 0.001$). This suggested that in environments where nucleotides and vitamins are deficient, elevated *lrp* expression increases the time required for *X. nematophila* to adapt to a new condition but permits higher growth yield if exogenous glucose and the amino acids are present.

When transitioning from LB to MM+AA (**Figure 4.3C, Figure 4.4GHI**), a glucose deficient condition, we observed significant differences among the strains in regard to growth rate and maximum OD_{600}, but not lag time. Interestingly, the growth rates for all four strains were significantly different from one another with wild-type (0.29 ± 0.01) having the highest growth rate followed by the fixed low-*lrp* strain (0.25 ± 0.00, $p < 0.05$), *lrp-2::kan* (0.21 ± 0.01, $p < 0.0001$), and fixed high-*lrp* (0.13 ± 0.01, $p < 0.0001$, One-Way ANOVA). Despite these differences, the wild-type, *lrp-2::kan*, and low-*lrp* strain reached similar maximum OD_{600} readings (~0.53) while the fixed high-*lrp* strain reached a maximum OD_{600} of 0.42 ± 0.01 ($p < 0.0001$, One-Way ANOVA). Together, these results suggest that *X. nematophila* cells expressing low levels of *lrp* are better adapted for transitions into amino acid replete, glucose deficient environments than those that have high levels of expression.

Table 4.2: The *X. nematophila* high-*lrp* P_{fliC}-*gfp* positive isolate maintains high P_{fliC}-*gfp* expression homogenously during growth in LB broth at the colony-level.

The P_{fliC}-*gfp* positive high-*lrp* isolate was grown in LB broth in biological triplicate and sampled throughout at initial inoculation, mid-exponential (OD_{600} = 0.5 - 0.6) and mid-stationary ($OD_{600} \geq 1.1$) growth phases for viable cell counts. Fluorescence phenotypes of the samples CFUs were assessed and are represented as a percentage of the total counted CFU.

Growth Phase	**Total CFU Analyzed**	**% P_{fliC} - *gfp* Positive**	**% P_{fliC} - *gfp* Negative**
Inoculum	321	99.7	0.3
Exponential	69	100	0
Stationary	116	100	0

In GMM (**Figure 4.3F, Figure 4.4PQR**), the fixed high-*lrp* strain was unable to grow over the 168-h experiment, while the *lrp-2::kan* and low-*lrp* strains grew at rates similar to wild-type. However, both strains exhibited longer lag times (*lrp-2::kan*: 74.9 ± 7.95, $p < 0.001$; low-*lrp*: 71.67 ± 1.28, $p<0.01$) and reached a lower maximum OD_{600} (*lrp-2::kan*: 0.28 ± 0.02, $p < 0.01$; low-*lrp*: 0.29 ± 0.02, $p<0.05$) compared to wild-type (0.33 ± 0.02, One-Way ANOVA). In GMM + ADAA (**Figure 4.3D, Figure 4.4JKL**) - a condition we identified in Chapter 1 that significantly reduced the lag time of *X. nematophila* compared to GMM alone – the strains performed similarly in regard to maximum OD_{600} and lag time. Only the wild-type strain exhibited a significantly higher growth rate (0.21 ± 0.06, $p < 0.05$, One-Way ANOVA) than the other three strains supporting our above conclusion that variability in *X. nematophila lrp* expression is more optimal than fixed or no *lrp* expression. We previously demonstrated that the ADAA Met was sufficient to reduce wild-type *X. nematophila* lag time in GMM. In the GMM + Met condition (**Figure 4.3E, Figure 4.4MNO**), the wild-type *X. nematophila* strain had a significantly shorter lag time (21.8 ± 3.04, $p < 0.01$, One-Way ANOVA) than the other tested strains. We also observed that the *lrp-2::kan* (28.8 ± 0.87, $p < 0.0001$) and low-*lrp* strains (29.3 ± 0.25, $p < 0.0001$) had significantly shorter lag times than the fixed high-*lrp* strain. The fixed high-*lrp* strain also had a significantly lower growth rate than the other tested strains (0.04 ± 0.00, $p < 0.05$), but was able to reach a maximum OD_{600} similar to wild-type (0.55 ± 0.02). The *lrp-2::kan* (0.40 ± 0.02, $p < 0.01$) and low-*lrp* (0.41 ± 0.01, $p < 0.01$) strains reached

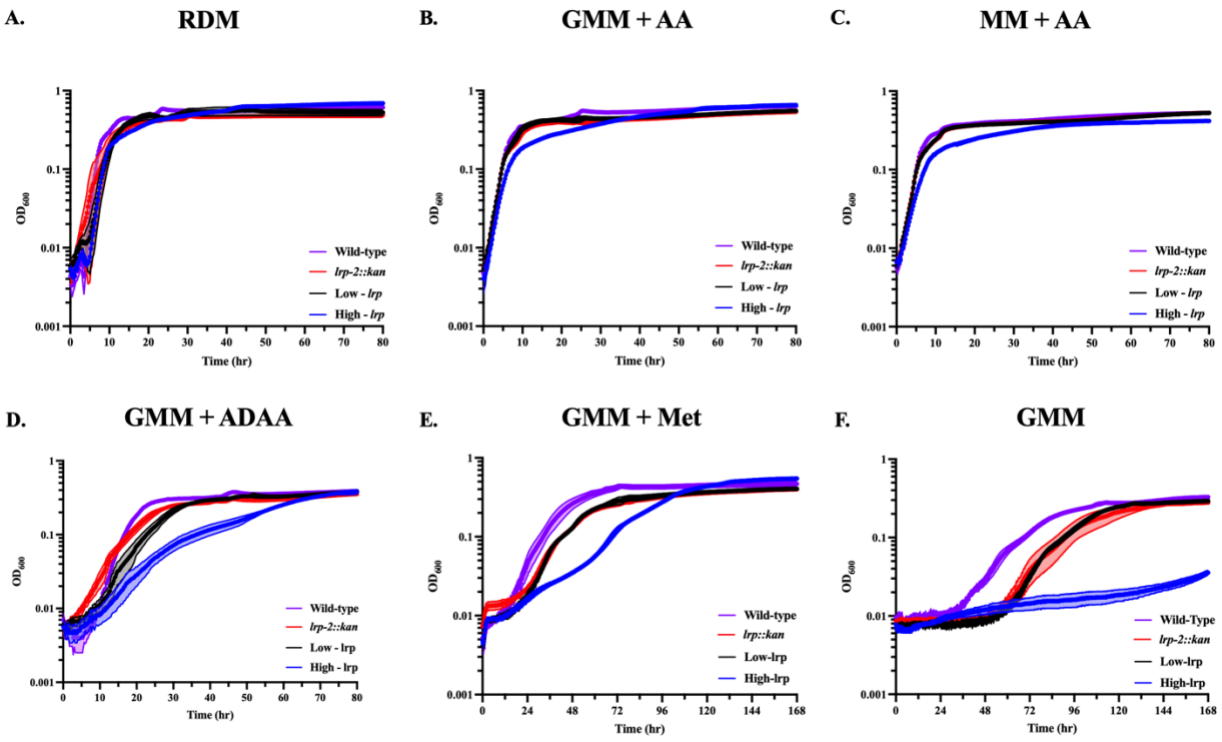


Figure 4.3: Fixed high-*lrp* expressing *X. nematophila* cells (blue) grow poorly in amino acid limiting growth conditions compared to wild-type (purple), *lrp-2::kan* (red), and fixed low-*lrp* (pink) strains.

Three biological replicates for each tested strain were inoculated into rich, defined medium (RDM, A), glucose minimal medium + all 20 of the amino acids (GMM + AA, B), MM+AA (C), GMM + aspartate-derived amino acids (ADAA, D), GMM + methionine (Met, E), and GMM (F) and grown for 80 or 168 h. Shaded regions indicate ±1 SEM.

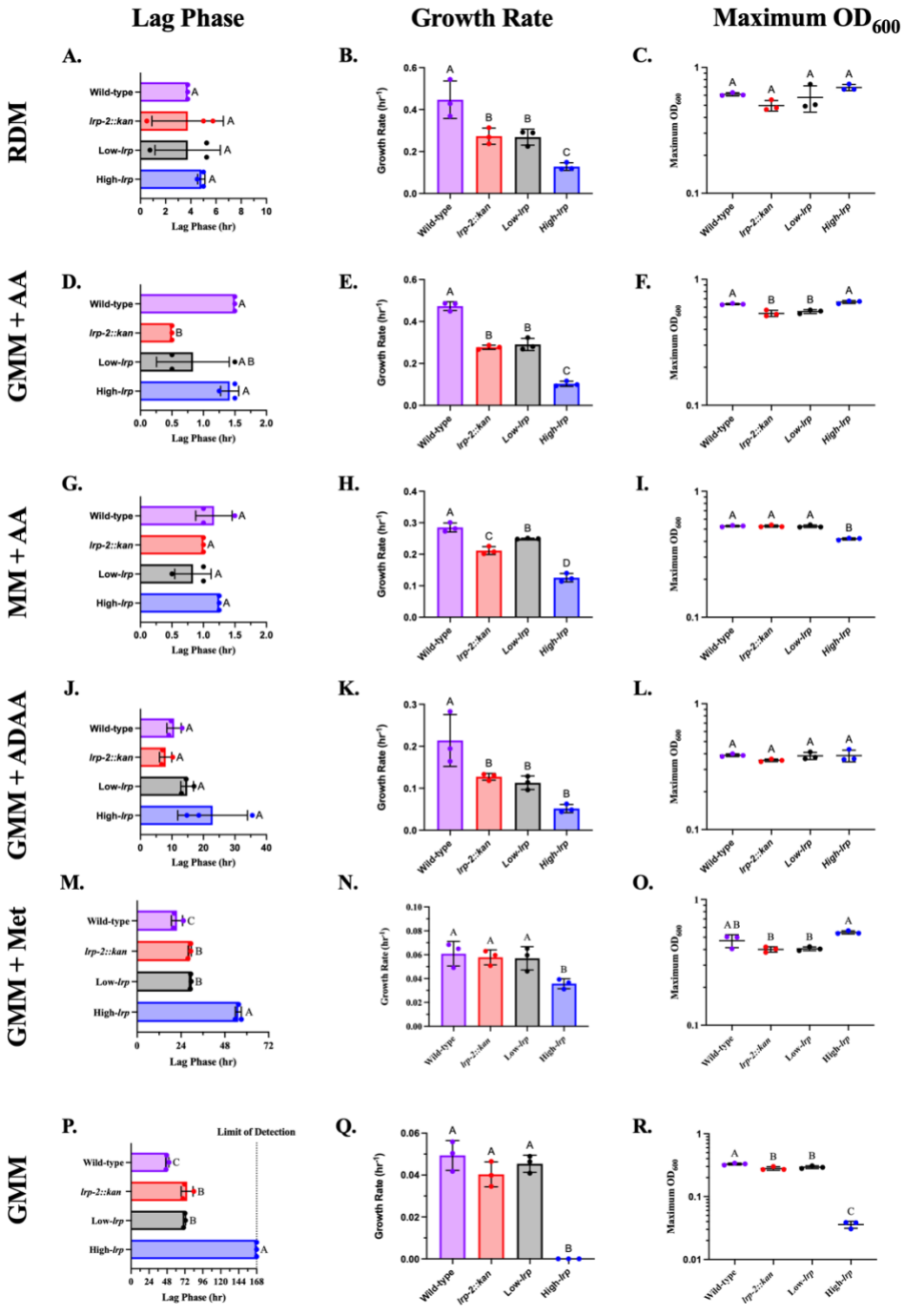


Figure 4.4: The length of lag phase (A, D, G, J, M, P), growth rate (B, E, H, K, N, Q), and maximum OD_{600} (C, F, I, L, O, R) determined from the growth curves in Figure 4.3.

These data represent the average of three biological replicates ±1 SD. Cultures were grown in RDM (A, B, C), GMM+AA (D, E, F), MM+AA (G, H, I), GMM+ADAA (J, K, L), GMM+Met (M, N, O), and GMM (P, Q, R) for 80 or 168 h.

a significantly lower maximum OD_{600} in GMM+Met than the high-*lrp* strain. Taken together, the data suggest that both high and low *lrp* expression levels in *X. nematophila* support growth in amino acid replete conditions, but when these expression states are fixed within the population only the low-*lrp* strain can grow in the absence of amino acids.

Lrp regulates 25% of the predicted genes found in the *X. nematophila* genome including those involved in symbiosis, metabolism, and essential cellular functions

The lack of observable amino acid dependent growth of the fixed high-*lrp* strain in GMM suggested that overexpression of *lrp* may lead to dysregulation of one or more genes involved in *X. nematophila* metabolism that are essential for bacterial growth/survival in amino acid deplete conditions. The influence of Lrp on the *X. nematophila* transcriptome has been examined previously via a microarray-based approach [14, 16, 23]. To build upon these findings, we performed RNA-seq on the *X. nematophila* and the *lrp-2::kan* strains during growth in LB. We identified 1157 coding sequences (CDS) whose transcript abundances were altered in the absence of *lrp* (**Figure 4.5A**). Of these transcripts, 670 of them were underrepresented (positively regulated by Lrp) in the *lrp-2::kan* mutant while the remaining 487 genes were overrepresented (negatively regulated by Lrp, **Figure 4.5B**). The *X. nematophila* genome is predicted to encode 4,570 ORFs and these data indicate that ~25% of the predicted coding potential of the genome is Lrp-regulated during growth in LB. Our previous microarray-based approach only identified that 7.3% of the *X. nematophila* genome was regulated by Lrp, suggesting that novel Lrp-regulated genes were identified using this approach [14].

To verify the accuracy of our transcriptomic analysis we examined if previously identified differentially expressed genes from the microarray were present in our dataset. Lrp has been previously shown to play an integral role in *X. nematophila* virulence by positively regulating expression of genes in the flagellar regulon hierarchy which are essential for insect infection [16, 21]. The transcriptional regulator *fliZ* exerts a strong regulatory influence on other flagellar regulatory proteins such as *flhDC* and *fliA* [25, 36, 37]. Expression of *fliZ* ($\log_2$(FC) = -1.59, $p < 0.001$), *flhD* ($\log_2$(FC) = -1.85, $p < 0.0001$), *flhC* ($\log_2$(FC) = -1.41, $p < 0.01$), and *fliA* ($\log_2$(FC) = -1.97, $p < 0.001$) were significantly lower in the *lrp-2::kan* mutant, which correlated with reduced expression of other chemotaxis and flagellar assembly associated genes like *fliC* ($\log_2$(FC) = -5.99, $p < 0.0001$). The secreted hemolysin *xhlA* and its co-regulated transport protein *xhlB* are required for *X. nematophila* virulence and expression of these genes is directly influenced by Lrp [21, 38]. In our dataset we observed that *xhlA* ($\log_2$(FC) = -2.99, $p < 0.0001$) and *xhlB* ($\log_2$(FC) = -2.20, $p < 0.001$) expression was reduced in the *lrp-2::kan* mutant consistent with these data.

The fecundity of the *S. carpocapsae* nematodes during insect infection is dependent upon the presence of *lrp* in *X. nematophila* as *lrp-2::kan* mutants do not support nematode reproduction at wild-type levels [19, 21]. The *X. nematophila* transcription factor LrhA and its regulon member XlpA, a secreted lipase, support *S. carpocapsae* nematode fecundity in an Lrp-dependent manner [39-41]. In the *lrp-2::kan* background, we noted that only *lrhA* ($\log_2$(FC) = -1.76, $p < 0.001$), but not *xlpA* ($\log_2$(FC) = 0.48), was significantly downregulated consistent with previous observations that Lrp positively regulates

expression of *lrhA* [39]. The fecundity of *S. carpocapsae* nematodes is also dependent upon production of secondary metabolites by *X. nematophila* [42]. Lrp is a known regulator of secondary metabolite production in *X. nematophila* and has been reported to positively and negatively regulate genes involved in their biosynthesis [23]. There are seventeen predicted secondary metabolism-associated loci in the genome of *X. nematophila* as predicted in MaGe Microscope [43] and by comparing these loci to our dataset we identified that Lrp is predicted to regulate genes present in all seventeen secondary metabolism-associated loci. Of the 690 genes found in these loci (15.1% of the genome), 208 of them were positively regulated by Lrp while 49 of them were negatively regulated. In support of previous published observations, this suggests that Lrp controls secondary metabolite production in *X. nematophila* [23].

Lrp is also a major regulator of *S. carpocapsae* IJ nematode colonization and directly regulates essential colonization factors such as the nematode intestinal localization gene, *nilC.* NilC is the specific, lipidated cargo of NilB, a type 11 secretion system is coordinately repressed by Lrp and the transcriptional repressor NilR [21, 44, 45]. Furthermore, Lrp negatively influences the expression of *nilR* [44]. Consistent with these observations, we observed that *nilC* ($\log_2$(FC) = 3.41, $p < 0.0001$) and *nilR* ($\log_2$(FC) = 3.54, $p < 0.0001$) expression were significantly higher in the *lrp-2::kan* strain. Together these observations indicate that the RNA-seq transcriptomic dataset is reflective of the Lrp regulon in *X. nematophila.*

We next submitted our transcriptomic dataset for gene ontology annotations using ShinyGO 0.85.1 [34]. GO terms for transcripts whose abundance was positively influenced

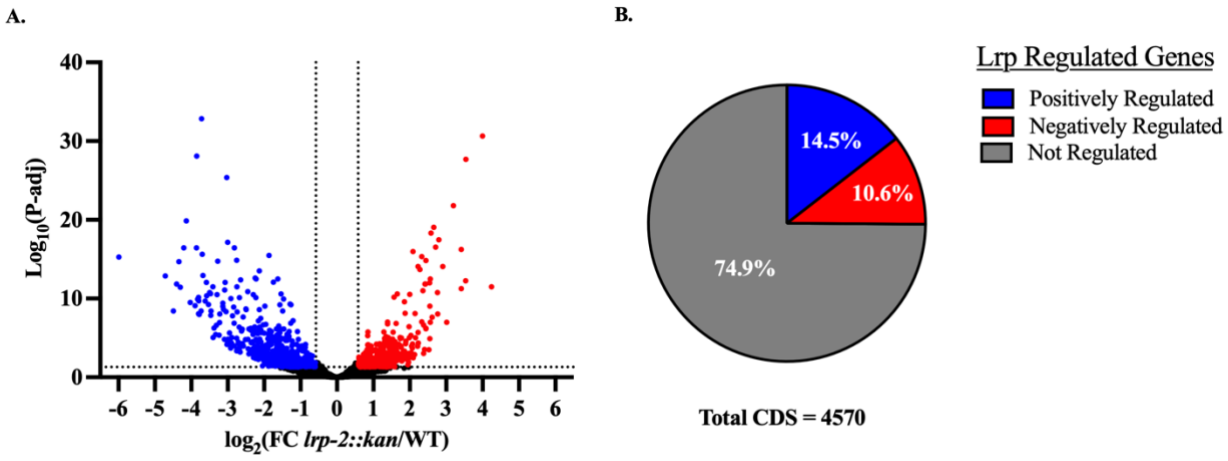


Figure 4.5: The presence of *lrp* influences gene expression of 25% of genes encoded in the *X. nematophila* genome when grown to stationary phase in a complex, rich medium.

A) Volcano plot of underrepresented (blue), overrepresented (red), and unrepresented (black) mRNA transcripts in an *X. nematophila lrp-2::kan* mutant compared to the parental wild-type strain. Dotted lines indicate cut-off values to determine which genes are differentially transcribed in X. *nematophila lrp-2::kan* mutant ($\log_{10}$(p-adj) = X, $\log_2$(Fold Change) = ±Y). **B)** Pie chart illustrating the percentage of genes positively (blue) and negatively (red) regulated by *X. nematophila* Lrp.

by the presence of *lrp* were associated with flagellar biosynthesis, chemotaxis, and secondary metabolism consistent with what we described above. For the negatively regulated transcripts, we noticed a preponderance of GO terms associated with general metabolism and cellular processes. We retrieved the predicted functions of these genes by using KEGG Mapper to analyze the locus tags of the corresponding genes. In some bacterial species, Lrp is an amino acid-responsive regulatory protein and can have a broad regulon that encompasses multiple modules of bacterial metabolism [46-48]. Consistent with our previous microarray-based transcriptomic analysis, we noted that the majority of metabolic genes under the Lrp regulon were associated with carbohydrate and amino acid metabolisms and included an expanded set of genes in both types of metabolism relative to previous datasets (**Figure 4.6** and **Table 4.3**, [14]). For example, Lrp positively influenced the expression of *manX* ($\log_2$(FC) = -1.47, $p < 0.05$) which is predicted to encode the EIIAB component of the ManXYZ phosphotransferase system as well as others involved in glycolysis. In contrast, Lrp negatively regulates the expression of genes downstream of glycolytic metabolism, in particular those involved in acetyl-CoA metabolism including the enzymes responsible for converting pyruvate into acetyl-CoA (AceE, AceF, and Lpd), acetate production and assimilation (Pta, AckA, and Acs), and CoA synthesis (PanBCE and IlvC). Together, this suggests that Lrp can exert control over *X. nematophila* carbon metabolism by modulating gene expression involved with carbon transport and catabolic activity at this growth phase.

In regard to amino acid metabolism, we observed that Lrp negatively influenced expression of genes associated with branched-chain amino acid (BCAA) biosynthesis. Lrp

and its regulatory effects have been best characterized in *E. coli* in the context of BCAA metabolism and our results affirm that this function is likely conserved in *X. nematophila* [49]. Furthermore, Lrp positively influenced the expression of *livH* (log_2(FC) = -1.33, $p < 0.05$) which is predicted to play a role in BCAA import (**Figure 4.6** and **Table 4.3**). Considering that LB is replete for BCAA, these data suggest that Lrp in *X. nematophila* may respond to extracellular abundances of BCAAs and modifies the transcriptome to promote nutrient uptake and reduce anabolic processes. Lrp also negatively influenced expression of genes indirectly associated with Met biosynthesis. While the core biosynthetic enzymes of the *X. nematophila* trans-sulfurylation pathway were not differentially expressed in the *lrp-2::kan* mutant, genes associated with sulfur assimilation, cysteine biosynthesis, aspartate-derived amino acid biosynthesis, and glycine degradation were negatively regulated by Lrp (**Figure 4.6** and **Table 4.3**). These pathways generate necessary Met precursors, like cysteine, homoserine, and 5-methylene tetrahydrofolate [50]. Met biosynthesis has been described as energetically costly in other bacteria and reducing the production of these products, and therefore Met, may be an adaptive measure when nutrient conditions are replete with Met [51]. Interestingly, we also saw that Lrp positively influenced the expression of MetY (log_2(FC) = -2.27, $p < 0.001$). MetY is a homocysteine synthase enzyme that is predicted to function in the Met direct sufurylation pathway that uses H_2S rather than cysteine as a sulfur donor [52]. In genomic analyses conducted in Chapter 2, we did not identify the enzymes MetX and MetW, which, in tandem with MetY, are predicted to engender Met synthesis via direct sulfurylation. It is nonetheless curious that Lrp positively regulates expression of MetY as it has not yet been

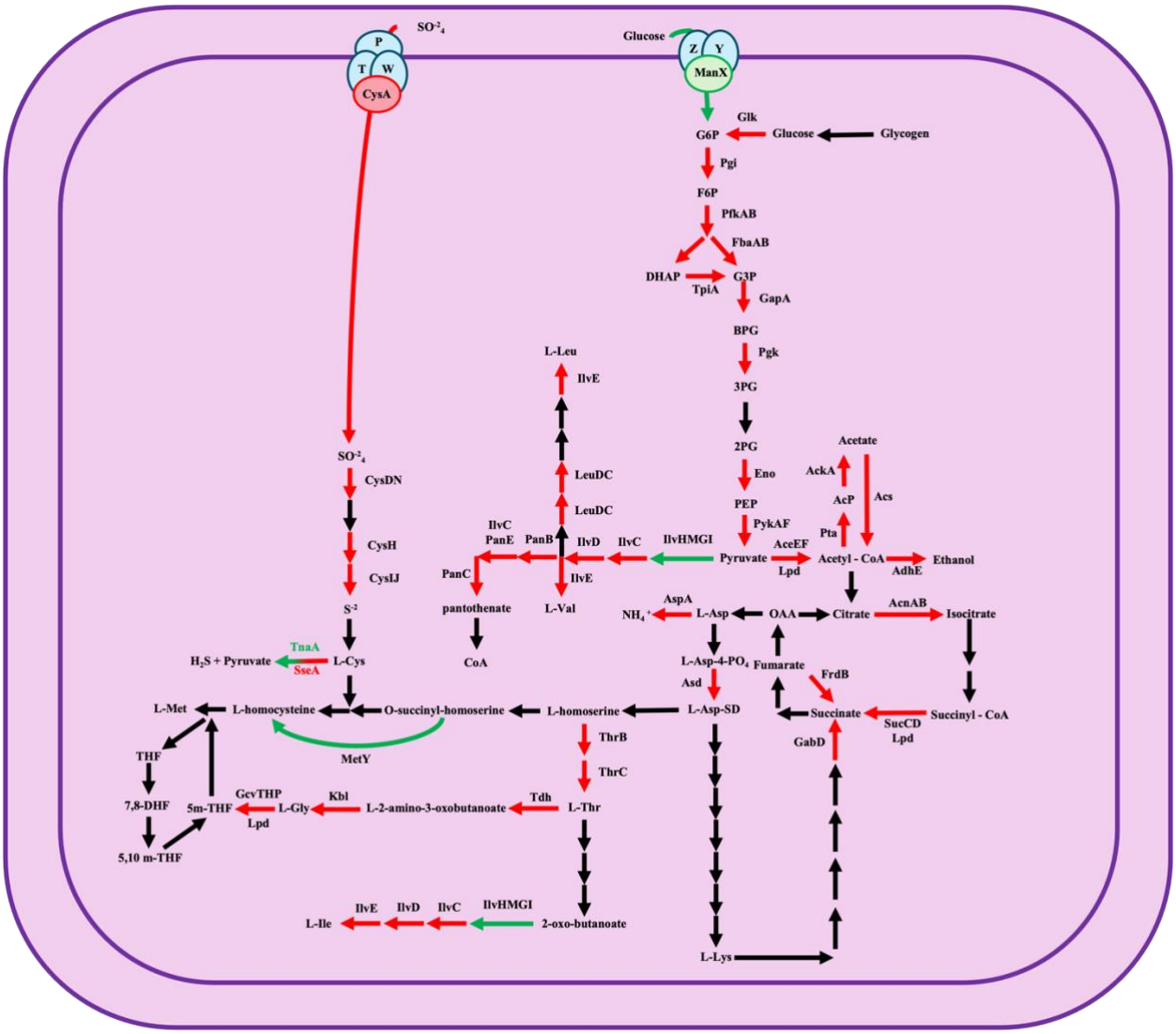


Figure 4.6: *X. nematophila* Lrp negatively regulates carbon and amino acid metabolism during early stationary phase growth in LB.

Graphic summary of Lrp-dependent gene regulation revealed by RNA-seq GO term analysis. Arrow color represents positive (green), negative (red), or little to no (black) regulation by Lrp.

Table 4.3: List of metabolism-associated genes (locus tags and annotations) that are differentially expressed in the *X. nematophila lrp-2::kan* mutant.

Shading indicates if these genes are positively (green) or negatively (red) regulated by *X. nematophila* Lrp.

Locus tag	Gene Annotation	$\log_2$(Fold Change)	Adj. p-value
XNC1_3737	*metY*	-2.266285	0.00048147
XNC1_2962	*tnaA*	-1.9517523	8.06E-05
XNC1_1932	*manX*	-1.4648054	0.03629008
XNC1_1046	*ilvH*	-0.642164	0.02087846
XNC1_2801	*pta*	0.58689083	0.01738572
XNC1_0052	*acs*	0.66530056	0.01870315
XNC1_3909	*glk*	0.76700696	0.01879391
XNC1_0900	*panB*	0.80711805	0.00688123
XNC1_0100	*pfkA*	0.88205953	0.03380803
XNC1_0818	*gabD*	0.91329159	0.04652939
XNC1_2822	*nuoM*	0.97952147	0.04095891
XNC1_0693	*thrB*	1.09405824	0.00060241
XNC1_0024	*atpC*	1.18758194	0.01369157
XNC1_2802	*ackA*	1.20143438	0.00053395
XNC1_2415	*acnA*	1.22689401	0.01624737
XNC1_3026	*pgk*	1.2368506	0.01724619
XNC1_0878	*eno*	1.24597558	0.03836802
XNC1_3115	*leuC*	1.28321047	0.01622989
XNC1_0025	*atpD*	1.28589192	0.02139401
XNC1_1414	*cydB*	1.29946215	0.04722283
XNC1_3856	*cysD*	1.31595161	0.03754078
XNC1_1082	*lpd*	1.33142486	0.00309342
XNC1_0007	*asd*	1.34669724	0.00801117
XNC1_1108	*gcvT*	1.35618438	0.04963696

Table 4.3 continued

Locus tag	Gene Annotation	log_2(Fold Change)	Adj. p-value
XNC1_1110	*gcvP*	1.37851752	0.01465168
XNC1_0637	*frdB*	1.38411857	0.04623003
XNC1_0371	*ilvD*	1.407261	8.65E-06
XNC1_3602	*aspA*	1.4314108	0.0449075
XNC1_1412	*sucD*	1.43645259	0.0198019
XNC1_0901	*panC*	1.447609	0.0001101
XNC1_3025	*fbaA*	1.45096037	0.01675157
XNC1_3940	*pgi*	1.47898352	0.00297437
XNC1_2171	*pykA*	1.47933141	0.01799947
XNC1_1081	*aceF*	1.48285504	1.95E-05
XNC1_1413	*cydA*	1.48314636	0.02070399
XNC1_0148	*tdh*	1.51177012	0.01012182
XNC1_1080	*aceE*	1.51739052	0.00011112
XNC1_3858	*cysH*	1.56088879	0.00247915
XNC1_3860	*cysJ*	1.6032224	0.00096368
XNC1_0694	*thrC*	1.66396927	7.39E-05
XNC1_3859	*cysI*	1.665985	0.00078694
XNC1_1472	*sseA*	1.68588084	0.00393141
XNC1_0370	*ilvE*	1.73022004	8.65E-06
XNC1_3855	*cysN*	1.73260936	0.00416232
XNC1_0208	*tpiA*	1.85174393	0.00236684
XNC1_0149	*kbl*	1.85717395	0.00141093
XNC1_1411	*sucC*	2.03510612	0.00077932
XNC1_2510	*gapA*	2.09164136	0.00341173
XNC1_2481	*adhE*	2.14589556	7.92E-09
XNC1_3226	*cysA*	2.23134022	4.54E-05
XNC1_0376	*ilvC*	3.99503868	2.28E-31

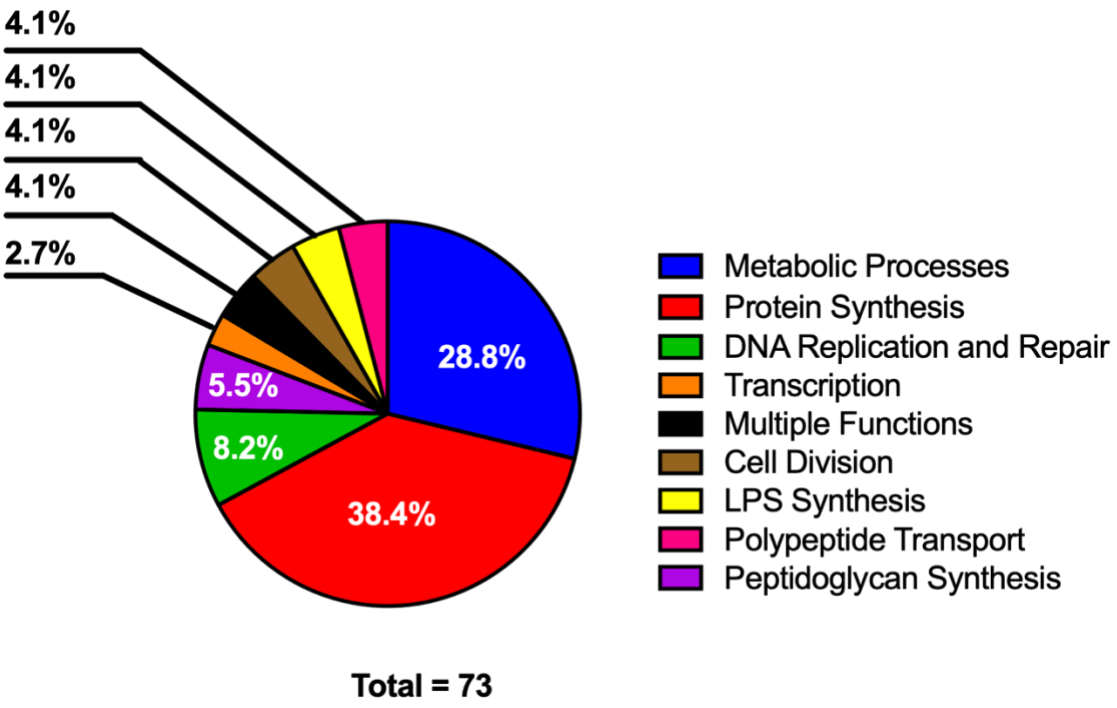


Figure 4.7: The majority of predicted essential genes negatively regulated by Lrp in *X. nematophila* are associated with protein synthesis and metabolism.

The pie chart is color coded by cellular function and the percentage of essential genes is presented within or alongside each wedge.

functionally characterized in *X. nematophila* and may possess alternative, unexplored functionality in the bacterium.

Given that a functional characterization of essential genes has not been performed in *X. nematophila*, we compared our dataset to those known to be essential in *E. coli* [53]. From this list we identified 77 predicted essential genes regulated by Lrp. Of these, only 4 genes (*yhhQ, fabG, acpS,* and *kdsB*) were positively regulated by Lrp, while the remaining 73 genes were negatively regulated by Lrp. The positively regulated essential genes were involved in lipid metabolism, lipopolysaccharide biosynthesis, and quenosine transport.

While the majority of negatively regulated genes were involved in metabolism, primarily central carbon metabolism, and protein synthesis (**Figure 1.7)**. The genes involved in protein synthesis included constituents of the 30S (*rpsB, rpsE, rpsF, rpsG, rpsL,* and *rpsR*) and 50S (*rplA, rplF, rplL, rplO, rplP, rplQ, rplR, rplS, rplT, rplY, rpmC,* and *rpmD*) ribosomal subunits as well as translation factors (*infB, tsf, fusA,* and *prfB*). The remaining genes were predicted to contributed to DNA replication and repair, cell division, transcription, lipopolysaccharide biosynthesis, peptidoglycan biosyntheis, and polypeptide transport. Taken together, these data indicate that in *X. nematophila* Lrp negatively influences the expression of predicted essential genes. Furthermore, these data also suggest that, in an amino acid-limited context, constitutive expression of *lrp* may cause growth arrest or cell death due.

DISCUSSION

The phenotypic heterogeneity of *X. nematophila* is likely adaptive for survival in dynamic environments. In this report, we demonstrate that fixation of Lrp at high levels in

X. nematophila populations is detrimental for persistence in the receptacle of aging *S. carpocapsae* IJs. Wild-type *X. nematophila* cells persist within *S. carpocapsae* IJs for long periods of time [54, 55]. Although their presence does reduce the longevity of *S. carpocapsae* IJs, it is imperative for *X. nematophila* to survive in this niche for subsequent insect infection as it contributes to both virulence and nematode reproduction in this environment [54, 56]. Early during IJ colonization, *X. nematophila* grows within the receptacle and has access to sufficient nutrients to support this growth [57]. However, as *S. carpocapsae* IJs age, the bacterial population size declines [54, 55]. Specific *X. nematophila* mutants that are defective in amino acid or vitamin biosynthesis (e.g, methionine and B6) experience greater population decline within IJs, suggesting that nutrient limitation is a primary driver of this phenomenon [55, 58]. Fixed high and low-*lrp* levels are adapted for different aspects of *X. nematophila* mutualism with *S. carpocapsae* nematodes. *X. nematophila* high-*lrp* cells are best adapted for supporting nematode fecundity during insect infection and for initiating colonization as higher frequencies of *S. carpocapsae* IJs are colonized by this strain compared to the low-*lrp* strain [19]. Although the fixed low-*lrp* strain is less ideal in these contexts, it exhibits greater fitness within the receptacle of *S. carpocapsae* IJs as it can reach higher bacterial loads per colonized nematode [17]. In wild-type populations of *X. nematophila* engineered with a Lrp-dependent P_{fliC}-*gfp* promoter, cells liberated from an aging nematode IJ population shift from a high Lrp state to a low Lrp state over time [17]. The failure of the high-*lrp* strain to persist within its nematode host compared to the fixed low-*lrp* strain over a 60-d aging experiment indicates that this physiological state may engender a higher metabolic demand

for essential nutrients like amino acids. This is likely due to the negative influence Lrp has on essential cellular and metabolic processes such as translation and amino acid biosynthesis, respectively, that may cause eventual growth arrest or cell death. Altogether, this suggests that nutrient limitation within aging *S. carpocapsae* IJs may potentiate Lrp-dependent shifts in wild type *X. nematophila* populations from predominantly high to predominantly low.

One aspect of the metabolic demand brought on by *X. nematophila* high-*lrp* expression was increased need for methionine in amino acid-deficient growth conditions. Indeed, by comparing growth dynamics of wild-type, *lrp-2::kan,* fixed low, and fixed high-*lrp* in various media conditions, we discerned that under most growth conditions the high-*lrp* strain was not as fit as its low and no *lrp* counterparts based on metrics such as lag time, growth rate, and maximum OD_{600}. In natural environments, high-*lrp X. nematophila* cells are dominant during the middle and late stages of insect infection and during early *S. carpocapsae* IJ colonization [17, 19, 25]. This suggests that these environments contain sufficient amino acids to support the growth of these *X. nematophila* cells. In Chapter 2 of this dissertation, we identified the ADAA (Lys, Thr, Asp, Met) as nutritional stimulants of wild-type *X. nematophila* growth in GMM by reducing time the time in lag phase and found that this effect was largely driven by Met. Similarly, the fixed high-*lrp* strain could only grow in GMM if Met was present and exhibited similar growth dynamics to the low and no *lrp* strains in GMM + ADAA. This suggests that presence of these amino acids is essential for optimal fitness of high-*lrp* cells. During insect infection, the transition from low to high *lrp* expression in *X. nematophila* occurs after the death of the insect [17, 19,

25]. Metabolomic analyses conducted by our group have shown that the abundance certain amino acids like methionine decrease during the transition between early and middle stages of infection suggesting that they are being incorporated into *X. nematophila* and *S. carpocapsae* biomass [14]. Since *X. nematophila* is the primary food source of its nematode host, we can reasonably hypothesize that the majority of insect-derived Met is being assimilated by the bacteria to support their own population growth [14]. In the early stage of infection, low-*lrp* cells are able to grow and proliferate due to low recognition and clearance from the insect immune system [20]. Conversely, the growth of high-*lrp* cells is suppressed as they are easily recognized by the insect immune system [20]. The availability of Met during this transitory period between early and middle infection could provide both low and high-*lrp X. nematophila* cells with the opportunity to proliferate; however, because high-*lrp* cells exhibit greater motility, exoenzyme production, and secondary metabolite production they are likely dominant within middle and late stages of infection despite their deficits in growth [16, 19]. The metabolome of aging *S. carpocapsae* IJs is not well described in regard to amino acid composition; bacterial Met biosynthesis is required for optimal outgrowth and long-term persistence of *X. nematophila* within *S. carpocapsae* IJs [55, 58]. In the absence of Met biosynthesis *X. nematophila* colonizes IJ nematodes at lower levels, suggesting that this amino acid is accessible within this niche either from the nematode or from pre-existing endogenous proteins [55, 58]. Given that *X. nematophila* high-*lrp* cells colonize IJs at a higher frequency, we could hypothesize that early access to Met within IJs is sufficient to establish temporary dominance [17, 19]. As Met levels diminish, *X. nematophila* cells must then shift to a low-*lrp* state to accommodate the more

stringent conditions of the aging *S. carpocapsae* IJ receptacle. Collectively, our data indicate that Met availability in the natural environments of *X. nematophila* may be contributing to shifts in Lrp-dependent phenotypic heterogeneity.

Re-evaluation of the Lrp-dependent regulon in *X. nematophila* via RNA-seq expanded the number of predicted genes whose expression is altered by Lrp. Similar to our previous analyses, we found that Lrp influences the expression of genes involved in chemotaxis and motility, secondary metabolite production, virulence towards insects, and mutualism with nematodes [16, 23]. In bacterial systems where the regulatory and physiological effects of Lrp are better characterized, Lrp-dependent gene expression elevates during the transition from exponential to stationary phase [59]. Consistent with this timing, Lrp directly or indirectly downregulates genes involved in entry into stationary phase, including those involved in amino acid biosynthesis and protein synthesis [24, 49]. Our data indicate that this occurs also in *X. nematophila* and confirms that Lrp is indeed a feast and famine regulatory protein. Our data also reveal that elevated Lrp regulation in *X. nematophila* is likely mal-adapted for growth in nutrient limited contexts since fixed high-*lrp* strains are unable to grow in GMM and are expected to have restricted amino acid biosynthesis and reduced protein translation.

Our finding that Met rescues the growth of the high-*lrp* strain in GMM suggests high-*lrp* expression specifically impacts metabolic demand for Met. In *E. coli*, supplementation with Met inhibits Lrp activity [47]. Similarly, Met has been shown to interact with the C-terminal ligand binding domain of transcription factors that share homology to *E. coli* Lrp in *Neisseria meningitidis* raising the possibility that Met may be a

putative Lrp ligand [60]. Conversely, supplementation may also be satisfying an elevated demand for Met within high-*lrp* expressing *X. nematophila.* Indeed, our transcriptomic analyses revealed that Lrp downregulates genes that contribute to Met biosynthesis such as *asd* (aspartate semi-aldehyde dehydrogenase, ADAA pathway), *gcvT* (aminomethyltransferase, folate cycle), *gcvP* (glycine decarboxylase, folate cycle), and multiple genes in the sulfur assimilation/cysteine biosynthesis pathway (*cysADNHIJ,* [50]). Paired with elevated expression of genes involved in energetically costly behaviors (e.g, motility and secondary metabolite production) and lowered expression of BCAA biosynthesis genes and protein synthesis genes, the high-*lrp* strain may be unable to maintain its regulatory state in the absence of exogenous amino acids [61, 62]. There are many limitations to these hypotheses. First and foremost, the conditions for which the RNA-seq based transcriptome was generated (e.g, LB) are amino acid replete, while GMM is amino acid deficient. Recent findings in *E. coli* revealed that the Lrp regulon is expansive and gene expression patterns vary based on the amino acid richness of the medium with some gene expression only being observed in the absence of amino acids [24]. To this end, we cannot be certain that the Lrp-dependent regulatory effects observed in LB will be similar in GMM. Furthermore, constitutive *lrp* expression does not inherently ensure elevated Lrp activity as post-translation acetylation, multimerization, coordinate regulation, and genome structure can alter the DNA binding ability of this transcription factor in other organisms [3, 24, 63, 64]. Finally it is also important to consider if the expression of *lrp* in the fixed high expression strain is environmentally relevant. This was addressed previously by our group, and we observed that relative, steady state levels of Lrp

in the fixed high-*lrp* strain greatly exceeded wild-type levels [16, 18]. However, wild-type populations of *X. nematophila* have been isolated previously that exhibit heterogenous Lrp-dependent gene expression (Vir-69-HET) or homogenously high Lrp-dependent gene expression (Vir-69-HOM, **Figure 4.8,** [18]). Corollary to their heterogeneity phenotypes, immunoblotting revealed that the Vir-69-Hom strain exhibited significantly higher Lrp levels than Vir-69-Het [18]. Furthermore, the Vir-69-Hom strain exhibited little to no grow yield (measured using viable cell counts) when cultivated in GMM, while the Vir-69-Het strain was largely able to grow in this condition (**Figure 4.8,** [18]**)**. This suggests that elevated *lrp* expression and Lrp levels within wild-type populations can causes similar growth inhibitory effects in *X. nematophila*. Altogether, these data and our own support a model where elevated Lrp levels in *X. nematophila* may have deleterious trade-offs during growth in amino acid deficient conditions.

Despite the physiological trade-offs associated with high levels of Lrp in *X. nematophila*, there is a clear adaptive benefit to maintain high *lrp* expression: it optimally supports nematode fecundity and maximizes early colonization [17, 19]. The formation of symbiotic relationships between animals and bacteria are often associated with physiological trade-offs in both organisms. This can manifest in the form of reduced fitness (e.g. lower growth rate) in host niches and/or metabolic dependence upon the host with these traits becoming fixed in the population via genome evolution [65, 66]. While *X. nematophila* is an obligately host - associated bacterium, it predictably faces environmental transitions from nematodes to insects where it must switch from a mutualistic state to an antagonistic state, respectively. *X. nematophila* is highly adapted for growth and survival

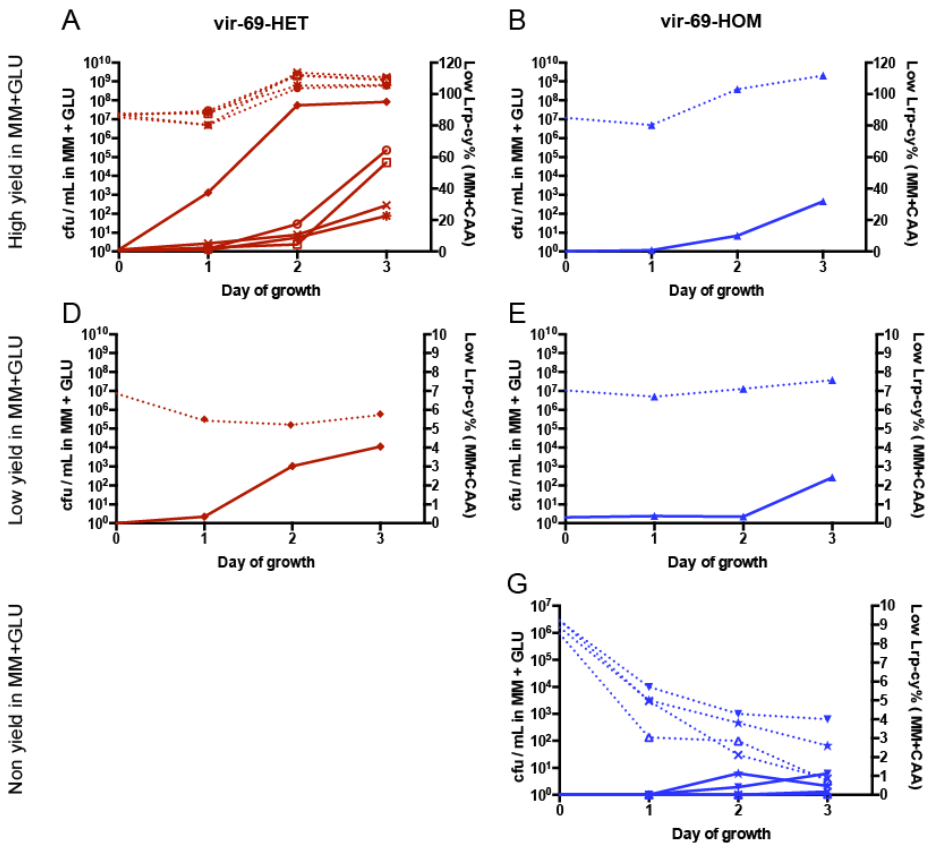


Figure 4.8: Variation in Lrp-dependent *P*$_{fliC}$*-gfp* in *X. nematophila* colonies grown in minimal medium supplemented with casamino acids (solid lines, right y-axis) correlates with bacterial growth yield in minimal medium supplemented with glucose (dashed lines, left).

Six biological replicates of two *X. nematophila* wild-type isolates that exhibit either Lrp-dependent P$_{fliC}$*-gfp* heterogeneity (A, vir-69-Het, red) or P$_{fliC}$*-gfp* homogeneity (B, vir-69-Hom, blue) on LB. Biological replicates are divided based on their growth yield in minimal medium supplemented with glucose. This figure is adapted from unpublished data collected and reported in in Chapter 3 of Dr. Mengyi Cao's dissertation [18].

in both contexts; however there are likely physiological trade-offs associate with each host environment. In this study, we identify that maintenance of fixed high-*lrp* expression in *X. nematophila* is mal-adapted for: 1) prolonged association with its mutualistic host *S. carpocapsae* and 2) growth in amino acid limiting conditions. This maladaptation may be associated with reduced expression of essential genes required for survival in these conditions or with elevated metabolic demand for essential amino acids like Met. Conversely, low-*lrp* expressing cells exhibit opposing phenotypes with increased fitness *in vivo* and *in vitro*. Our findings suggest that Lrp-dependent phenotypic heterogeneity in *X. nematophila* may serve as an adaptive strategy for optimizing fitness in distinct host environments where nutrient limitation and abundance may vary overtime.

REFERENCES

1. Smits, W.K., O.P. Kuipers, and J.-W. Veening, *Phenotypic variation in bacteria: the role of feedback regulation.* Nature Reviews Microbiology, 2006. **4**(4): p. 259-271.
2. Grimbergen, A.J., et al., *Microbial bet-hedging: the power of being different.* Current Opinion in Microbiology, 2015. **25**: p. 67-72.
3. van der Woude, M., B. Braaten, and D. Low, *Epigenetic phase variation of the pap operon in Escherichia coli.* Trends in Microbiology, 1996. **4**(1): p. 5-9.
4. Ikeda, J.S., et al., *Flagellar phase variation of Salmonella enterica serovar Typhimurium contributes to virulence in the murine typhoid infection model but does not influence Salmonella-induced enteropathogenesis.* Infect Immun, 2001. **69**(5): p. 3021-30.
5. Putrinš, M., et al., *Phenotypic heterogeneity enables uropathogenic Escherichia coli to evade killing by antibiotics and serum complement.* Infect Immun, 2015. **83**(3): p. 1056-67.
6. Chin, C.Y., et al., *A high-frequency phenotypic switch links bacterial virulence and environmental survival in Acinetobacter baumannii.* Nat Microbiol, 2018. **3**(5): p. 563-569.
7. Tsai, C.N. and B.K. Coombes, *The Role of the Host in Driving Phenotypic Heterogeneity in Salmonella.* Trends in Microbiology, 2019. **27**(6): p. 508-523.
8. Lerner, A., et al., *Phenotypic variation in Azospirillum brasilense exposed to starvation.* Environ Microbiol Rep, 2010. **2**(4): p. 577-86.

9. Joyce, S.A. and D.J. Clarke, *A hexA homologue from Photorhabdus regulates pathogenicity, symbiosis and phenotypic variation.* Molecular Microbiology, 2003. **47**(5): p. 1445-1457.

10. Grewal, S.I. and P.B. Rainey, *Phenotypic variation of Pseudomonas putida and P. tolaasii affects the chemotactic response to Agaricus bisporus mycelial exudate.* J Gen Microbiol, 1991. **137**(12): p. 2761-8.

11. Hussa Elizabeth, A., M. Casanova-Torres Ángel, and H. Goodrich-Blair, *The Global Transcription Factor Lrp Controls Virulence Modulation in Xenorhabdus nematophila.* Journal of Bacteriology, 2015. **197**(18): p. 3015-3025.

12. Park, Y., et al., *Clonal variation in Xenorhabdus nematophila virulence and suppression of Manduca sexta immunity.* Cellular Microbiology, 2007. **9**(3): p. 645-656.

13. Snyder, H., et al., *New insights into the colonization and release processes of Xenorhabdus nematophila and the morphology and ultrastructure of the bacterial receptacle of its nematode host, Steinernema carpocapsae.* Appl Environ Microbiol, 2007. **73**(16): p. 5338-46.

14. Mucci, N.C., et al., *Apex Predator Nematodes and Meso-Predator Bacteria Consume Their Basal Insect Prey through Discrete Stages of Chemical Transformations.* mSystems, 2022. **7**(3): p. e0031222.

15. Casanova-Torres, A.M., et al., *The Global Transcription Factor Lrp Is both Essential for and Inhibitory to Xenorhabdus nematophila Insecticidal Activity.* Appl Environ Microbiol, 2017. **83**(12).

16. Hussa, E.A., A.M. Casanova-Torres, and H. Goodrich-Blair, *The Global Transcription Factor Lrp Controls Virulence Modulation in Xenorhabdus nematophila.* J Bacteriol, 2015. **197**(18): p. 3015-25.

17. Cao, M. and H. Goodrich-Blair, *Xenorhabdus nematophila bacteria shift from mutualistic to virulent Lrp-dependent phenotypes within the receptacles of Steinernema carpocapsae insect-infective stage nematodes.* Environ Microbiol, 2020. **22**(12): p. 5433-5449.

18. Cao, M., *Lrp dependent virulence modulation in bacterium Xenorhabdus nematophila.* , in *Microbiology* 2017, University of Wisconsin - Madison: Madison, Wisconsin.

19. Cao, M., et al., *High Levels of the Xenorhabdus nematophila Transcription Factor Lrp Promote Mutualism with the Steinernema carpocapsae Nematode Host.* Appl Environ Microbiol, 2017. **83**(12).

20. Casanova-Torres Ángel, M., et al., *The Global Transcription Factor Lrp Is both Essential for and Inhibitory to Xenorhabdus nematophila Insecticidal Activity.* Applied and Environmental Microbiology, 2017. **83**(12): p. e00185-17.

21. Cowles, K.N., et al., *The global regulator Lrp contributes to mutualism, pathogenesis and phenotypic variation in the bacterium Xenorhabdus nematophila.* Cell Microbiol, 2007. **9**(5): p. 1311-23.

22. Heungens, K., C.E. Cowles, and H. Goodrich-Blair, *Identification of Xenorhabdus nematophila genes required for mutualistic colonization of Steinernema carpocapsae nematodes.* Mol Microbiol, 2002. **45**(5): p. 1337-53.

23. Engel, Y., et al., *The Global Regulators Lrp, LeuO, and HexA Control Secondary Metabolism in Entomopathogenic Bacteria.* Front Microbiol, 2017. **8**: p. 209.

24. Kroner, G.M., M.B. Wolfe, and L. Freddolino, *Escherichia coli Lrp Regulates One-Third of the Genome via Direct, Cooperative, and Indirect Routes.* J Bacteriol, 2019. **201**(3).

25. Jubelin, G., et al., *Studies of the dynamic expression of the Xenorhabdus FliAZ regulon reveal atypical iron-dependent regulation of the flagellin and haemolysin genes during insect infection.* Environ Microbiol, 2011. **13**(5): p. 1271-84.

26. Xu, J., et al., *Transformation of Xenorhabdus nematophilus.* Appl Environ Microbiol, 1989. **55**(4): p. 806-12.

27. Neidhardt, F.C., P.L. Bloch, and D.F. Smith, *Culture medium for enterobacteria.* J Bacteriol, 1974. **119**(3): p. 736-47.

28. McMullen, J.G., 2nd and S.P. Stock, *In vivo and in vitro rearing of entomopathogenic nematodes (Steinernematidae and Heterorhabditidae).* J Vis Exp, 2014(91): p. 52096.

29. Lee, M.M. and S.P. Stock, *A multilocus approach to assessing co-evolutionary relationships between Steinernema spp. (Nematoda: Steinernematidae) and their bacterial symbionts Xenorhabdus spp. (gamma-Proteobacteria: Enterobacteriaceae).* Syst Parasitol, 2010. **77**(1): p. 1-12.

30. Chaston, J.M., et al., *Previously unrecognized stages of species-specific colonization in the mutualism between Xenorhabdus bacteria and Steinernema nematodes.* Cellular microbiology, 2013. **15**(9): p. 1545-1559.

31. Schindelin, J., et al., *Fiji: an open-source platform for biological-image analysis.* Nature Methods, 2012. **9**(7): p. 676-682.

32. Ansari, N., et al., *Chapter 13 - Quantitative 3D Cell-Based Assay Performed with Cellular Spheroids and Fluorescence Microscopy*, in *Methods in Cell Biology*, P.M. Conn, Editor. 2013, Academic Press. p. 295-309.

33. Community, T.G., *The Galaxy platform for accessible, reproducible, and collaborative data analyses: 2024 update.* Nucleic Acids Research, 2024. **52**(W1): p. W83-W94.

34. Ge, S.X., D. Jung, and R. Yao, *ShinyGO: a graphical gene-set enrichment tool for animals and plants.* Bioinformatics, 2020. **36**(8): p. 2628-2629.

35. Kanehisa, M., Y. Sato, and M. Kawashima, *KEGG mapping tools for uncovering hidden features in biological data.* Protein Sci, 2022. **31**(1): p. 47-53.

36. Lanois, A., G. Jubelin, and A. Givaudan, *FliZ, a flagellar regulator, is at the crossroads between motility, haemolysin expression and virulence in the insect pathogenic bacterium Xenorhabdus.* Molecular microbiology, 2008. **68**(2): p. 516-533.

37. Jubelin, G., et al., *FliZ is a global regulatory protein affecting the expression of flagellar and virulence genes in individual Xenorhabdus nematophila bacterial cells.* PLoS genetics, 2013. **9**(10): p. e1003915-e1003915.

38. Cowles, K.N. and H. Goodrich-Blair, *Expression and activity of a Xenorhabdus nematophila haemolysin required for full virulence towards Manduca sexta insects.* Cell Microbiol, 2005. **7**(2): p. 209-19.

39. Richards Gregory, R., et al., *Xenorhabdus nematophila lrhA Is Necessary for Motility, Lipase Activity, Toxin Expression, and Virulence in Manduca sexta Insects.* Journal of Bacteriology, 2008. **190**(14): p. 4870-4879.

40. Park, D. and S. Forst, *Co-regulation of motility, exoenzyme and antibiotic production by the EnvZ-OmpR-FlhDC-FliA pathway in Xenorhabdus nematophila.* Mol Microbiol, 2006. **61**(6): p. 1397-412.

41. Richards Gregory, R. and H. Goodrich-Blair, *Examination of Xenorhabdus nematophila Lipases in Pathogenic and Mutualistic Host Interactions Reveals a Role for xlpA in Nematode Progeny Production.* Applied and Environmental Microbiology, 2010. **76**(1): p. 221-229.

42. Singh, S., et al., *Role of secondary metabolites in establishment of the mutualistic partnership between Xenorhabdus nematophila and the entomopathogenic nematode Steinernema carpocapsae.* Appl Environ Microbiol, 2015. **81**(2): p. 754-64.

43. Vallenet, D., et al., *MicroScope in 2017: an expanding and evolving integrated resource for community expertise of microbial genomes.* Nucleic Acids Res, 2017. **45**(D1): p. D517-d528.

44. Cowles, C.E. and H. Goodrich-Blair, *nilR is necessary for co-ordinate repression of Xenorhabdus nematophila mutualism genes.* Mol Microbiol, 2006. **62**(3): p. 760-71.

45. Grossman, A.S., et al., *A Surface Exposed, Two-Domain Lipoprotein Cargo of a Type XI Secretion System Promotes Colonization of Host Intestinal Epithelia Expressing Glycans.* Frontiers in microbiology, 2022. **13**: p. 800366-800366.

46. Yokoyama, K., et al., *Feast/famine regulatory proteins (FFRPs): Escherichia coli Lrp, AsnC and related archaeal transcription factors.* FEMS Microbiol Rev, 2006. **30**(1): p. 89-108.

47. Hart, B.R. and R.M. Blumenthal, *Unexpected coregulator range for the global regulator Lrp of Escherichia coli and Proteus mirabilis.* J Bacteriol, 2011. **193**(5): p. 1054-64.

48. Baek, C.-H., et al., *Leucine-responsive regulatory protein (Lrp) acts as a virulence repressor in Salmonella enterica serovar Typhimurium.* Journal of bacteriology, 2009. **191**(4): p. 1278-1292.

49. Calvo, J.M. and R.G. Matthews, *The leucine-responsive regulatory protein, a global regulator of metabolism in Escherichia coli.* Microbiol Rev, 1994. **58**(3): p. 466-90.

50. Hondorp, E.R. and R.G. Matthews, *Methionine.* EcoSal Plus, 2006. **2**(1).

51. Kaleta, C., et al., *Metabolic costs of amino acid and protein production in Escherichia coli.* Biotechnology Journal, 2013. **8**(9): p. 1105-1114.

52. Hasebe, F., *MetW regulates the enzymatic activity of MetX in Pseudomonas.* Biosci Biotechnol Biochem, 2021. **85**(2): p. 351-358.

53. Goodall, E.C.A., et al., *The Essential Genome of Escherichia coli K-12.* mBio, 2018. **9**(1).

54. Mitani, D.K., H.K. Kaya, and H. Goodrich-Blair, *Comparative study of the entomopathogenic nematode, Steinernema carpocapsae, reared on mutant and wild-type Xenorhabdus nematophila.* Biological Control, 2004. **29**(3): p. 382-391.

55. Flores-Lara, Y., et al., *Influence of nematode age and culture conditions on morphological and physiological parameters in the bacterial vesicle of Steinernema carpocapsae (Nematoda: Steinernematidae).* J Invertebr Pathol, 2007. **95**(2): p. 110-8.

56. Emelianoff, V., et al., *Effect of bacterial symbionts Xenorhabdus on mortality of infective juveniles of two Steinernema species.* Parasitology Research, 2007. **100**(3): p. 657-659.

57. Martens, E.C., K. Heungens, and H. Goodrich-Blair, *Early colonization events in the mutualistic association between Steinernema carpocapsae nematodes and Xenorhabdus nematophila bacteria.* J Bacteriol, 2003. **185**(10): p. 3147-54.

58. Martens, E.C., F.M. Russell, and H. Goodrich-Blair, *Analysis of Xenorhabdus nematophila metabolic mutants yields insight into stages of Steinernema carpocapsae nematode intestinal colonization.* Mol Microbiol, 2005. **58**(1): p. 28-45.

59. Landgraf, J.R., J. Wu, and J.M. Calvo, *Effects of nutrition and growth rate on Lrp levels in Escherichia coli.* Journal of bacteriology, 1996. **178**(23): p. 6930-6936.

60. Ren, J., et al., *The Structure and Transcriptional Analysis of a Global Regulator from Neisseria meningitidis*.* Journal of Biological Chemistry, 2007. **282**(19): p. 14655-14664.

61. Santamaria, G., et al., *Evolution and regulation of microbial secondary metabolism.* eLife, 2022. **11**: p. e76119.

62. Schavemaker, P.E. and M. Lynch, *Flagellar energy costs across the tree of life.* Elife, 2022. **11**.

63. Chen, S., M.H. Rosner, and J.M. Calvo, *Leucine-regulated self-association of leucine-responsive regulatory protein (Lrp) from Escherichia coli11Edited by M. F. Moody.* Journal of Molecular Biology, 2001. **312**(4): p. 625-635.

64. Qin, R., et al., *The Bacterial Two-Hybrid System Uncovers the Involvement of Acetylation in Regulating of Lrp Activity in Salmonella Typhimurium.* Frontiers in microbiology, 2016. **7**: p. 1864-1864.

65. Chong, R.A., H. Park, and N.A. Moran, *Genome Evolution of the Obligate Endosymbiont Buchnera aphidicola.* Molecular Biology and Evolution, 2019. **36**(7): p. 1481-1489.

66. Koga, R., et al., *Single mutation makes Escherichia coli an insect mutualist.* Nat Microbiol, 2022. **7**(8): p. 1141-1150.

CHAPTER 5: CONCLUSIONS AND FUTURE DIRECTIONS

Authors: Cameron Moore and Heidi Goodrich-Blair

INTRODUCTION

This dissertation project began with a small, simple question: *How do I get an obligately symbiotic bacterium to grow in a chemically, defined minimal medium?* What started as an endeavor to overcome a methodological challenge, grew into a project that filled knowledge gaps in our current understanding of *Xenorhabdus* physiology. In this dissertation, I focused first on how nutrient limitation impacted the *in vitro* growth dynamics of *X. nematophila* where I discovered that methionine (Met) limitation caused a prolonged lag length in amino acid deficient conditions (Chapter 2). A broader assessment of growth across *Xenorhabdus* species revealed that the prolonged lag physiology was not conserved but that Met-dependent reduction of lag was fairly wide-spread suggesting variable demand for Met *in vitro*. Paired with comparative genomic and phylogenetic analyses, I speculated that niche-specific adaptation among *Xenorhabdus* may have driven this physiology to arise. I tested this in Chapter 3 by assessing how disruption of Met biosynthesis altered the niche-specific association of *X. bovienii*-Sf-FL with its cognate nematode host *Steinernema feltiae*-FL. Here I demonstrated that Met proficiency in *X. bovienii* positively impacts colonization of *S. feltiae*-FL IJs and *S. feltiae*-FL reproduction. In support of the data collected in from Chapter 2 and 3, I suggest that variable metabolic demand for Met among *Xenorhabdus* is likely correlated with the Met biosynthetic demands required to maintain mutualistic associations with *Steinernema* nematode hosts. In Chapter 4, I assessed the impact of Lrp-dependent phenotypic heterogeneity on *X. nematophila* fitness *in vitro* and *in vivo.* Within *S. carpocapsae* IJs and in amino acid replete conditions, *X. nematophila* cells with high-*lrp expression* struggled to persist or

grow, respectively, while the low-*lrp* strain seemed to thrive by comparison. The *in vitro* growth defect of the high-*lrp* strain could be rescued by exogenous supplementation of Met, suggesting that increased metabolic demand for this amino acid or Met-dependent inhibition of Lrp activity alters this strain's growth dynamics. Transcriptomics revealed that Lrp negatively regulates many genes involved in essential cellular processes such as carbon catabolism, amino acid biosynthesis, and protein synthesis, all of which would be necessary for growth in conditions where amino acids are deficient. Even with these physiological trade-offs, X. *nematophila* high-*lrp* cells are beneficial to their nematode host in certain symbiotic contexts; therefore, we speculate that Met availability may be driving Lrp-dependent shifts in *X. nematophila* populations [1-5]. Together these data suggest that, for a subset of *Xenorhabdus* species, Met is a critical metabolite that modulates bacterial physiology, gene regulation, and symbiotic associations with animals.

QUESTION 1:

What are the factors that contribute variable lag length among *Xenorhabdus*?

The observation that *Xenorhabdus* species have variable lag times in GMM led us to hypothesize that distinct *Xenorhabdus* species have differential demands for Met under amino acid limiting growth conditions. A reasonable, alternative hypothesis is that long lag Xenorhabdus species synthesize Met at a slower rate than intermediate or short lag *Xenorhabdus*. In Chapter 3, I demonstrated that even in the presence of a Met synthesis proficient symbiont, the presence of a Met synthesis deficient *X. bovienii* symbiont could suppress *S. feltiae* reproduction. Furthermore, long-term association (30 d) between *S. feltiae* IJs with a Met synthesis deficient symbiont diminished its ability to effectively

reproduce in insects. While these observations are not lag-related, they support the idea that satisfying demand for Met in a long lag *Xenorhabdus* species can come at a cost to its *Steinernema* host if biosynthesis is not functional. In subsequent analyses, it will be important to determine if the physiological differences in *Xenorhabus* lag observed in Chapter 2 were the result of demand for Met or less efficient synthesis. To address this, I would first determine the rate of Met biosynthesis in select long, intermediate, and short lag *Xenorhabdus* species using a computational approach (e.g. Flux Balance Analysis) [6, 7]. If the predicted rate of methionine synthesis is similar among *Xenorhabdus* species, this would suggest that demand for methionine is variable between these organisms. If the rate is significantly different among the tested *Xenorhabdus*, then this would indicate a reduced rate of Met synthesis.

I would next endeavor to determine the genetic factors contributing to the prolonged lag phenotype. To do this I would use a targeted approach where I would focus on the three genomic "predictors" of *Xenorhabdus* lag time: *argD*, the MtcC-like protein encoding locus, and *pixA*. The presence of ArgD was primarily observed in short lag *Xenorhabdus* species, *X. nematophila*, and *X. griffiniae*. An ortholog to *E. coli* ArgD was not identified in most long lag *Xenorhabdus* species, *X.* poinarii, and *X. cabanillasii.* It is important to note, only the genome of *X. cabanillasii* is considered closed in this group of *Xenorhabdus* where ArgD was not detected. Prior to any downstream experimentation on this predictor, it is important to confirm that *argD* is truly absent in these organisms. ArgD is functionally redundant aminotransferase that contributes to the synthesis of both lysine and arginine [8]. While deletion of *argD* does not cause auxotrophy of either amino acid,

it does elicit a prolonged, variable lag phase in *E. coli* [8]. The second lag predictor was the presence of a gene of unknown function whose encoded protein shared sequence similarity to MtcC – a cystathionine γ-lyase which allows bacteria to utilize Met as a sulfur source by converting it into L-cysteine [9]. This gene was identified in short-lag (*X. thuongxuanensis, X. ehlersii*, and *X. doucetiae*) and intermediate-lag (*X. griffiniae* and *X. poinarii*) *Xenorhabdus*. Furthermore, this protein was encoded proximally to genes predicted to be involved in cysteine metabolism [10-12]. The final lag predictor was PixA, a methionine-rich inclusion protein found in all the long lag *Xenorhabdus* and in *X. doucetiae*. While previous studies have endeavored to investigate PixA in *X. nematophila,* the function of this protein remains elusive, and its presence only modestly impacts the ability of the bacterium to colonize its nematode host [13]. PixA is hypothesized to be an endogenous nutrient reservoir that *Xenorhabdus* species can degrade to liberate essential amino acids in times of starvation, though no evidence to date has strongly supported this [13, 14]. In Chapter 1, we suggest that PixA degradation may be an alternative mechanism by which *Xenorhabdus* generate Met when transitioning from amino acid replete to amino acid deficient conditions. To test if these genes contribute to 1) *Xenorhabdus* lag length and 2) influence Met demand or synthesis, I would also utilize established gene deletion and complementation strategies to determine if these genomic predictors are involved in either of the aforementioned phenotypes. In the event that these predictors have no impact on *Xenorhabdus* lag and/or Met demand, I would use an untargeted approach where I utilize a high-throughput genetic screening technique (e.g. transposon-mutant library) to

identify genes in select *Xenorhabdus* species that contribute to long, intermediate, and short lag times [15-17].

Finally to complete this line questioning, I would next attempt to determine if the Met-responsiveness nature of *Xenorhabdus* lag phase in GMM is due to Met's contribution to protein synthesis and/or S-adenosylmethionine (AdoMet) pools [18]. In other bacteria, such as *Escherichia coli* and Phaeobacter *inhibens*, processes associated with Met metabolism have been shown to modulate lag dynamics. In *E. coli* nutrient downshifts in amino acid composition (e.g. transition from LB to GMM) required sequential restoration of endogenous amino acid pools, with Met being the first pool fulfilled, in order to initiate protein synthesis and resume growth [19]. In *P. inhibens*, supplementation of methylated compounds, but not Met, increased endogenous AdoMet levels by feeding into the one-carbon pool and Met cycle eliciting a lag reduction [19, 20]. These two observations highlight that supplementation of Met to *Xenorhabdus* cultures could be reducing lag times by modulating one or both of those pathways. To address this, I would again leverage isotope tracing and mass spectrometry. Here I would supplement *Xenorhabdus* GMM cultures with ^{13}C-labelled Met, similar to what was done for *P. inhibens*, and determine if, during lag, Met accumulates in newly synthesized proteins or AdoMet [20]. In addition to a Met-responsive *Xenorhabdus* species, I would also select a control, non-Met responsive *Xenorhabdus* species for comparison.

QUESTION 2:

How does *Xenorhabdus* Met biosynthesis influence the reproductive physiology of *Steinernema* nematodes *in vitro*?

I consider the most striking finding of my second data chapter (Chapter 3) to be the demonstration that disruption of Met biosynthesis in *X. bovienii*-Sf-FL suppresses *S. feltiae*-FL reproduction *in vitro* and *in vivo*. In addition to this symbiotic pair, I also assessed the impact of other Met auxotrophic *Xenorhabdus* symbionts on the emergence of their cognate *Steinernema* host *in vitro* **(Fig 1).** Unlike *X. bovienii,* Met auxotrophy in *X. nematophila* (long lag in GMM) did not significantly alter emergence of *S. carpocapsae* IJs. This suggests that there is not a correlation between *Xenorhabdus* lag length and Met-dependent support of *Steinernema* host reproduction. Findings from two short lag *Xenorhabdus* species agreed with this finding. Disruption of Met biosynthesis in *X. griffiniae* did not significantly alter the emergence of *S. hermaphroditum* IJs. However, disruption of *X. cabanillasii* Met biosynthesis led to a marked improvement in *S. riobrave* nematode emergence suggesting that here the symbiont was suppressing host reproduction. I attempted to follow-up on this phenotype in *X. cabanillasii* but was inhibited by this potential reproductive suppression as I was unable to reproducibly isolate aposymbiotic *S. riobrave* eggs when reared on the wild-type symbiont. Both *X. bovienii*-Sf-FL and *X. cabanillasii* phylogenetically group together in a clade basal to the *Xenorhabdus* phylogeny (Chapter 2). Given that modulation of host reproduction, albeit in an opposing fashion, is shared among these two organisms, this leads me to hypothesize that other bacterial species within this clade (e.g. *X. innexi* and other *X. bovienii* isolates) may exert Met-dependent effects on their cognate nematode host's reproduction. To test this I would generate deletions of the *metE* gene (as well as complement strains) in select *Xenorhabdus* isolates and assess the impact of these mutations on host reproduction and bacterial colonization as

described in Chapter 3. To this end I have generated a *metE* deletion construct for *X. innexi;* however, I was unsuccessful in generating this mutant. Unlike other *Xenorhabdus* species, *X. innexi* is not easily genetically manipulated (an observation made by previous researchers from our group) and may require further optimization for this goal to be achieved. The findings from these assessments will broaden or narrow our scope of focus regarding Met-dependent modulation of *Steinernema* reproduction among *Xenorhabdus* species.

While *X. bovienii*-Sf-FL is highly adapted to its cognate nematode host, work from our group and others has shown that this symbiont can also limitedly support the reproduction of other nematode species closely related to *S. feltiae*-FL (e.g. *S. feltiae*-MD, *S. feltiae*-FR, and *S. puntavense*) [21, 22]. To assess if reproductive support of non-cognate nematode hosts is also Met-dependent, I would isolate aposymbiotic J1 juveniles for the nematode species listed above and initially measure their IJ emergence phenotypes. If the emergence of these nematodes is dependent on Met biosynthesis in the non-cognate symbiont, I would enumerate the number of immature *Steinernema* IJs developed on each tested condition (wild-type, *metE* mutant, and complement) to determine if emergence defects are reproductive or behavior as I did in Chapter 3. The results from these experiments would illuminate whether the mechanism of Met-dependent reproductive support is specific to the *X. bovienii*-*S. feltiae*-FL symbiosis or is more generalized for other *Steinernema* nematodes.

In the bacterial feeding nematode *Caenorhabditis elegans*, a link between dietary restriction of Met and reducing fecundity has been described. Briefly, Met restriction was

induced by limiting the number of consumable bacteria – *E. coli* OP50 – available to *C. elegans* and observable decreases in nematode egg laying behavior and egg viability were observed [23]. Supplementation of the nematode growth medium with methionine was sufficient to restore *C. elegans* egg laying and egg survivability [23]. I hypothesize that similar reproductive defects are occurring in *S. feltiae* – FL when reared on a Met deficient *X. bovienii*-Sf-FL symbiont. To address this hypothesis, I would assess the aforementioned phenotypes in *S. feltiae*-FL nematodes when reared on wild-type, *metE* deficient, and *metE* complement strains of *X. bovienii*. If significant differences in egg laying and egg viability are not observed, I would next assess if the *S. feltiae* nematodes are able to develop and progress through their lifecycle when reared on Met synthesis deficient *X. bovienii*-Sf-FL by quantifying the number of juvenile and adult nematodes and comparing them to the wild-type and complement conditions [24]. We also made the observation in Chapter 3, that the presence of a Met auxotrophic symbiont in a predominantly Met prototrophic population was sufficient to suppress *S. feltiae* reproduction. From this finding I hypothesized that the Met deficient symbiont was assimilating and sequestering environmental Met from *S. feltiae*-FL impeding *S. feltiae* reproduction (Chapter 3). To test this, ideally, I would need to generate a *metE* deficient strain that was incapable of taking up exogenous Met. The *X. bovienii*-Sf-FL genome contains the genes *metINQ*, which are predicted to encode a Met-specific ABC-type transport protein (Chapter 2); however, if this transporter serves as the sole Met import system, then generation of a *metINQ* mutant in a *metE* deficient background would be potentially lethal. To account for this possibility, I would instead construct a conditional expression strain where *metINQ* was under

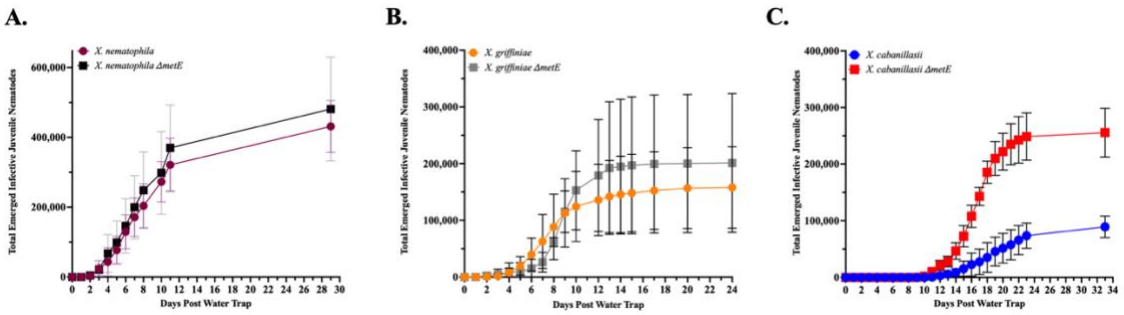


Figure 5.1: Emergence behavior of *Steinernema* nematodes when reared on wild-type and *metE*-deficient *Xenorhbadus* symbionts.

A) *S. carpocapsae* IJ emergence from wild-type (maroon) and *metE* deficient *X. nematophila* (black). **B)** *S. hermaphroditum* IJ emergence from wild-type (orange) and *metE* deficient *X. griffiniae* (grey). **C)** *S. riobrave* IJ emergence from wild-type (blue) and *metE* deficient *X. griffiniae* (red). Curves are the average of four biological replicates and error bars indicate ±1 SD.

the control of an arabinose inducible promoter in the *X. bovienii*-Sf-FL *metE* deficient background (*ΔmetE* P_{ara}-*metINQ*) as well as the wild-type [25]. I would then co-cultivate *S. feltiae*-FL nematodes on these strains when exposed to low, intermediate, and high doses of arabinose and compare IJ emergence. If I observe elevated emergence on a *ΔmetE* P_{ara}-*metINQ* strain with low induction, this suggests that sequestration of Met by a Met auxotrophic symbiont is suppressing nematode reproduction. This would not be true if I observed no effect or even a negative effect during these experiments. Collectively, these proposed experiments would provide mechanistic insights into the *X. bovienii*-Sf-FL Met-dependent support of reproduction in *S. feltiae* nematodes.

QUESTION 3:

How do exogenous Met levels influence *X. nematophila* Lrp-dependent phenotypes?

In Chapter 4, I identify that the *X. nematophila* fixed high-*lrp* is unable to persist for 60 d inside the receptacle of aging *S. carpocapsae* IJs, while also failing to grow under amino acid limiting conditions *in vitro* unless Met is present. This suggests that in environments where *X. nematophila* high-*lrp* cells are dominant, Met and other amino acids may be available in sufficient quantities to support this sub-population's outgrowth. Based on data presented previously, I would expect that Met would be available within insect cadavers and in the receptacle of unaged *S. carpocapsae* IJs [26, 27]. To test this hypothesis, I would generate a deletions of *metINQ* in the fixed high-*lrp* strain of *X. nematophila* to determine if exogenous Met assimilation is essential for nematode fecundity – a nematode host phenotype that is Lrp-dependent and that correlates with successful bacterial proliferation within insect cadavers – and *S. carpocapsae* colonization

initiation [1, 2]. To perform this assay, I would rear up aposymbiotic *S. carpocapsae* IJ nematodes and co-inject them with the *X. nematophila* high-*lrp* strain that does or does not contain *metINQ* into *Galleria mellonella* [2]. If exogenous Met levels contribute to the proliferative success of the high-*lrp* strain in *G. mellonella*, I would expect to see reduced *S. carpocapsae* IJ emergence in the high-*lrp metINQ* mutant compared to the control conditions. This would suggest that fitness of the high-*lrp* strain in this context would be dependent upon exogenous Met levels. If there is no difference, then this would indicate that an alternative metabolic factor may be potentiating this interaction. Following this assay, I would collect *S. carpocapsae* IJs that emerged from these co-infected *Galleria* and assess the frequency of colonization and bacterial carriage of the high-*lrp* strain with and without *metINQ*. I would predict that the loss of *metINQ* in the high-*lrp* background would reduce colonization frequency of the strain and significantly reduce bacterial carriage in unaged *S. carpocapsae* IJs suggesting that nematode-derived Met is influencing these colonization dynamics in *X. nematophila* high-*lrp* cells. If we do not see significant differences in these phenotypes, we could repeat these experiments using a high-*lrp* background that does or does encode *pixA*. As stated above PixA is considered Met rich and modestly contributes to colonization of *S. carpocapsae* IJs [13]. It has been hypothesized, but never proven, to be a potential endogenous source of Met in *X. nematophila* [13, 14]. If endogenous Met reserves supports the success of *X. nematophila* high-*lrp* cells, we would expect to see deficits in the aforementioned fecundity and colonization phenotypes during this assay. Together, these experiments address if

exogenous or endogenous Met levels in *X. nematophila* contribute to the success of high-*lrp* cells in their natural ecosystem.

A separate line of inquiry would be to investigate the role of Met in Lrp-dependent gene expression. In order to address this I would utilize pre-existing promoter fusion constructs generated by previous lab members to address the impact of exogenous Met on *lrp* expression as well as expression of genes directly regulated by Lrp such as *nilC* and *xhlBA* [4, 5, 28-30]. In *E. coli* supplementation of Met reduces Lrp activity to a similar extent to leucine, particularly in its repression of the P_{livK} promoter [31]. Furthermore, supplementation of Met to GMM restored growth to the high-*lrp* which was predicted to negatively regulated a variety of essential and conditionally essential genes (Chapter 4). This suggest that in *X. nematophila* Met may reduce Lrp activity (e.g. DNA-binding) by some unknown mechanism. Based on these observations, I would predict that the presence of Met would alleviate the autogenous, negative regulation of Lrp exerts on its own promoter, which was observed previously in *X. nematophila* [4]. Moreover, I would expect to see increased promoter activity of *nilC* (repressed by Lrp) and decreased *xhlBA* promoter activity (activated by Lrp) in the presence Met [5, 29, 30]. If we do not see these phenotypes and instead see the opposite phenotype or observe no effects, this information would still be important as it would suggest that the effect of Met on Lrp activity is more complex and likely context dependent as asserted in other bacterial models [32]. I would also assess the effect of Met on population-wide phenotypic heterogeneity using previously described strains containing the P_{fliC}-*gfp* express construct [1, 2, 33]. This promoter is Lrp-dependent (either directly or indirectly) and was used previously to observe phenotypic heterogeneity

in *X. nematophila* populations [1, 2, 33]. I would predict that supplementation of Met into cultures containing wild-type strains that exhibit heterogeneous or homogenously high P_{fliC}-*gfp* expression would reduce the proportion of *fliC* expressing cells in both populations; however, because the heterogenous strain is more phenotypically variable I anticipate that this phenotype would be more dramatic compared to the homogenous strain [1, 33]. If these phenotypes are not observed or the opposite occurs, again this indicates that the impact of Met on Lrp activity may be context dependent. Both sets of experiments would enhance our current knowledge on how environmental nutrients impact Lrp-dependent gene expression as, to date, there are no published studies demonstrating Lrp nutrient-responsivity in *X. nematophila*.

CONCLUDING STATEMENT

The multi-faceted roles of Met in various biological phenomena across all life forms is has not been underappreciated; however, it remained limitedly explored in *Xenorhabdus* bacteria prior to this dissertation. Here I assembled experimental evidence implicating this key amino acid in reducing the lag time of some *Xenorhabdus* species in amino acid deficient conditions (Chapter 1), in modulating growth dynamics of symbiotically relevant, Lrp-dependent phenotypic states in *X. nematophila*, and in maintaining the obligate (Chapter 4), strain-specific mutualism between *X. bovienii*-Sf-FL and *S. feltiae*-FL nematode host (Chapter 3). Collectively, I provide strong evidence that Met serves as biochemical mediator of bacterial fitness and symbioses in a sub-set of *Xenorhabdus* bacteria. Furthermore, I highlight in this chapter the key questions raise but

unanswered in this dissertation and examine the possible contributions these inquiries could have on our knowledge of *Xenorhabdus*-*Steinernema* symbioses.

REFERENCES

1. Cao, M. and H. Goodrich-Blair, *Xenorhabdus nematophila bacteria shift from mutualistic to virulent Lrp-dependent phenotypes within the receptacles of Steinernema carpocapsae insect-infective stage nematodes.* Environ Microbiol, 2020. **22**(12): p. 5433-5449.
2. Cao, M., et al., *High Levels of the Xenorhabdus nematophila Transcription Factor Lrp Promote Mutualism with the Steinernema carpocapsae Nematode Host.* Appl Environ Microbiol, 2017. **83**(12).
3. Casanova-Torres, A.M., et al., *The Global Transcription Factor Lrp Is both Essential for and Inhibitory to Xenorhabdus nematophila Insecticidal Activity.* Appl Environ Microbiol, 2017. **83**(12).
4. Hussa, E.A., A.M. Casanova-Torres, and H. Goodrich-Blair, *The Global Transcription Factor Lrp Controls Virulence Modulation in Xenorhabdus nematophila.* J Bacteriol, 2015. **197**(18): p. 3015-25.
5. Cowles, K.N., et al., *The global regulator Lrp contributes to mutualism, pathogenesis and phenotypic variation in the bacterium Xenorhabdus nematophila.* Cell Microbiol, 2007. **9**(5): p. 1311-23.
6. Basan, M., et al., *A universal trade-off between growth and lag in fluctuating environments.* Nature, 2020. **584**(7821): p. 470-474.
7. Orth, J.D., I. Thiele, and B. Palsson, *What is flux balance analysis?* Nat Biotechnol, 2010. **28**(3): p. 245-8.

8. Lal, P.B., et al., *The redundant aminotransferases in lysine and arginine synthesis and the extent of aminotransferase redundancy in Escherichia coli.* Mol Microbiol, 2014. **94**(4): p. 843-56.

9. Seiflein, T.A. and J.G. Lawrence, *Two transsulfurylation pathways in Klebsiella pneumoniae.* J Bacteriol, 2006. **188**(16): p. 5762-74.

10. Yamamoto, K., et al., *Induction of the Escherichia coli yijE gene expression by cystine.* Biosci Biotechnol Biochem, 2015. **79**(2): p. 218-22.

11. Soutourina, J., S. Blanquet, and P. Plateau, *Role of d-Cysteine Desulfhydrase in the Adaptation of Escherichia coli to d-Cysteine **.* Journal of Biological Chemistry, 2001. **276**(44): p. 40864-40872.

12. Nagasawa, T., et al., *D-Cysteine desulfhydrase of Escherichia coli. Purification and characterization.* Eur J Biochem, 1985. **153**(3): p. 541-51.

13. Goetsch, M., et al., *Analysis of the PixA inclusion body protein of Xenorhabdus nematophila.* J Bacteriol, 2006. **188**(7): p. 2706-10.

14. Couche, G.A. and R.P. Gregson, *Protein inclusions produced by the entomopathogenic bacterium Xenorhabdus nematophilus subsp. nematophilus.* J Bacteriol, 1987. **169**(11): p. 5279-88.

15. Alani, O.S., et al., *Conjugation and transposon mutagenesis of Xenorhabdus griffiniae HGB2511, the bacterial symbiont of the nematode Steinernema hermaphroditum (India).* MicroPubl Biol, 2023. **2023**.

16. Heungens, K., C.E. Cowles, and H. Goodrich-Blair, *Identification of Xenorhabdus nematophila genes required for mutualistic colonization of Steinernema carpocapsae nematodes.* Mol Microbiol, 2002. **45**(5): p. 1337-53.

17. Richards, G.R., et al., *Isolation and characterization of Xenorhabdus nematophila transposon insertion mutants defective in lipase activity against Tween.* J Bacteriol, 2009. **191**(16): p. 5325-31.

18. Hondorp, E.R. and R.G. Matthews, *Methionine.* EcoSal Plus, 2006. **2**(1).

19. Wu, C., et al., *Enzyme expression kinetics by Escherichia coli during transition from rich to minimal media depends on proteome reserves.* Nature Microbiology, 2023. **8**(2): p. 347-359.

20. Sperfeld, M., et al., *Algal methylated compounds shorten the lag phase of Phaeobacter inhibens bacteria.* Nature Microbiology, 2024. **9**(8): p. 2006-2021.

21. McMullen, J.G., 2nd, et al., *Fitness costs of symbiont switching using entomopathogenic nematodes as a model.* BMC Evol Biol, 2017. **17**(1): p. 100.

22. Murfin, K.E., et al., *Xenorhabdus bovienii Strain Diversity Impacts Coevolution and Symbiotic Maintenance with Steinernema spp. Nematode Hosts.* mBio, 2015. **6**(3): p. e00076.

23. Zhou, G., et al., *Methionine increases yolk production to offset the negative effect of caloric restriction on reproduction without affecting longevity in C. elegans.* Aging (Albany NY), 2020. **12**(3): p. 2680-2697.

24. Chaston, J.M., et al., *Previously unrecognized stages of species-specific colonization in the mutualism between Xenorhabdus bacteria and Steinernema nematodes.* Cellular microbiology, 2013. **15**(9): p. 1545-1559.

25. Abebew, D., et al., *Uncovering Nematicidal Natural Products from Xenorhabdus Bacteria.* Journal of Agricultural and Food Chemistry, 2022. **70**(2): p. 498-506.

26. Martens, E.C., F.M. Russell, and H. Goodrich-Blair, *Analysis of Xenorhabdus nematophila metabolic mutants yields insight into stages of Steinernema carpocapsae nematode intestinal colonization.* Mol Microbiol, 2005. **58**(1): p. 28-45.

27. Mucci, N.C., et al., *Apex Predator Nematodes and Meso-Predator Bacteria Consume Their Basal Insect Prey through Discrete Stages of Chemical Transformations.* mSystems, 2022. **7**(3): p. e0031222.

28. Cowles, C.E. and H. Goodrich-Blair, *The Xenorhabdus nematophila nilABC genes confer the ability of Xenorhabdus spp. to colonize Steinernema carpocapsae nematodes.* J Bacteriol, 2008. **190**(12): p. 4121-8.

29. Cowles, C.E. and H. Goodrich-Blair, *nilR is necessary for co-ordinate repression of Xenorhabdus nematophila mutualism genes.* Mol Microbiol, 2006. **62**(3): p. 760-71.

30. Cowles, K.N. and H. Goodrich-Blair, *Expression and activity of a Xenorhabdus nematophila haemolysin required for full virulence towards Manduca sexta insects.* Cell Microbiol, 2005. **7**(2): p. 209-19.

31. Hart, B.R. and R.M. Blumenthal, *Unexpected coregulator range for the global regulator Lrp of Escherichia coli and Proteus mirabilis.* J Bacteriol, 2011. **193**(5): p. 1054-64.

32. Kroner, G.M., M.B. Wolfe, and L. Freddolino, *Escherichia coli Lrp Regulates One-Third of the Genome via Direct, Cooperative, and Indirect Routes.* J Bacteriol, 2019. **201**(3).

33. Cao, M., *Lrp dependent virulence modulation in bacterium Xenorhabdus nematophila.* , in *Microbiology* 2017, University of Wisconsin - Madison: Madison, Wisconsin.

VITA

Cameron Moore was raised in the Dutch Valley community of Clinton, TN where he attended Dutch Valley Elementary, Clinton Middle, and Clinton High School. In 2016, he attended Maryville College (Maryville, TN) where he obtained a B.S. in biology with a minor in chemistry, while also participating in the institution's instrumental music program as the principal student euphonium player. During his time as an undergraduate, Cameron participated in two summer internships through the HERE program at Oak Ridge National Laboratory where he participated in research efforts in the areas of toxicology and risk hazard assessment (2017) and plant metabolomics and bioconversion (2018). In 2019, Cameron participated in the NSF REU in Molecular and Synthetic Microbiology at the University of Georgia – Athens where he worked under Dr. Eric Stabb studying the squid-*Vibrio* symbiosis. In 2020, he enrolled at the University of Tennessee – Knoxville in pursuit of a Ph.D. in Microbiology where he joined the laboratory of Dr. Heidi Goodrich-Blair. His dissertation project focused on investigating how methionine metabolism in symbiotic *Xenorhabdus* bacteria influenced growth behavior, phenotypic heterogeneity, and animal host interactions. Cameron looks forward to returning to the "land of the living" after graduate school and investing more time enjoying his hobbies (e.g. playing the euphonium, reading fiction novels, and cooking both new and old recipes).